

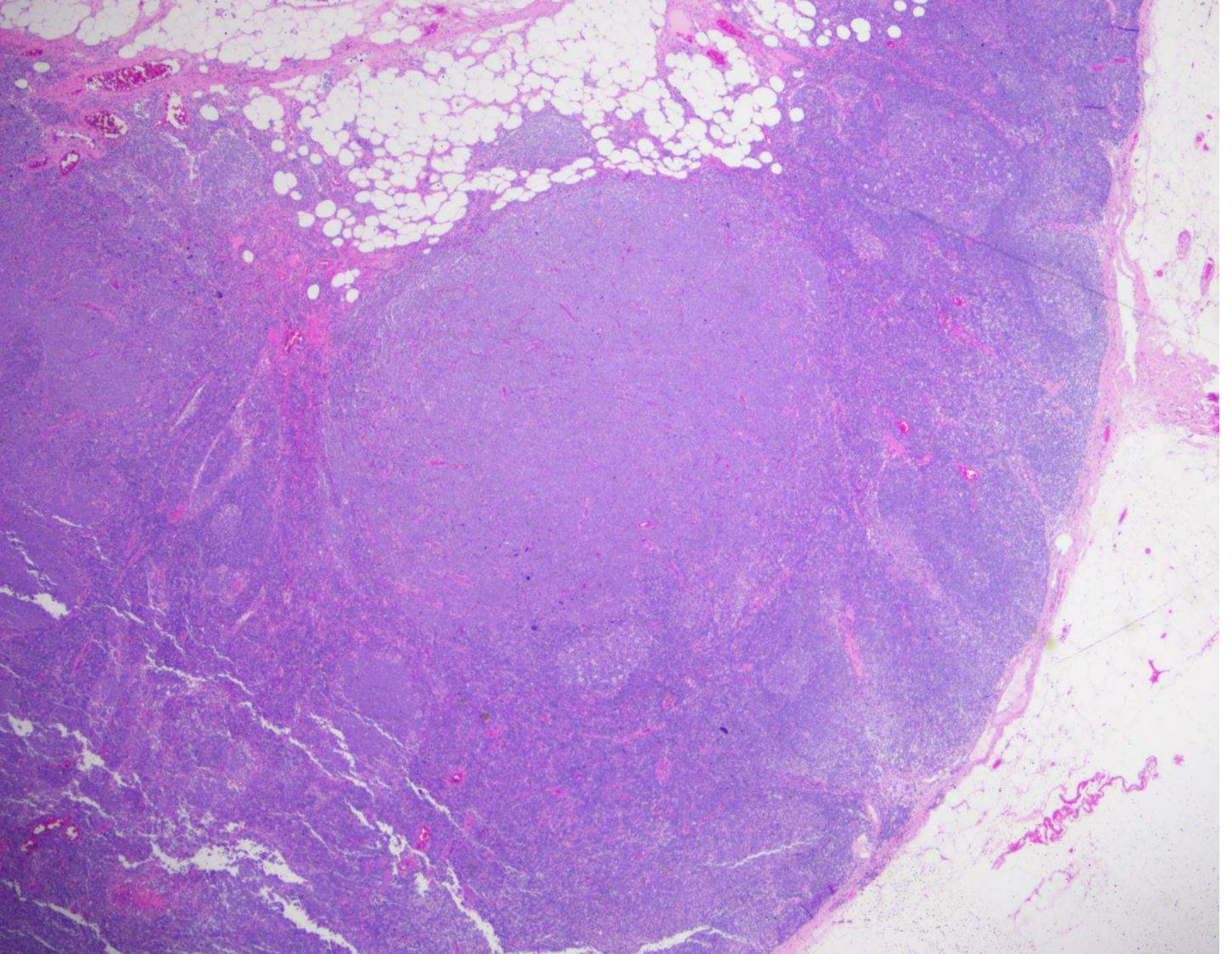
OCT 2020 DIAGNOSIS LIST

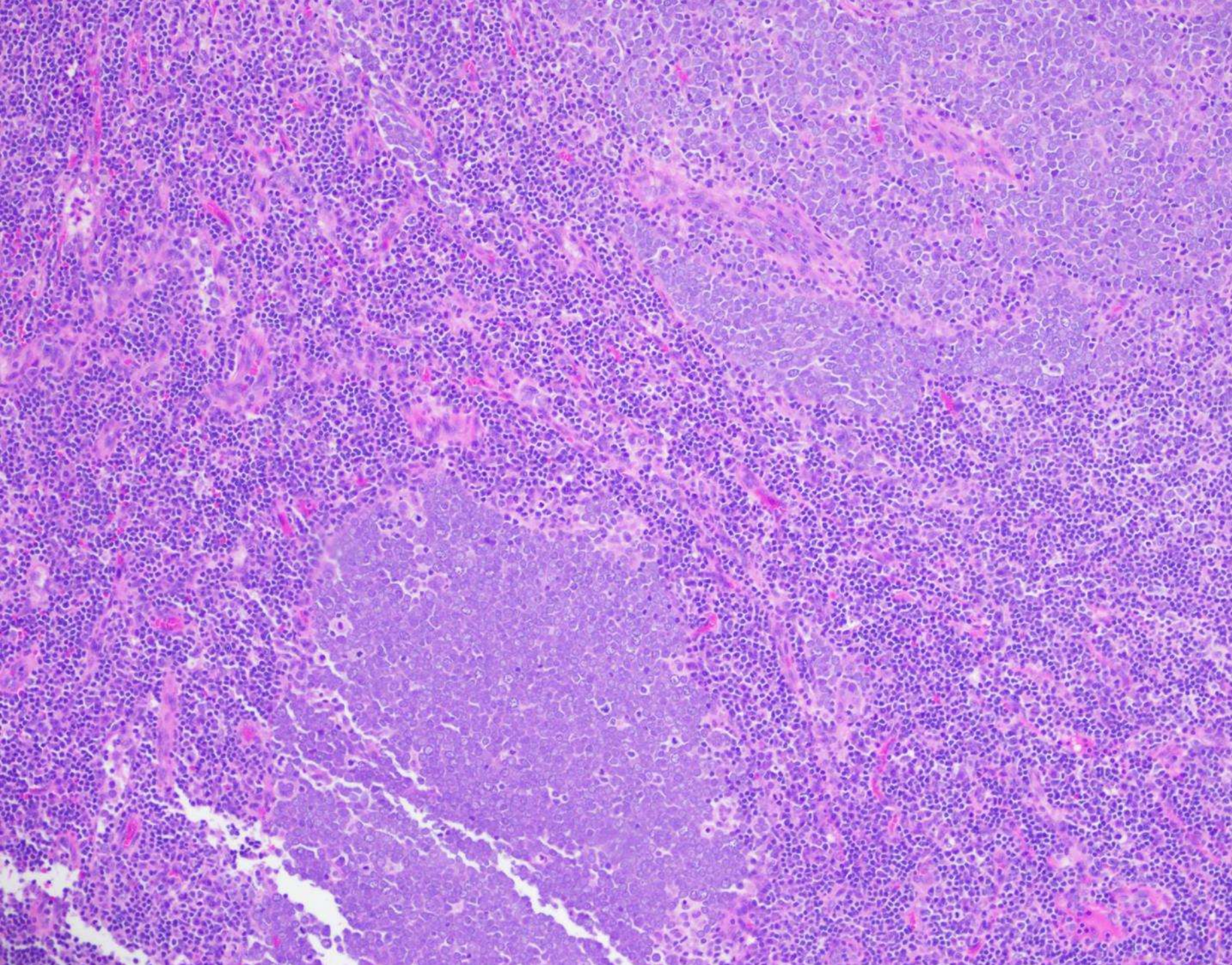
- 20-0101: metastatic Merkel cell carcinoma and Kaposi sarcoma (lymph node; soft tissue pathology and dermatopathology)
- 20-1002: calcified amorphous tumor (heart; cardiovascular pathology)
- 20-0103: myocyte vacuolization/atypia & fatty infiltration (s/p Maze procedure for atrial fibrillation (heart; cardiovascular pathology)
- 20-0104: intimal sarcoma (heart; cardiovascular pathology)
- 20-0105: Rosai-Dorfman disease (dura; soft tissue pathology)
- 20-0106: metastatic urothelial carcinoma (brain/neuropathology/GU pathology)
- 20-0107: florid mesothelial hyperplasia (testis; GU pathology)

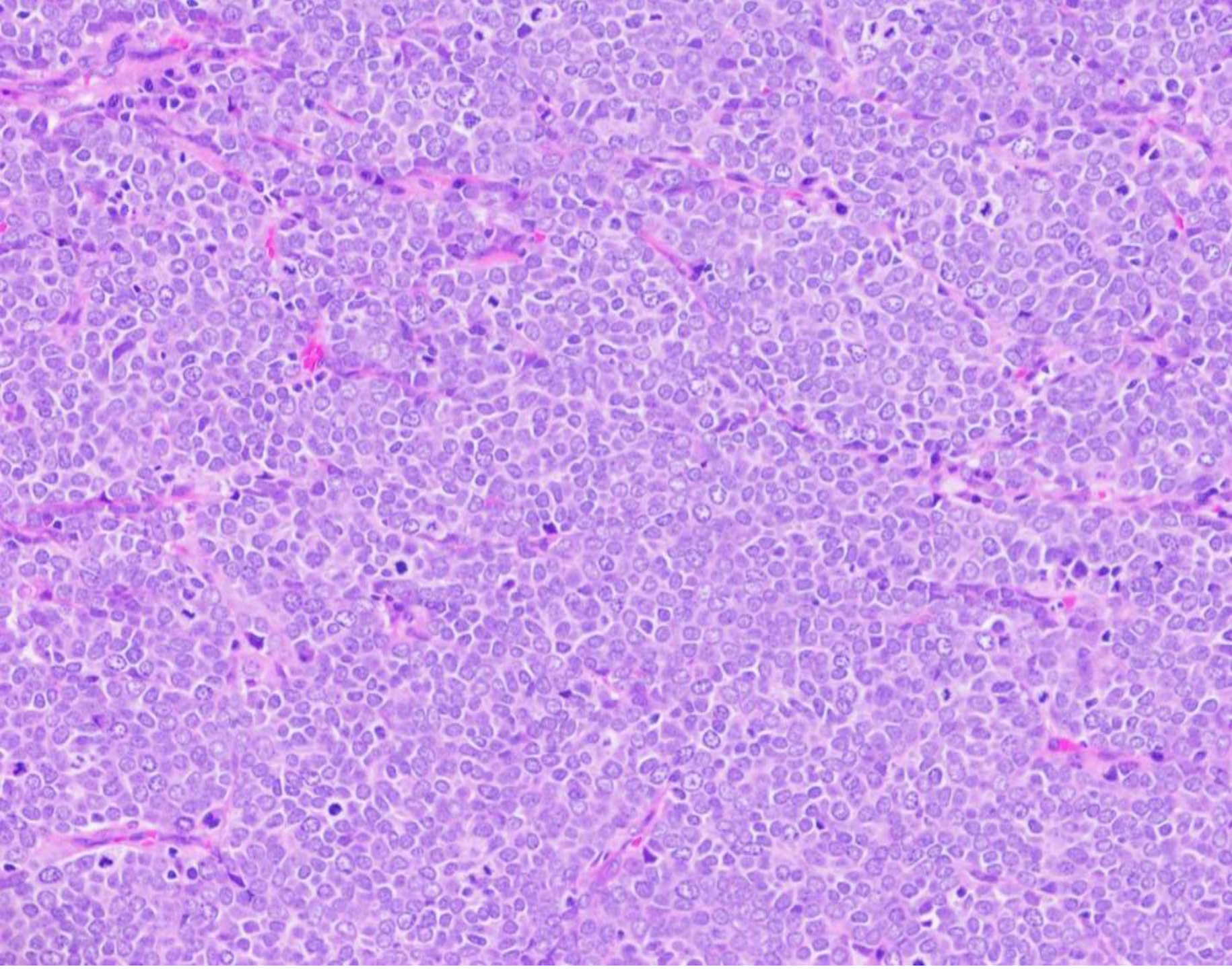
20-1001

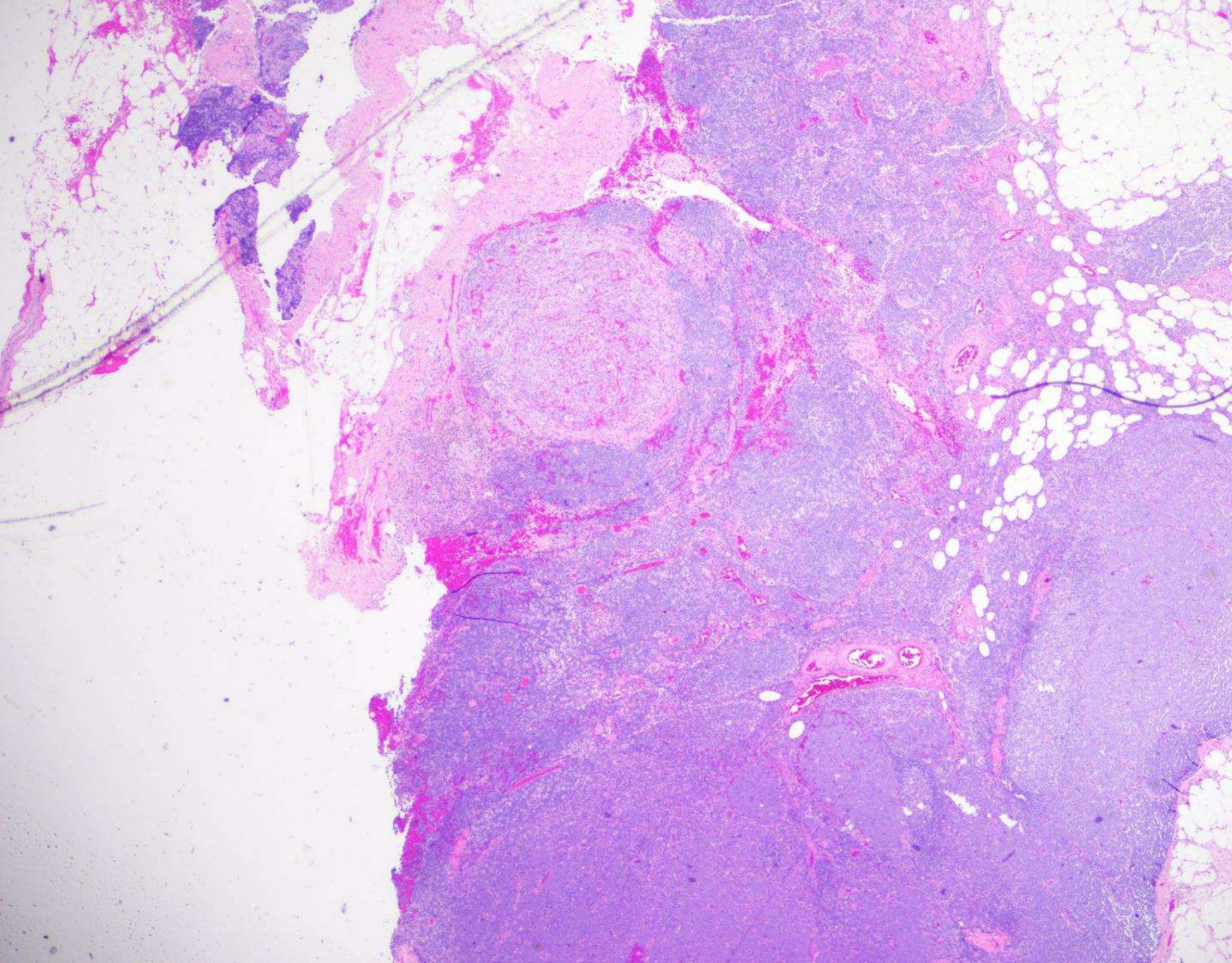
Armen Khararjian; Kaiser Walnut Creek

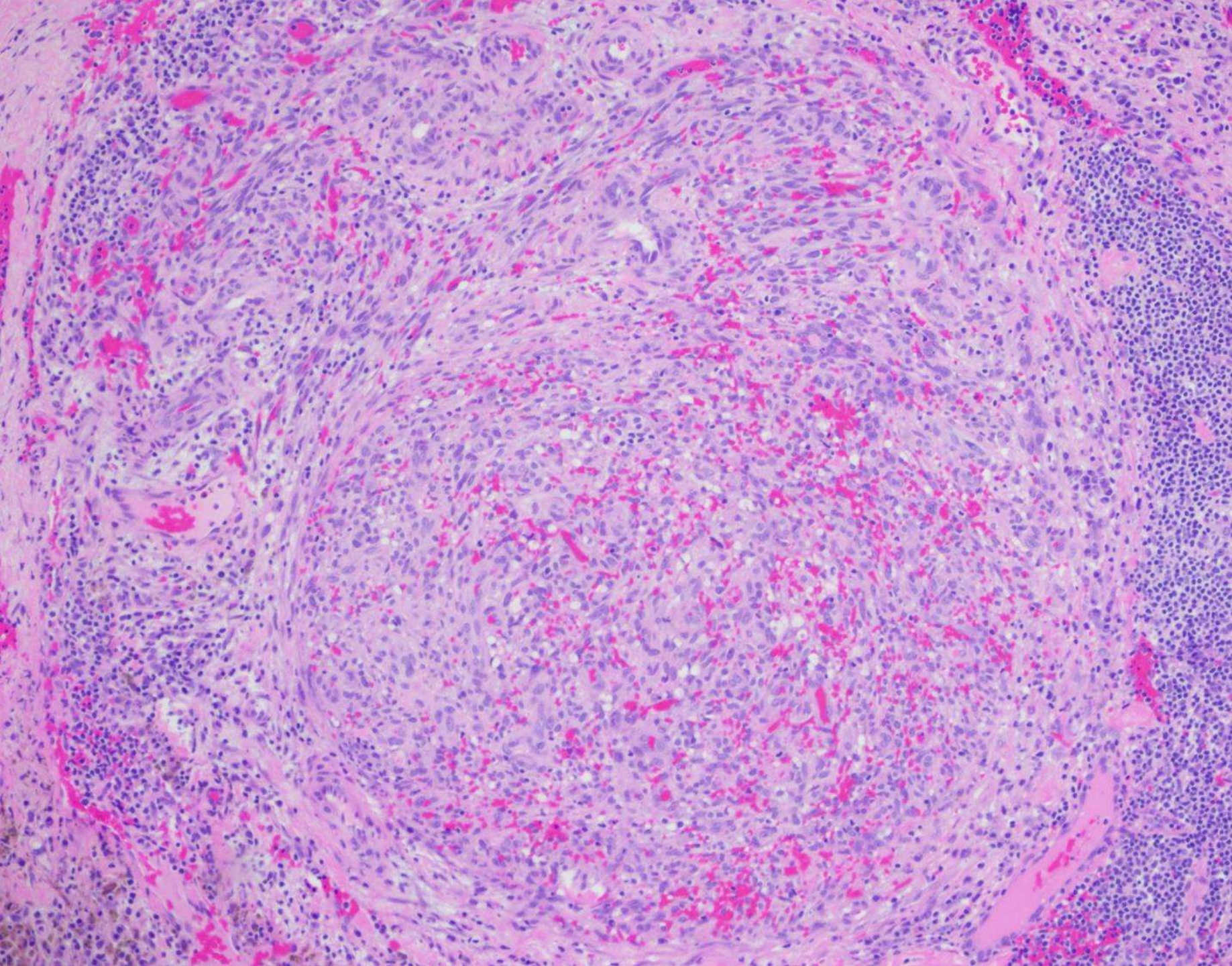
82-year-old M who presented for WLE and SLN bx for
buttock mass.

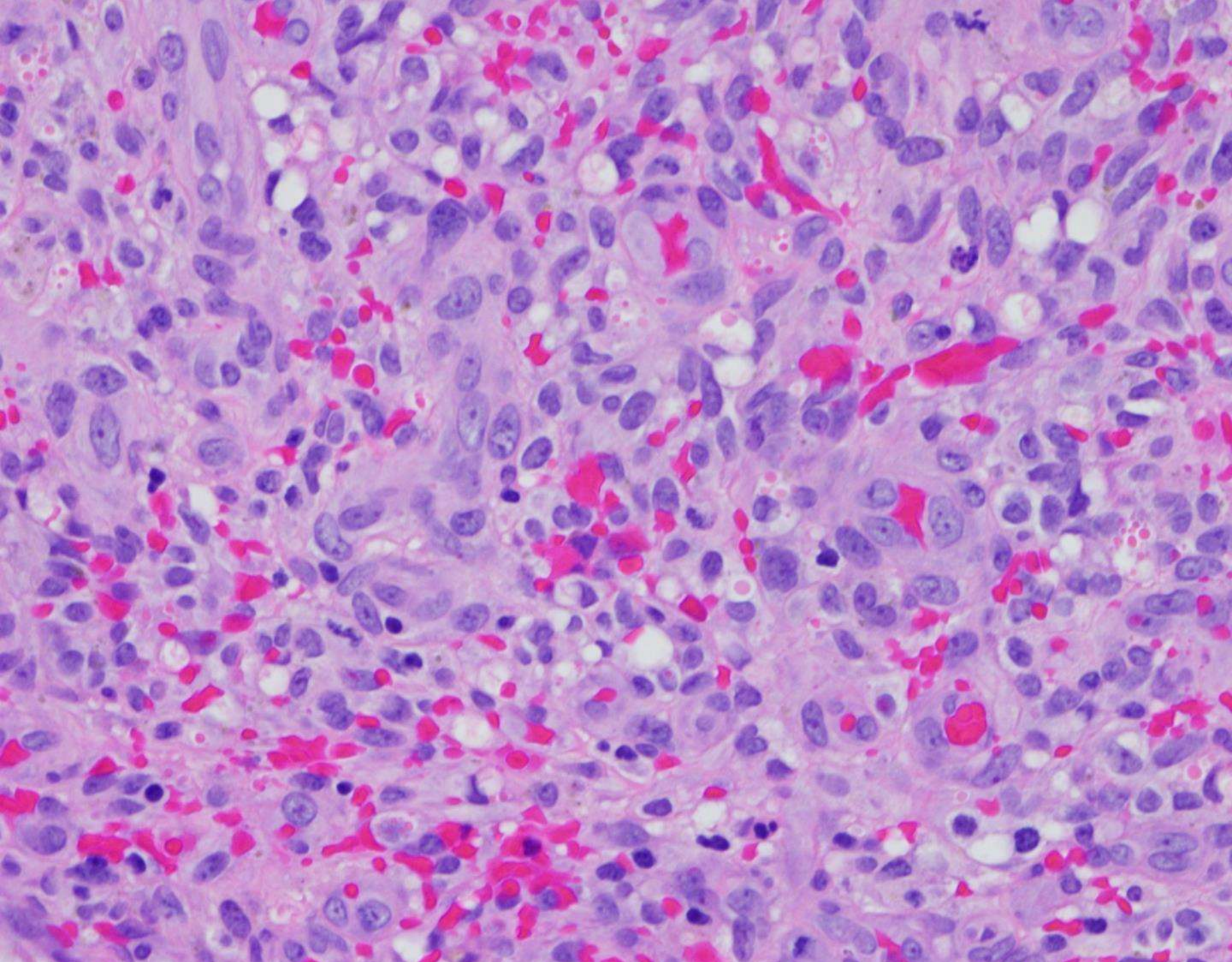


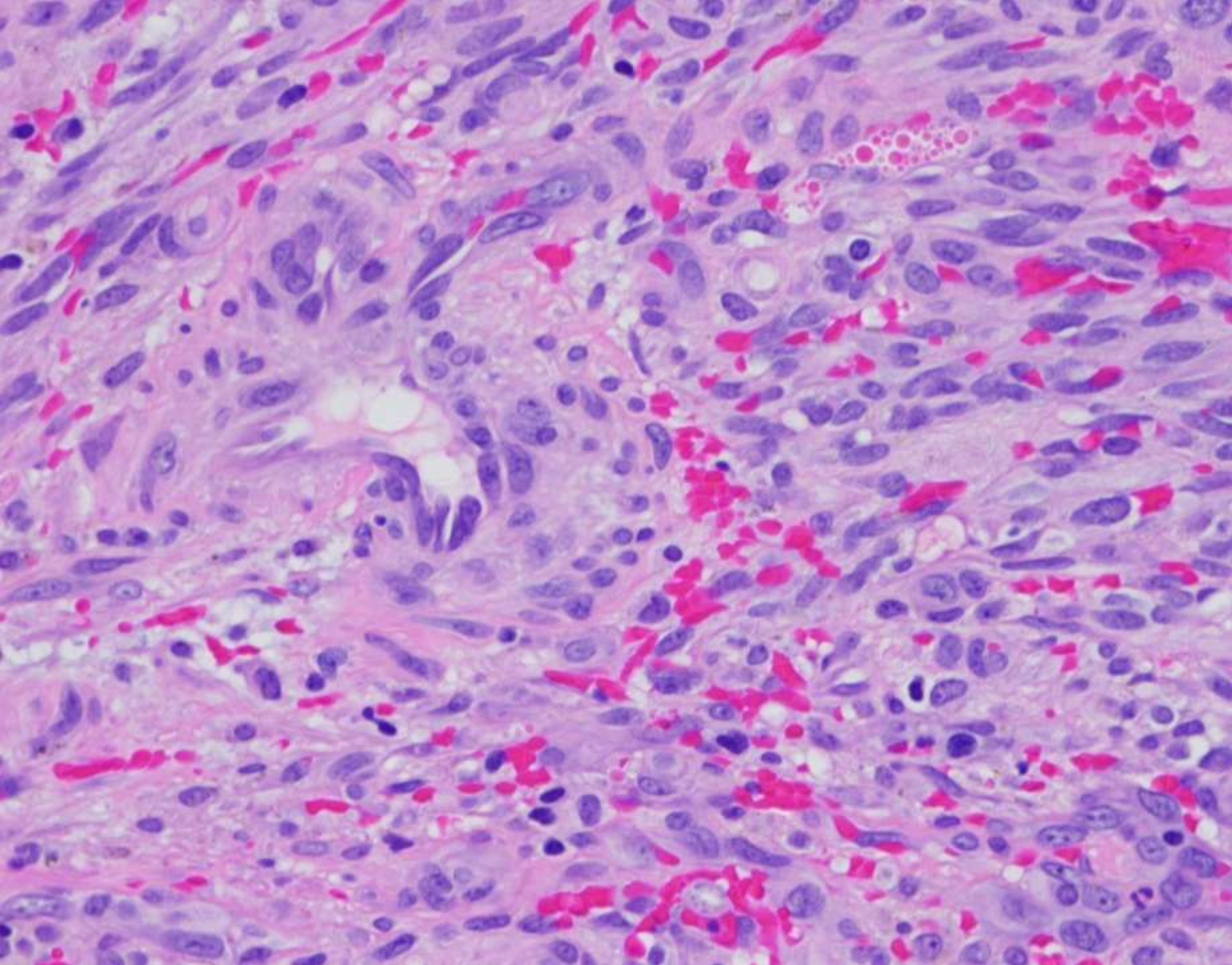


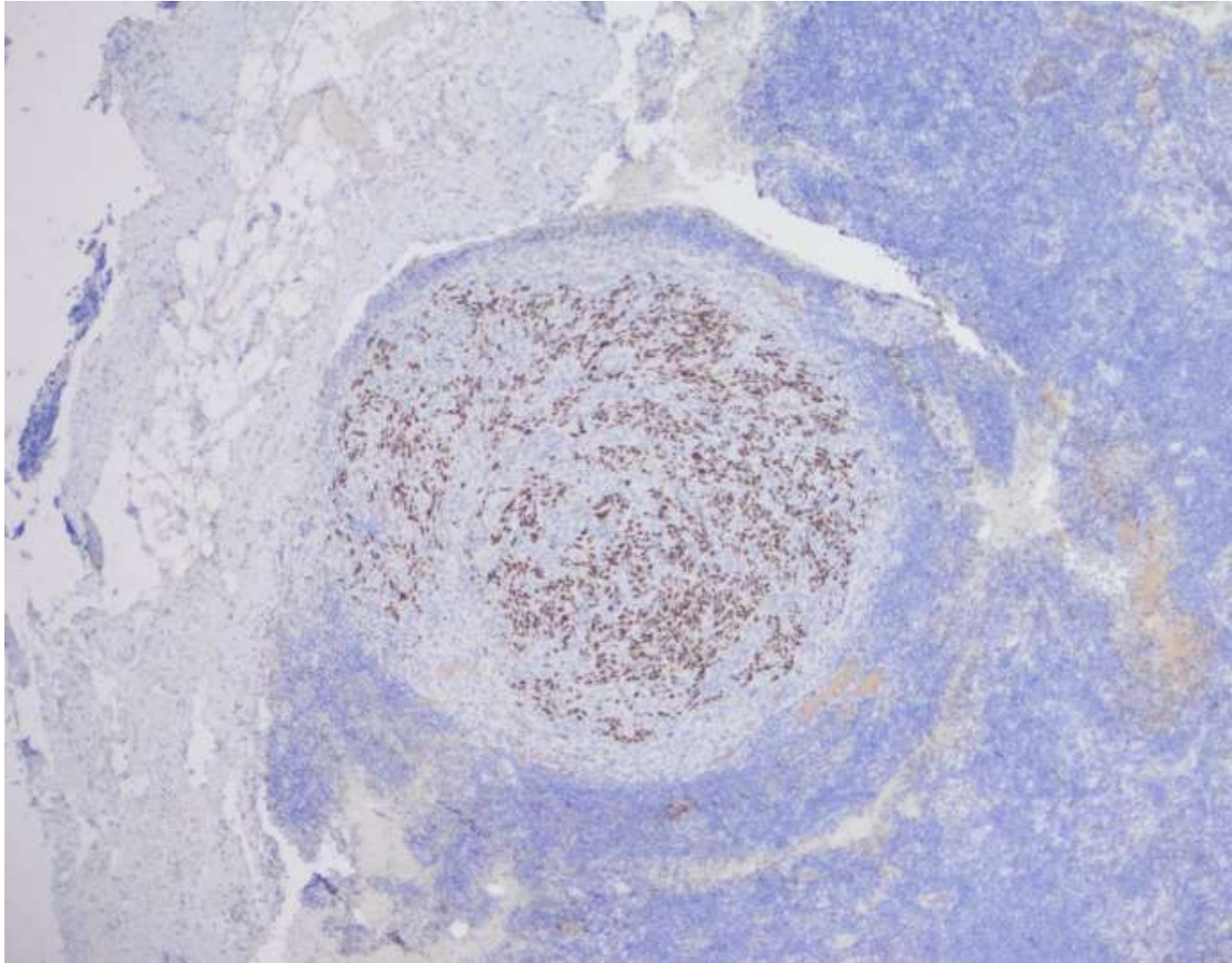




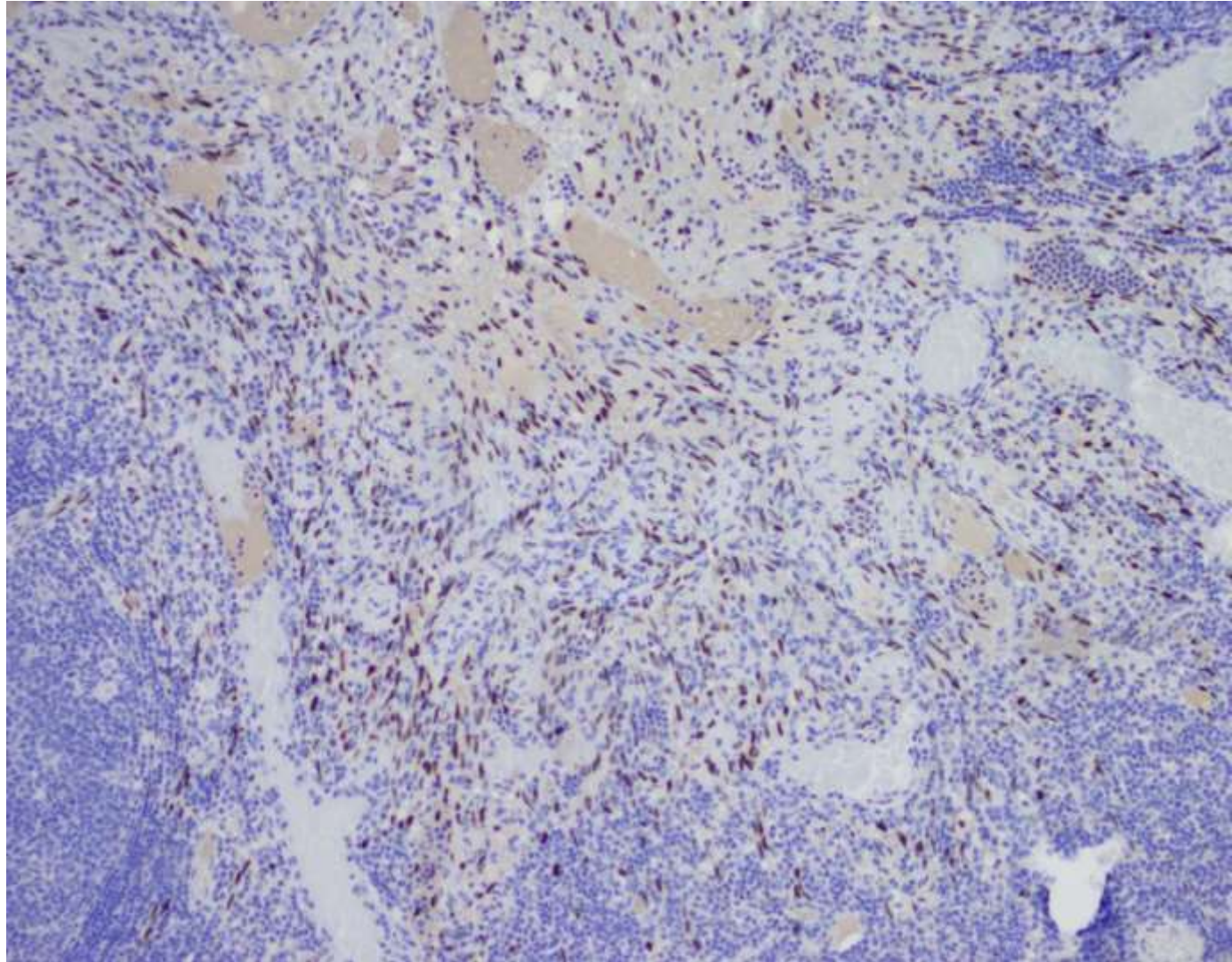








HHV8



Kaposi Sarcoma

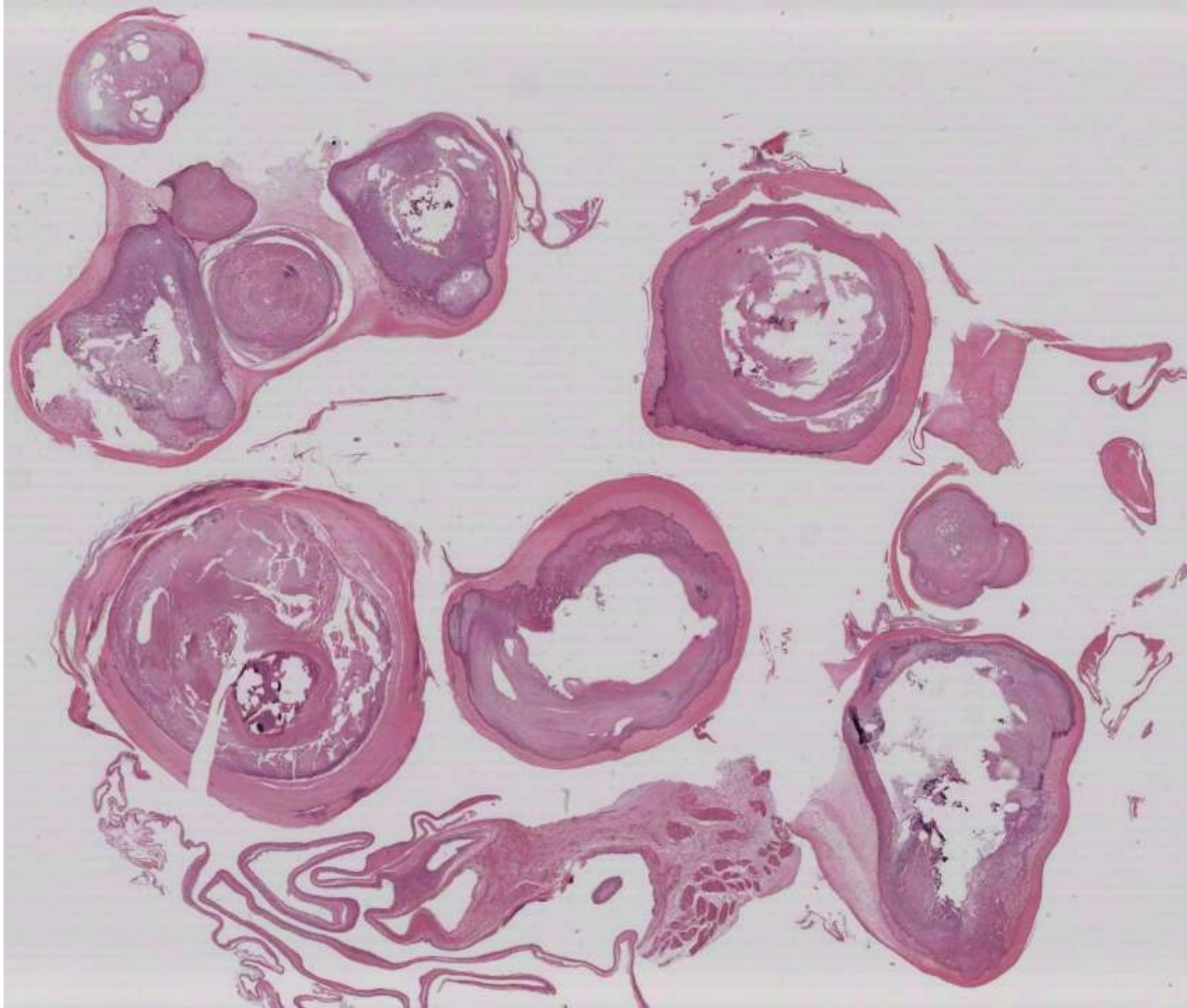
- Pt with excision and LN dissection for Merkel cell CA
- Incidental vascular lesion in LN
 - No history of KS
 - Patient not HIV+
 - Patient not of Mediterranean descent

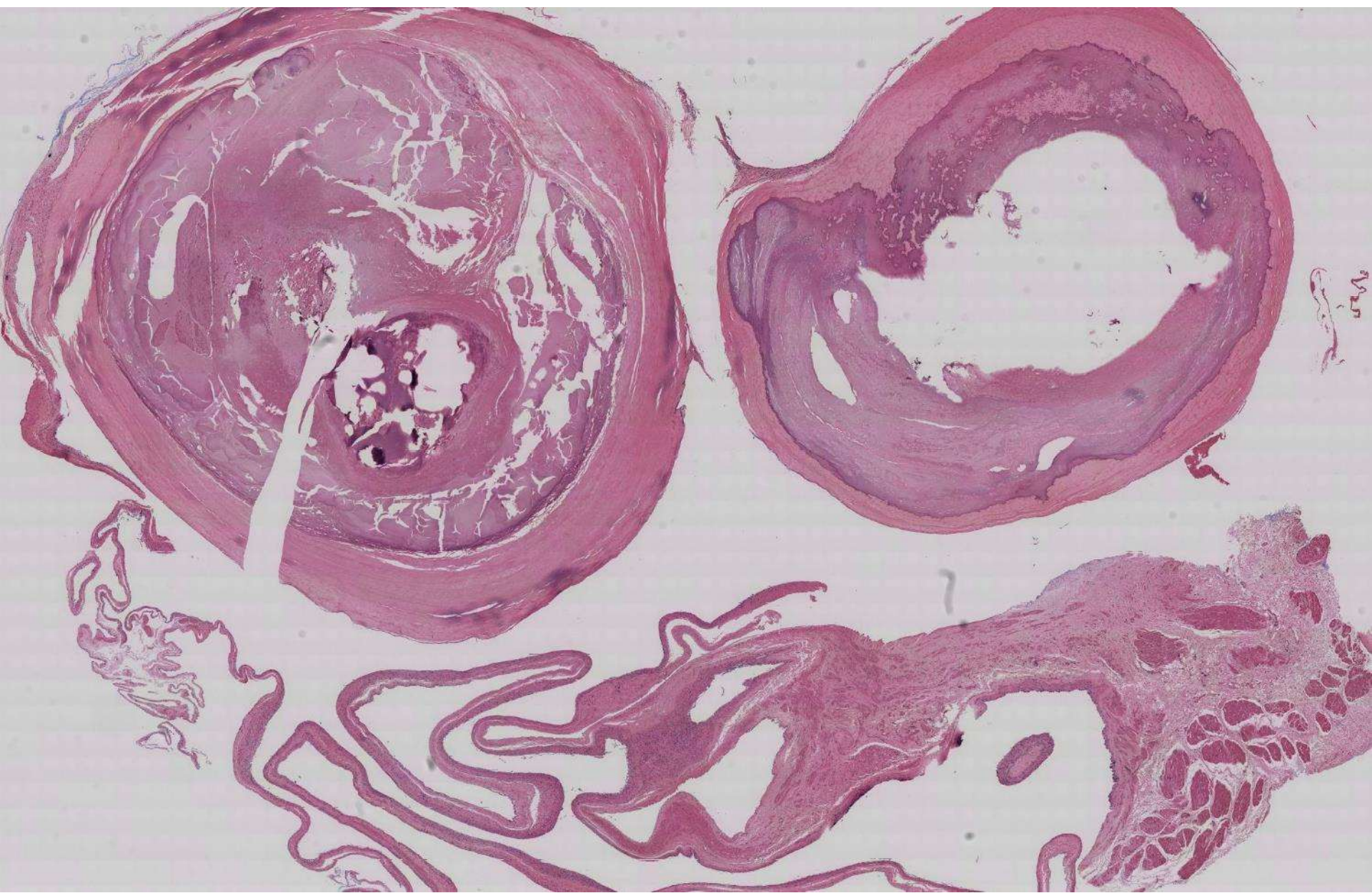
20-1002

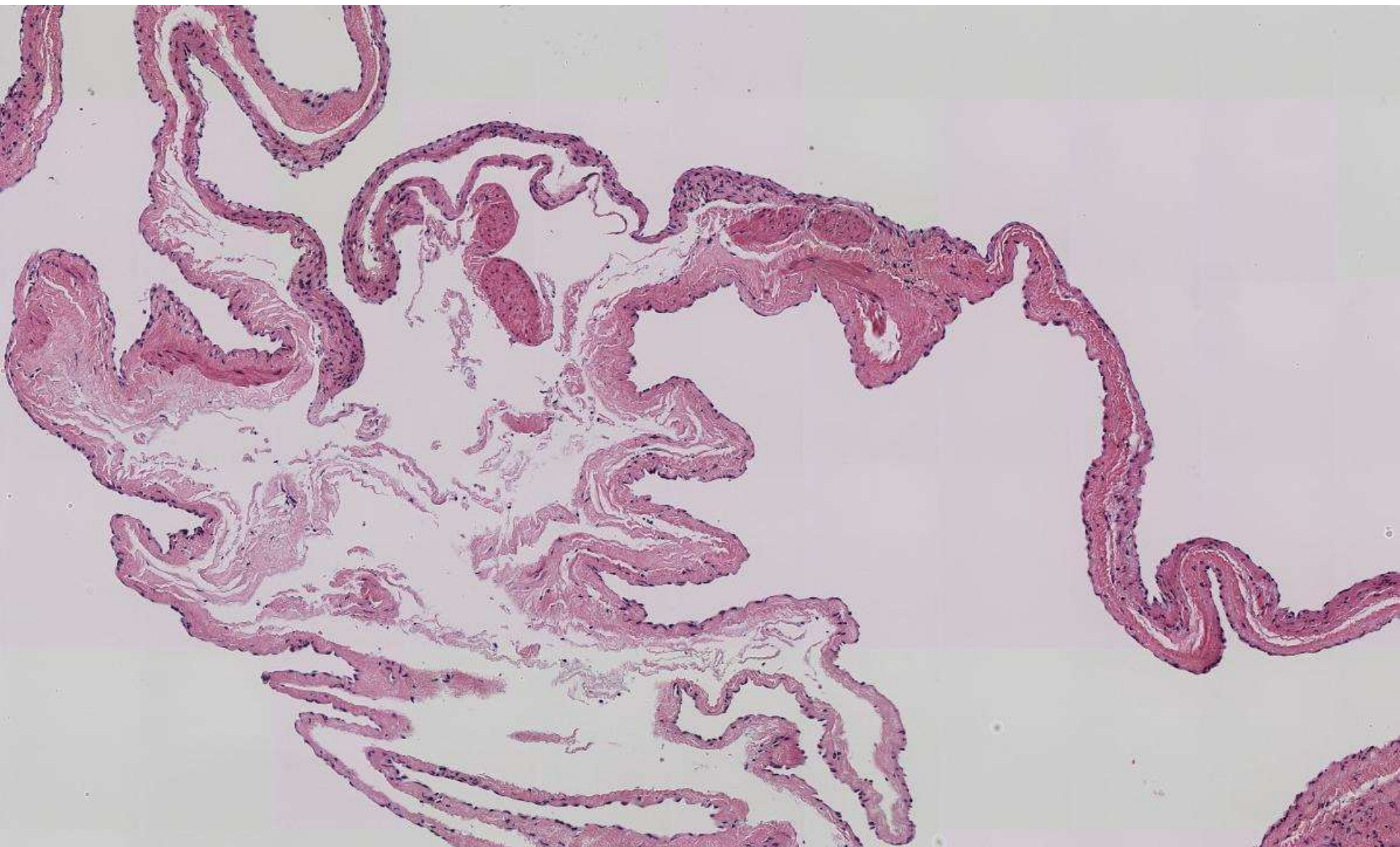
scanned slide available!

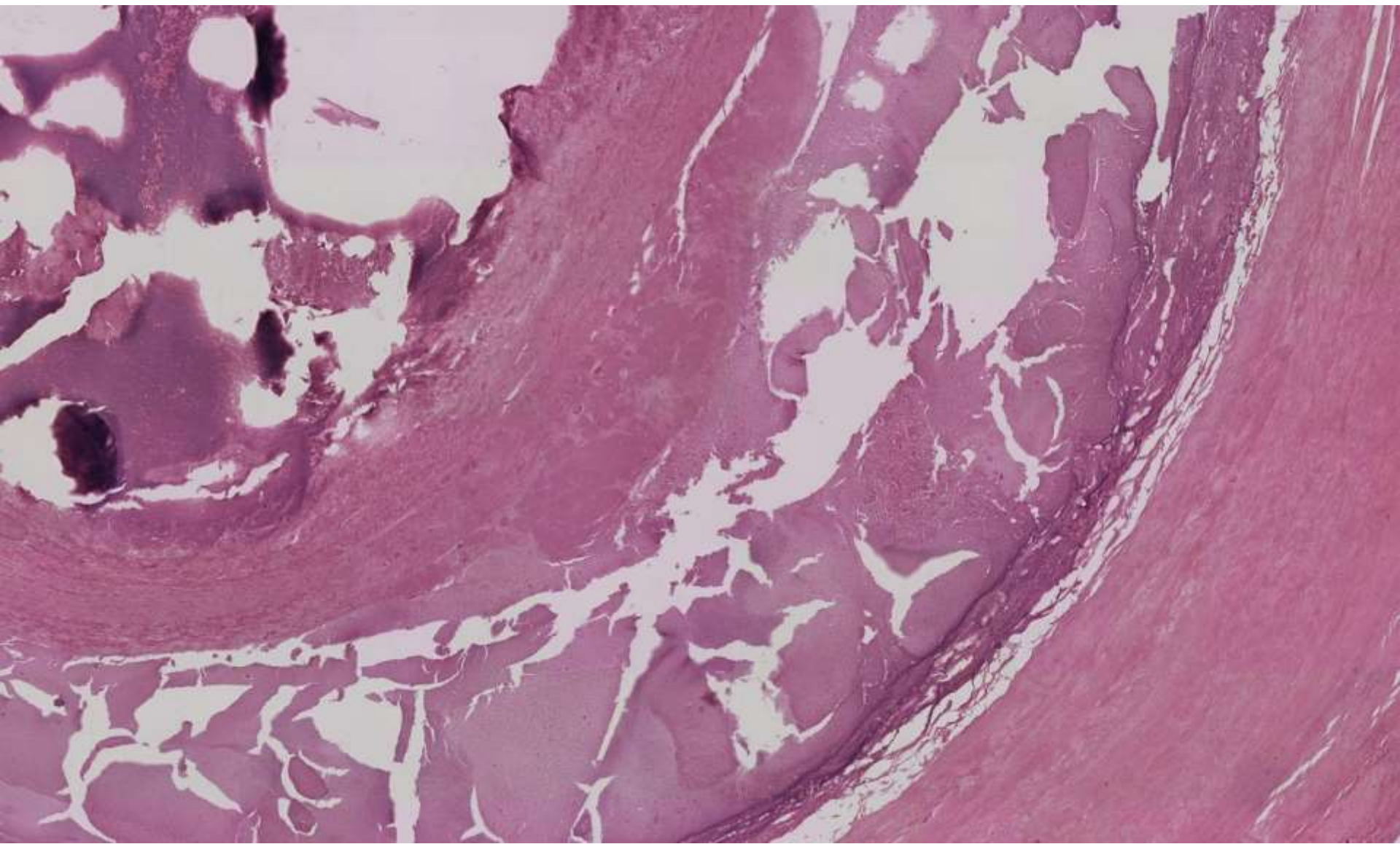
Natalie Patel; El Camino Hospital

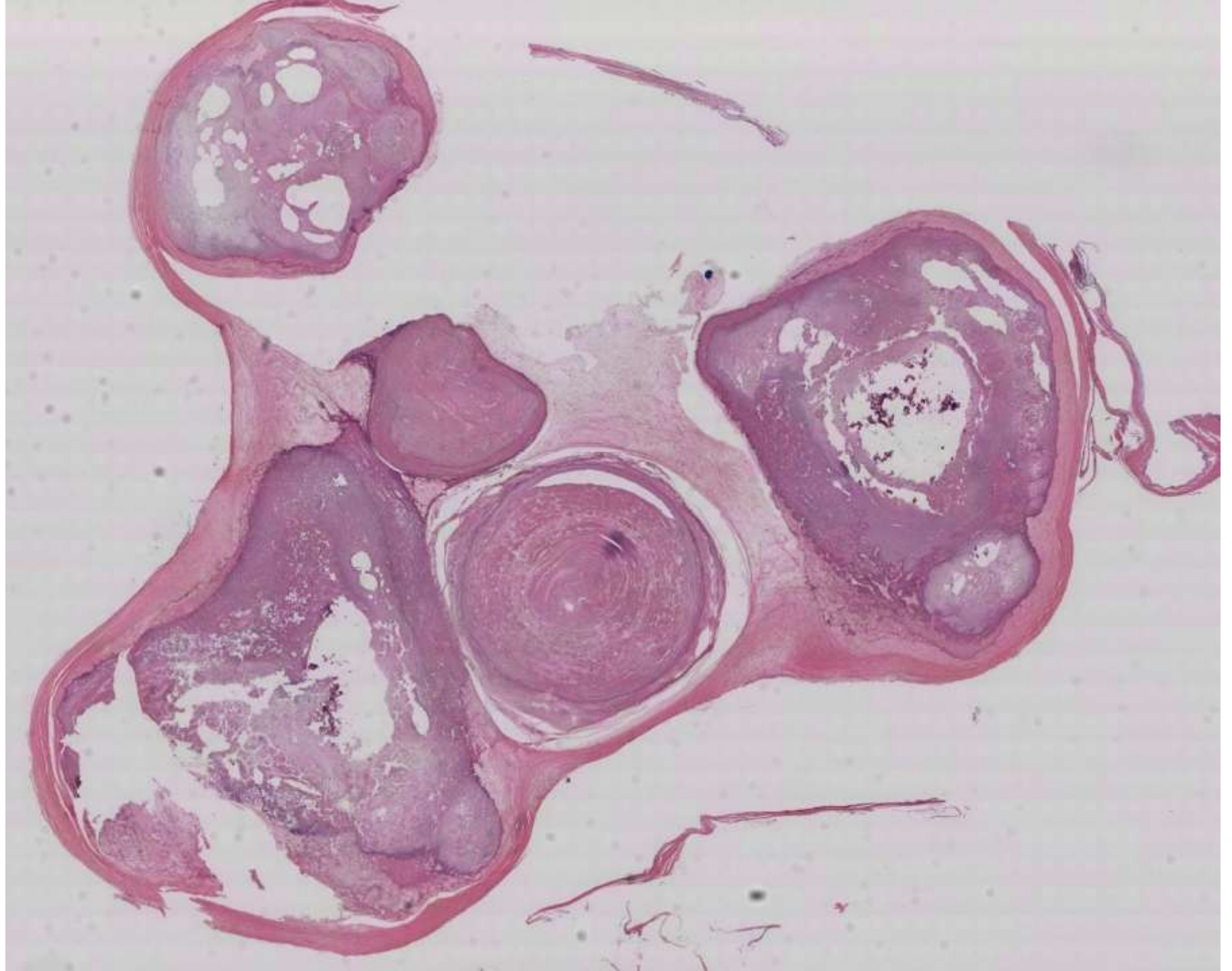
57-year-old M with right atrial mass, excised.

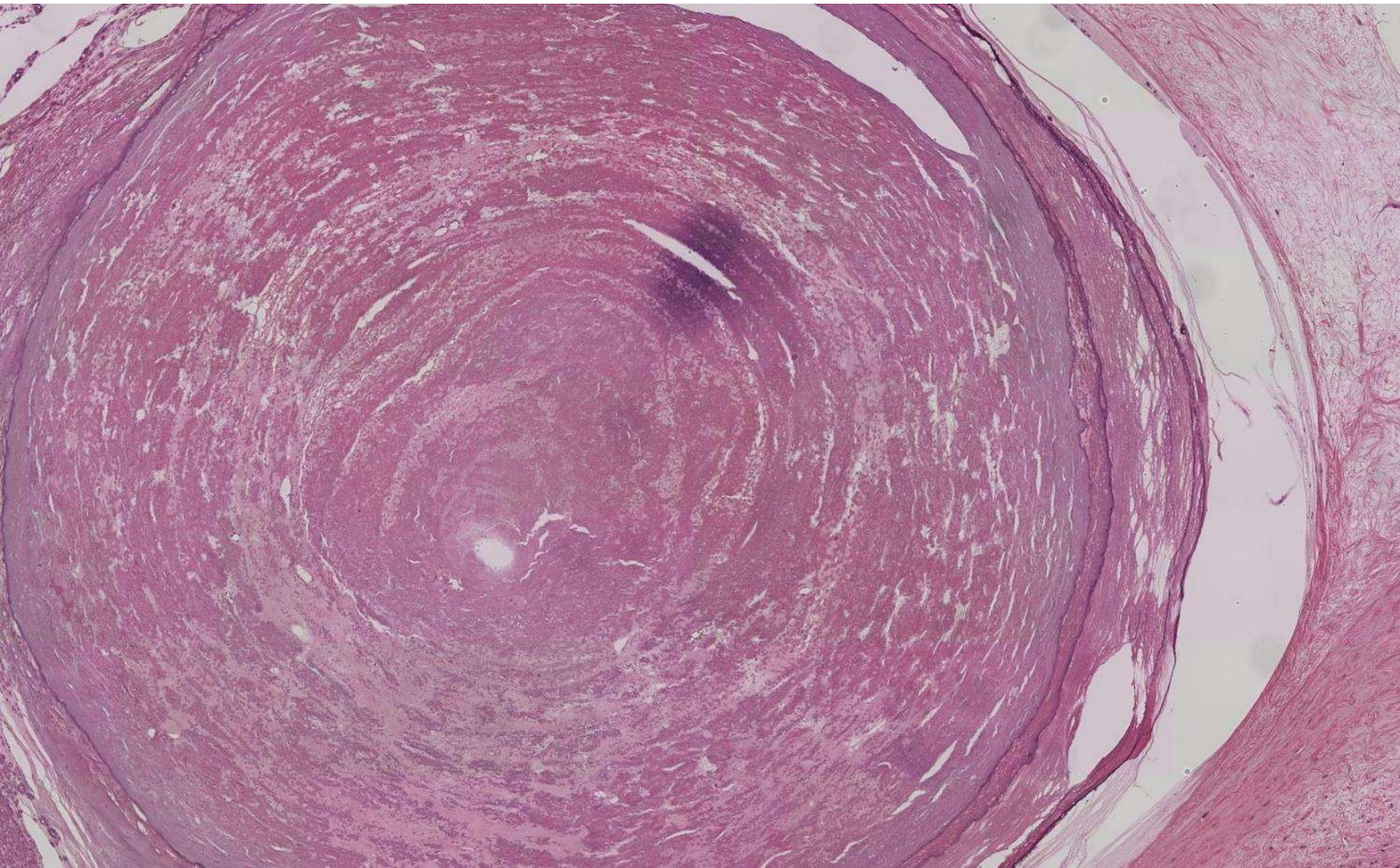


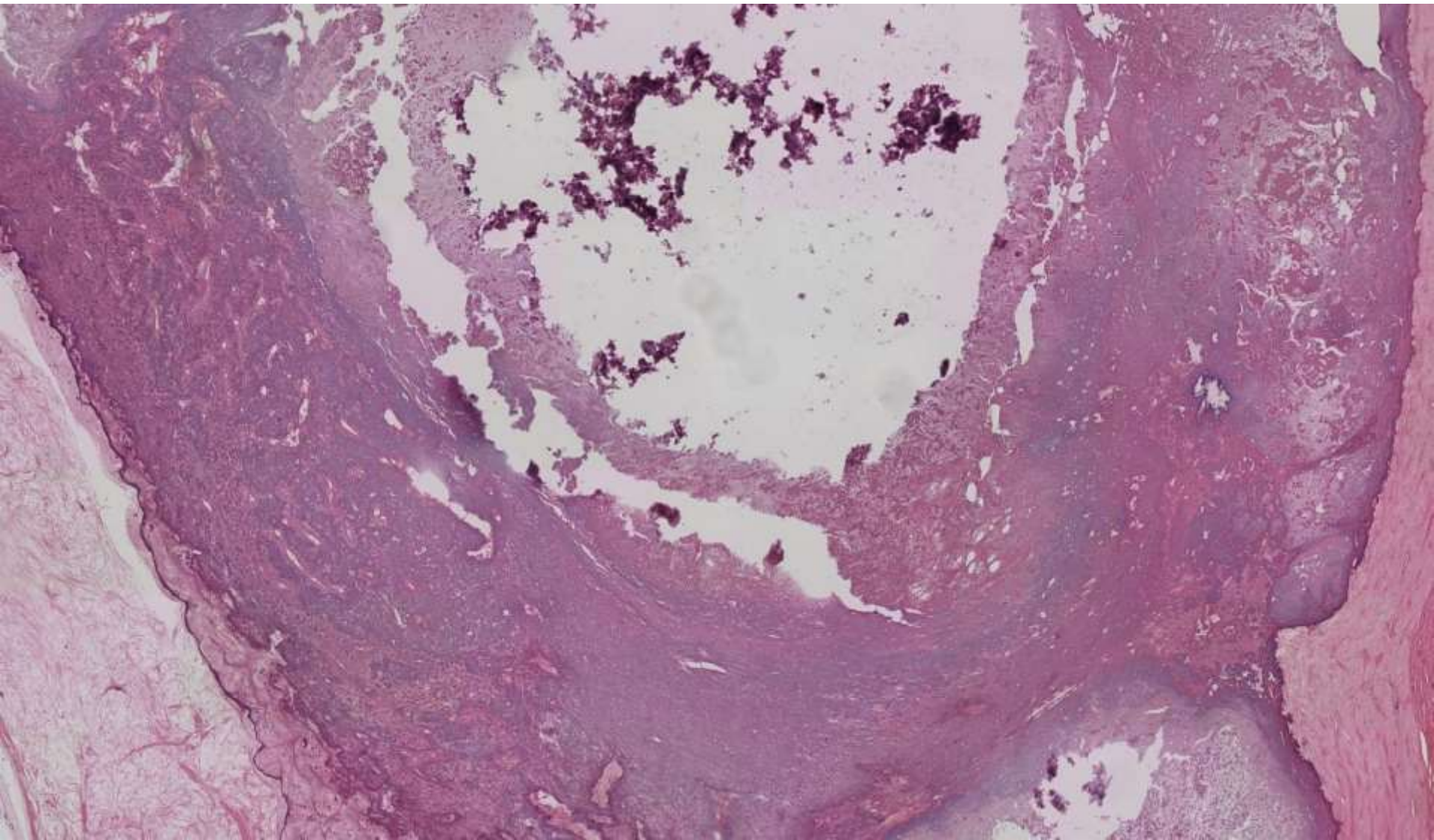


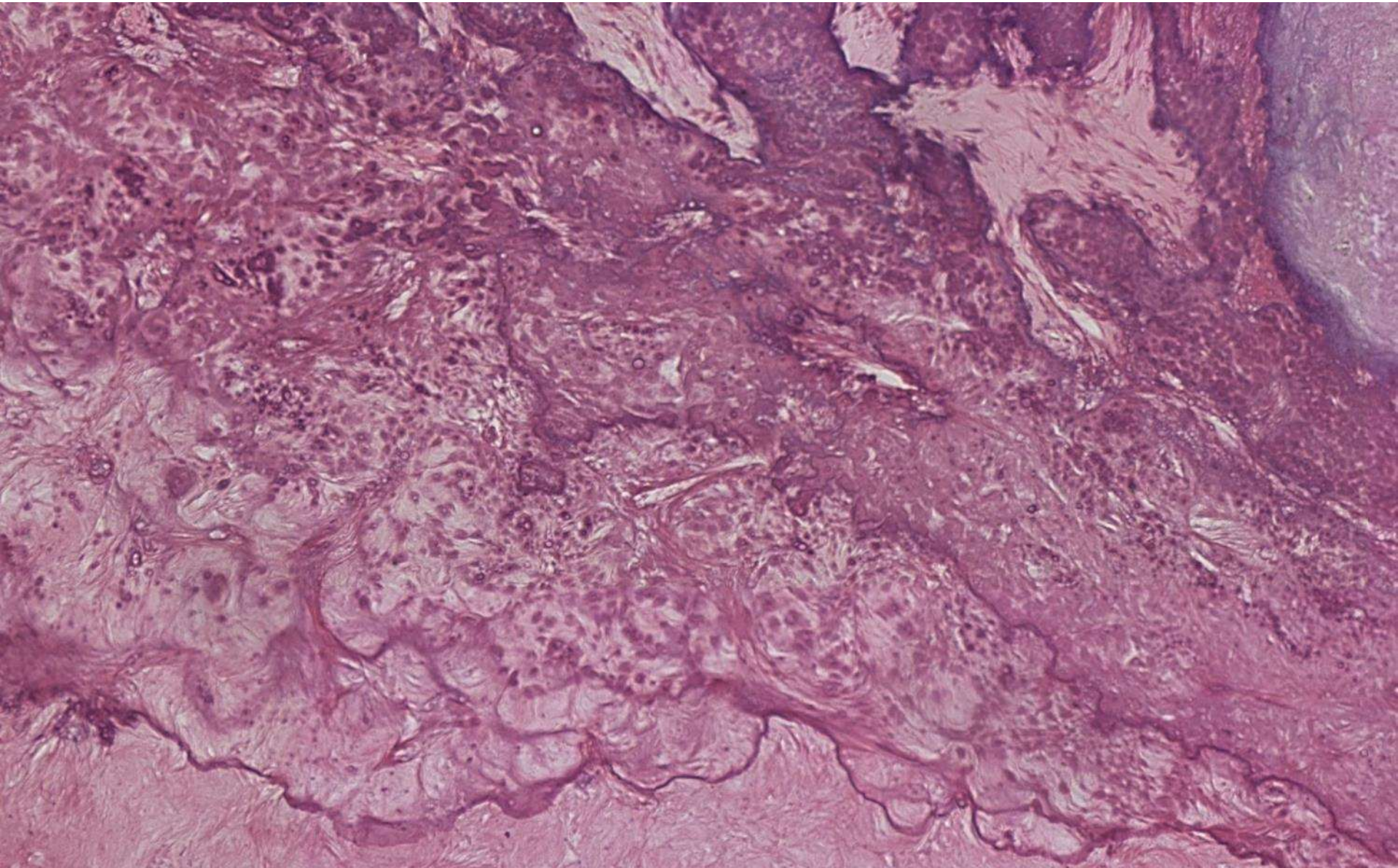












DDX

- Myxoma
- Calcified amorphous tumor
- Vegetation
- Fibroma
- Amyloid
- Thrombus

Clinical findings

- 57 y/o male, good health
- Diastolic murmur prompted TTE
- Runs 6 miles a day
- TTE – 2cm partially calcified mass in lower right atrium

CAT (pseudoneoplasm)

- Rare non-neoplastic intracavitary cardiac mass
- features = calcification and amorphous fibrinous material
- Described in 1997 by Reynolds and colleagues
- ~ 42 cases reported in the literature

Clinical characteristics

- Mean age: 54 (F>M)
- Intracavitary mass in all cardiac chambers
 - MV or annulus (36%)
 - RA (21%)
 - RV (17%)
 - Rare diffuse LV infiltration
- Mean size: 2.9cm (1.7mm-9cm)
- Symptoms: dyspnea (45%)>syncope>PE or systemic emboli > incidental (17%)

Etiology

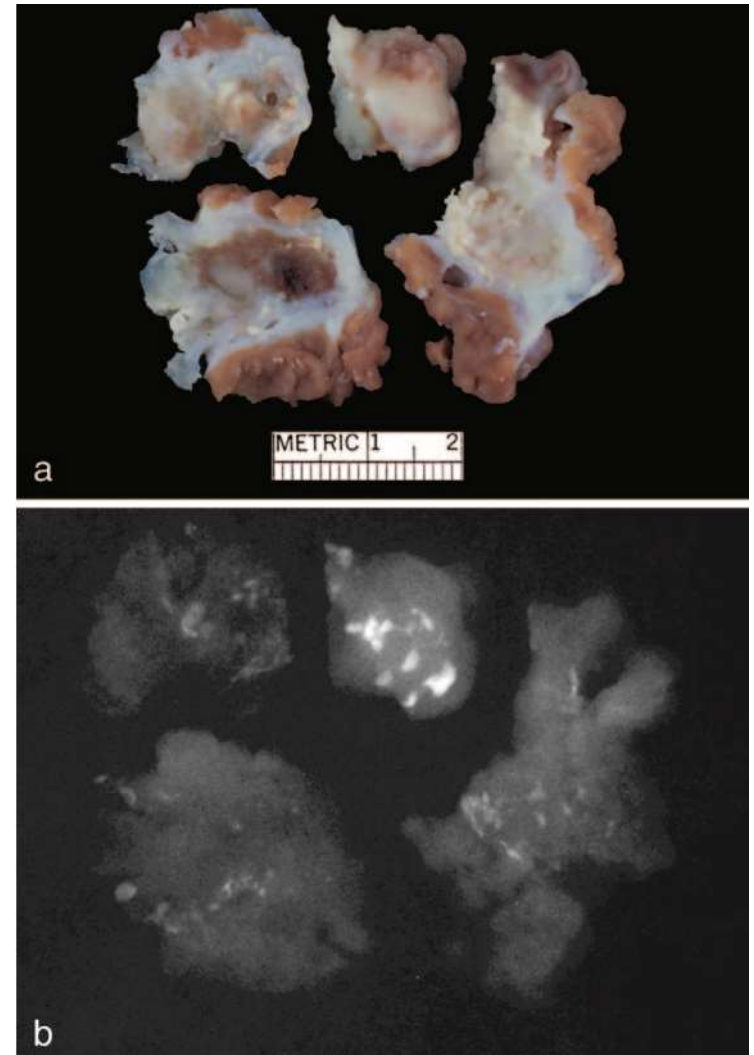
- Hypotheses:
 - Organized thrombus origin favored by hypercoagulability
 - And/or phosphocalcic metabolism abnormalities
- Tumor growth unclear
 - Spans 6 wk – 1 yr

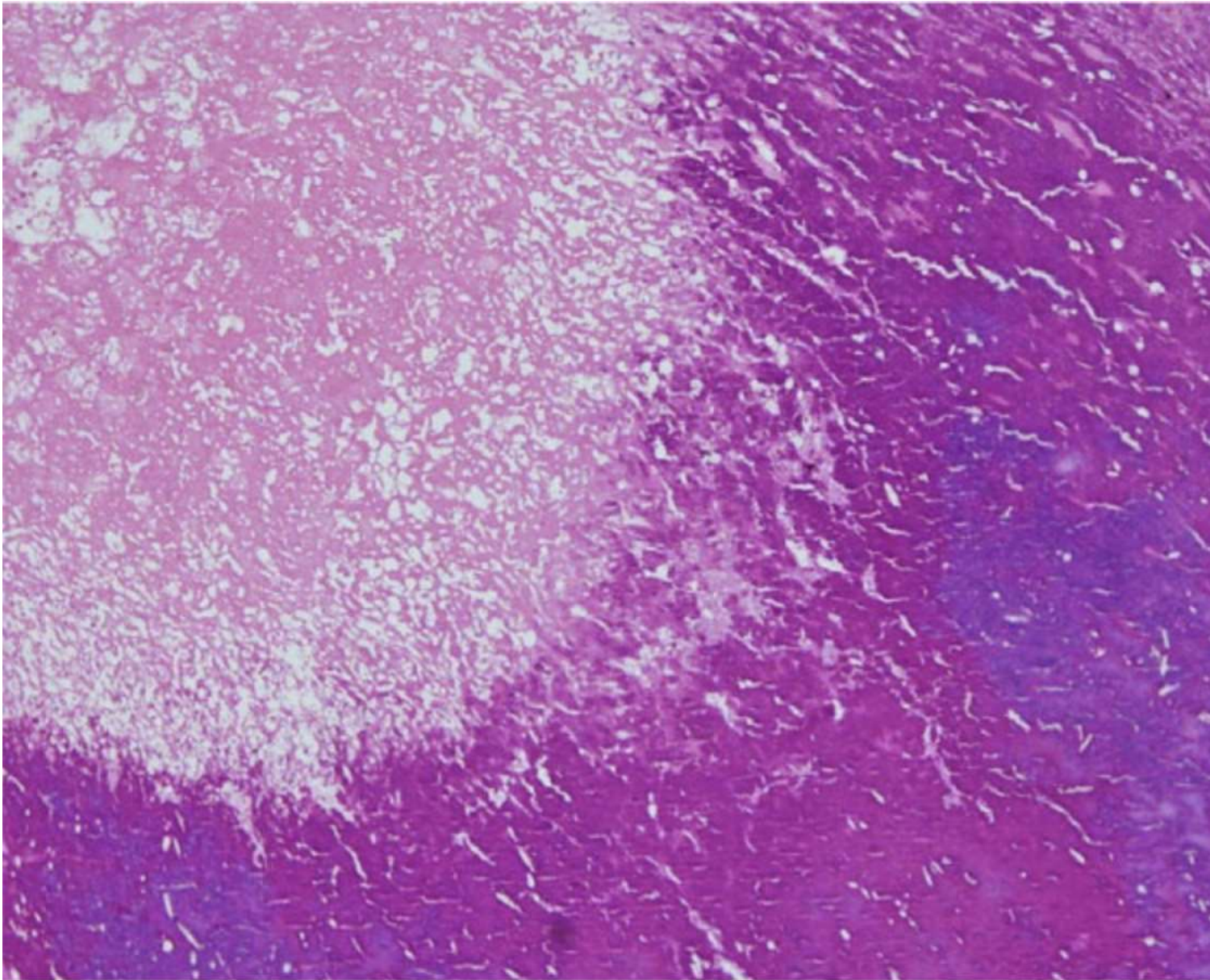
Imaging

- Can not differentiate cardiac CAT from other masses
- On echo:
 - Appears as a calcified mass
 - Size can vary from small punctate lesions to very large masses.
 - Rarely, diffuse LV myocardial infiltrations
- DDX on imaging: osteosarcoma, calcified myxoma or vegetations

Pathology

- Degenerating fibrin with variable/central, nodular calcium deposits
- Rare osseous metaplasia has been described
- Mild to moderate chronic inflammation, especially near the base of the lesion, +/-, capillaries may also be present
- Organization, hemosiderin deposition and cholesterol clefts typically absent
- Resemble noninfectious thrombotic endocarditis
- Nodular calcium deposits surrounded by an amorphous hyalinized material





Gupta, R., Hote, M. and Ray, R., 2010. Calcified amorphous tumor of the heart in an adult female: a case report. *Journal of medical case reports*, 4(1), p.278.

Treatment

- Surgical resection
- Recurrence is rare

Summary

- CAT = pseudoneoplasm
- Any heart chamber, most commonly MV or annulus
- Nodular deposits or flecks of calcium
- Background of eosinophilic, amorphous, sometimes fibrillary material

References

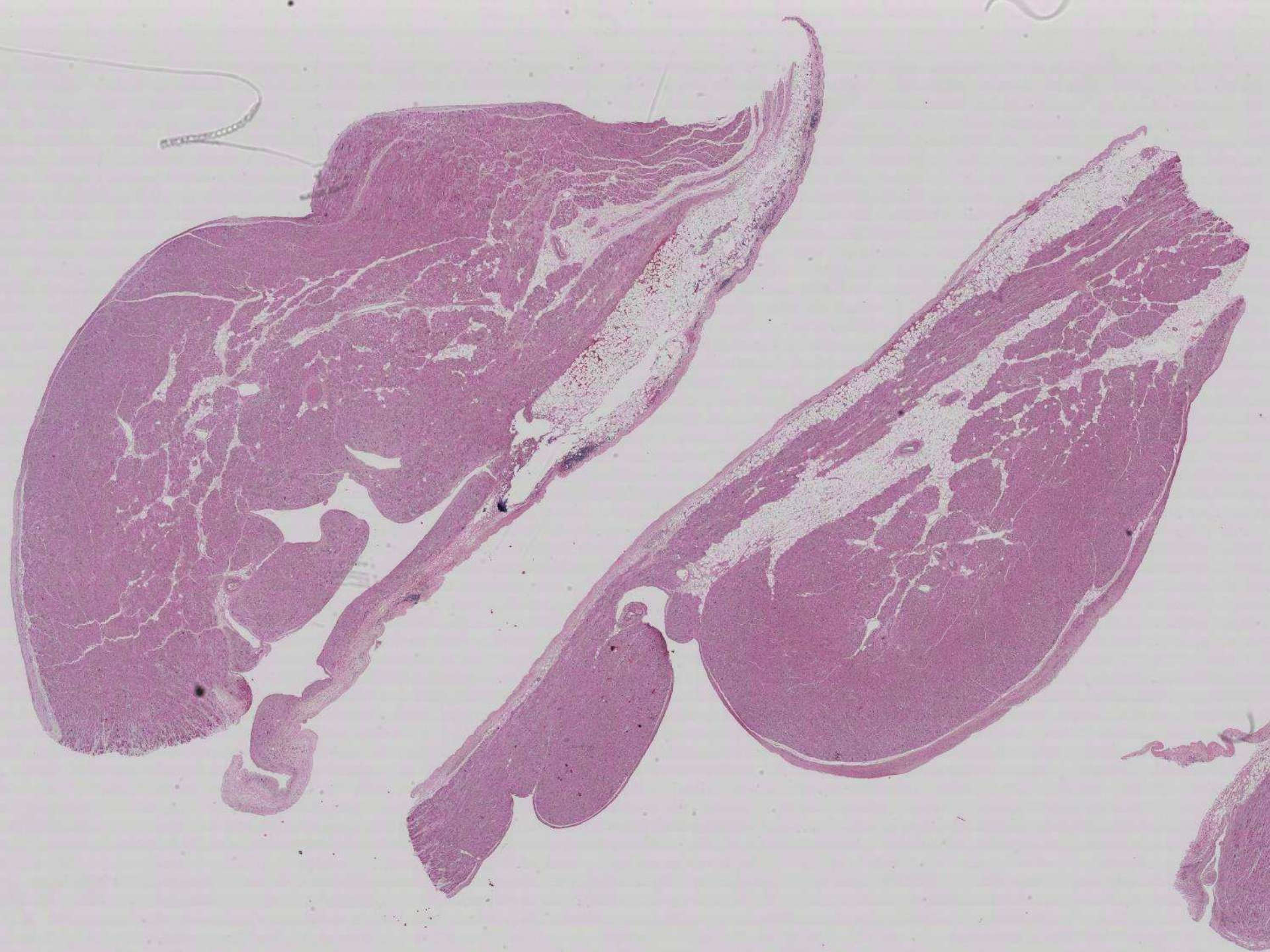
- Reynolds C., Tazelaar H.D., Edwards W.D. Calcified amorphous tumor of the heart (cardiac CAT) Hum Pathol. 1997;28:601–606.
- Vlasseros I., Katsi V., Tousoulis D., Tsiachris D., Bousiotou A., Souretis G. Visual loss due to cardiac calcified amorphous tumor: a case report and brief review of the literature. Int J Cardiol. 2011;152:e56–e57.
- Miller D.V., Tazelaar H.D. Cardiovascular pseudoneoplasms. Arch Pathol Lab Med. 2010;134:362–368.
- Hussain N., Rahman N., Rehman A. Calcified amorphous tumors (CATs) of the heart. Cardiovasc Pathol. 2014

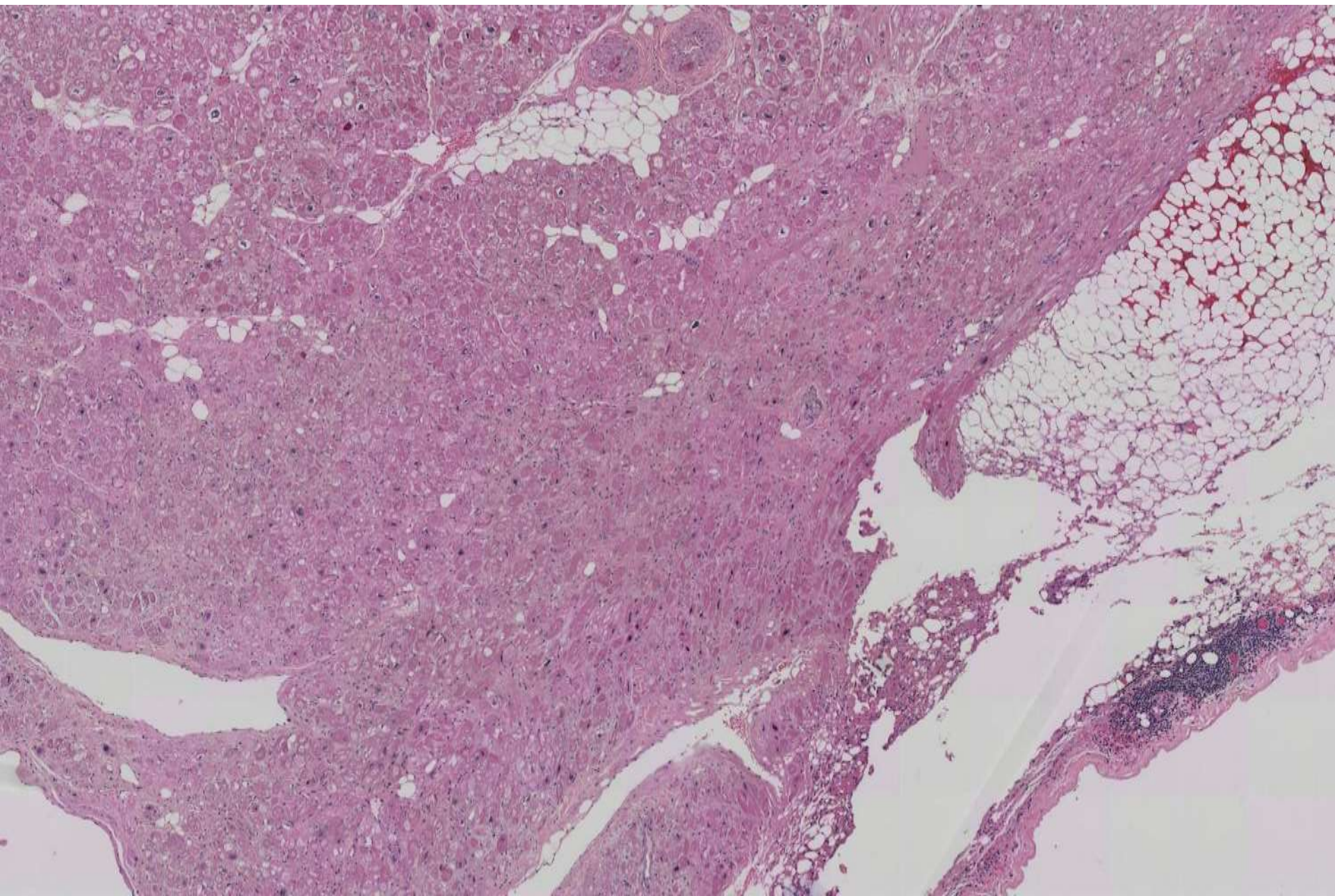
20-1003

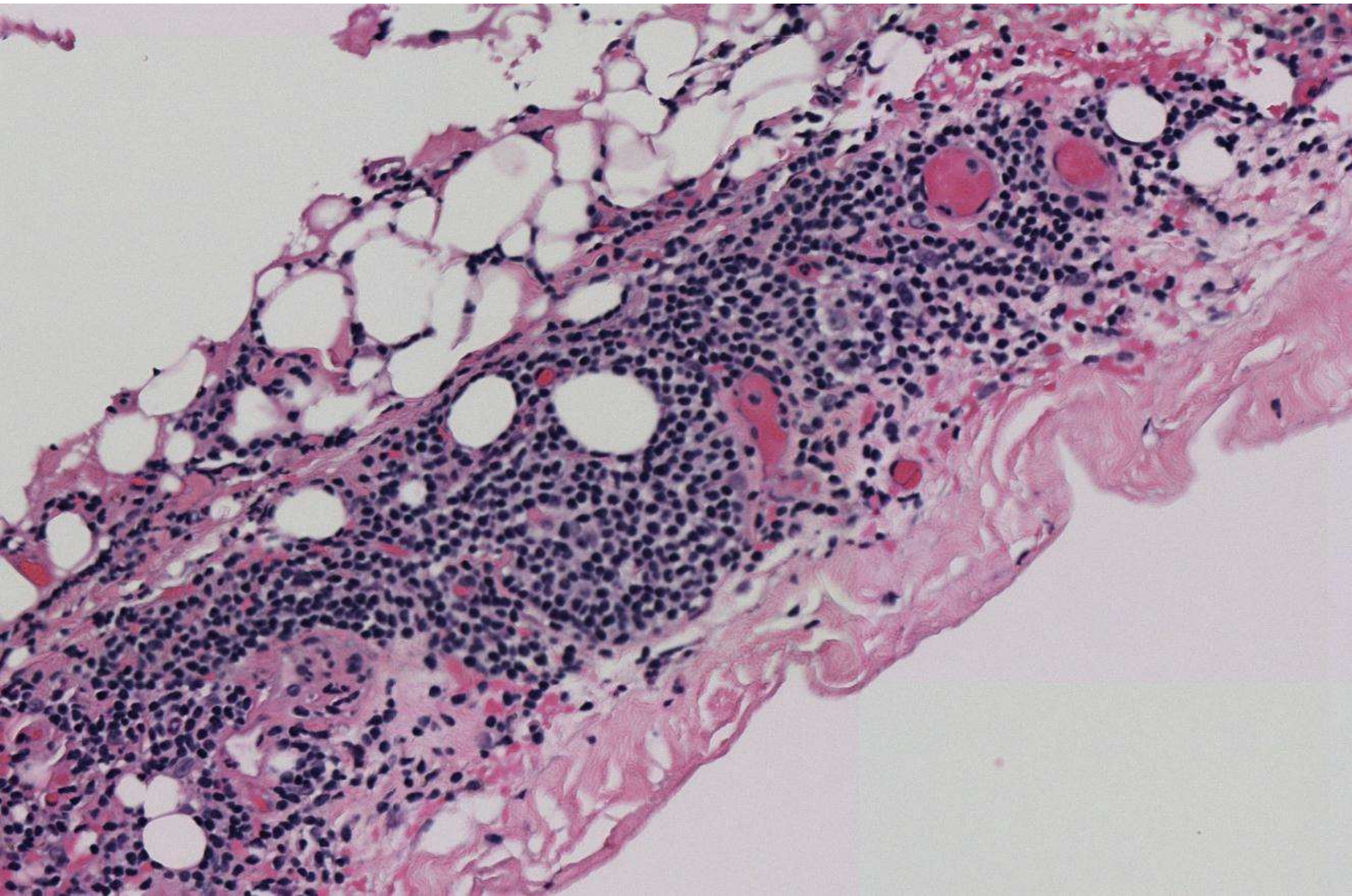
scanned slide available!

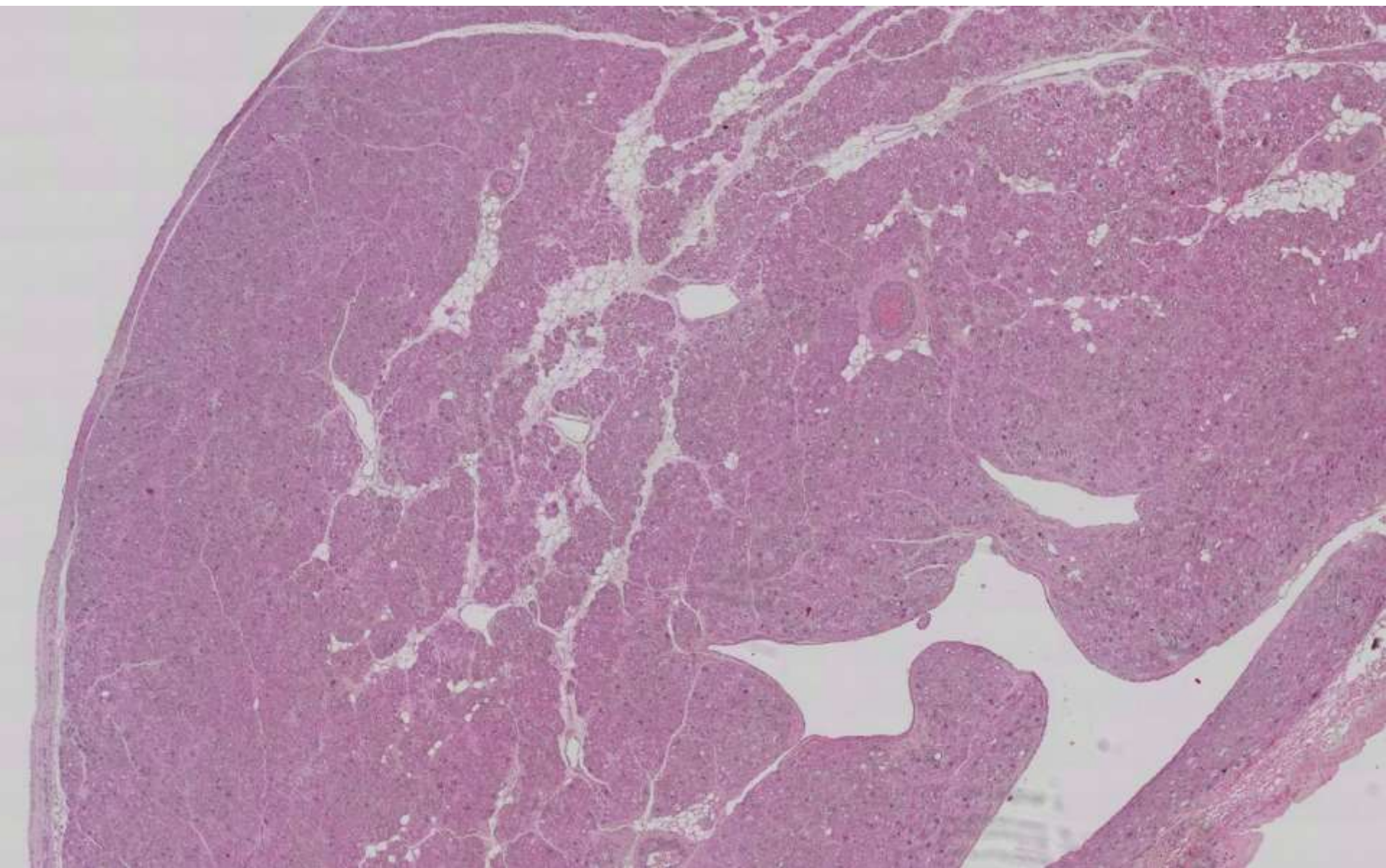
Ankur Sangoi; El Camino Hospital

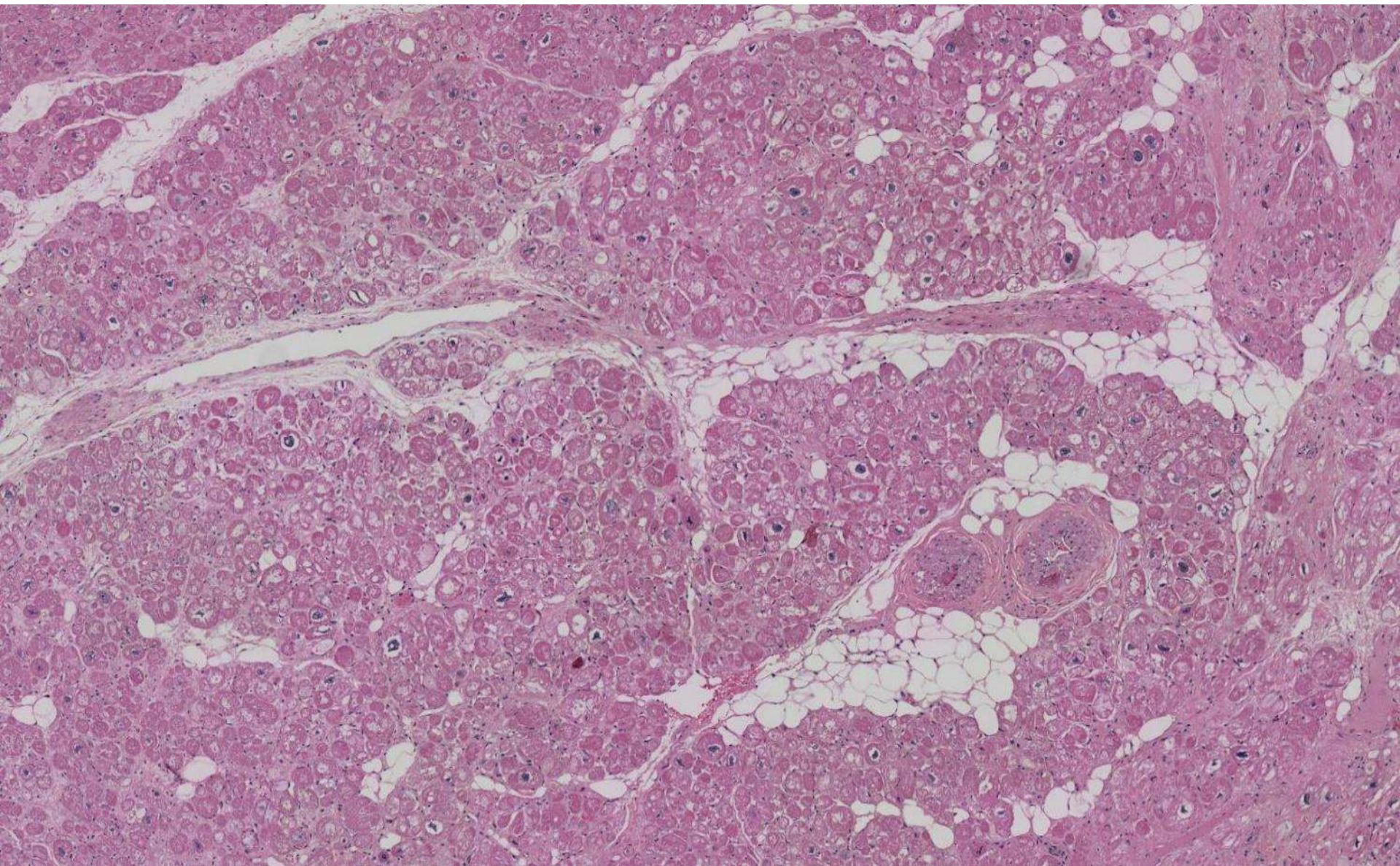
71-year-old M undergoes ascending aorta repair and right atrial resection (latter submitted).

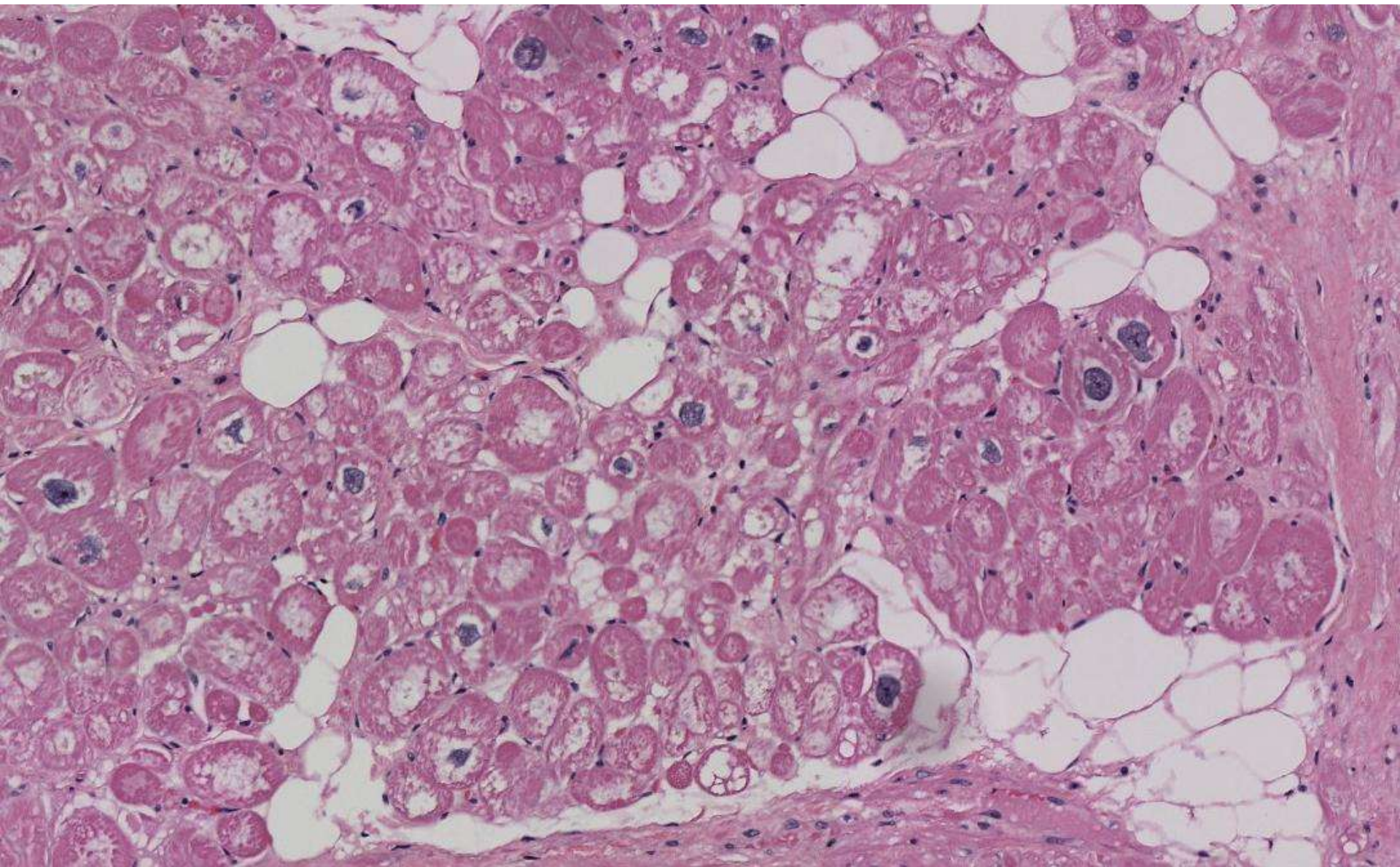


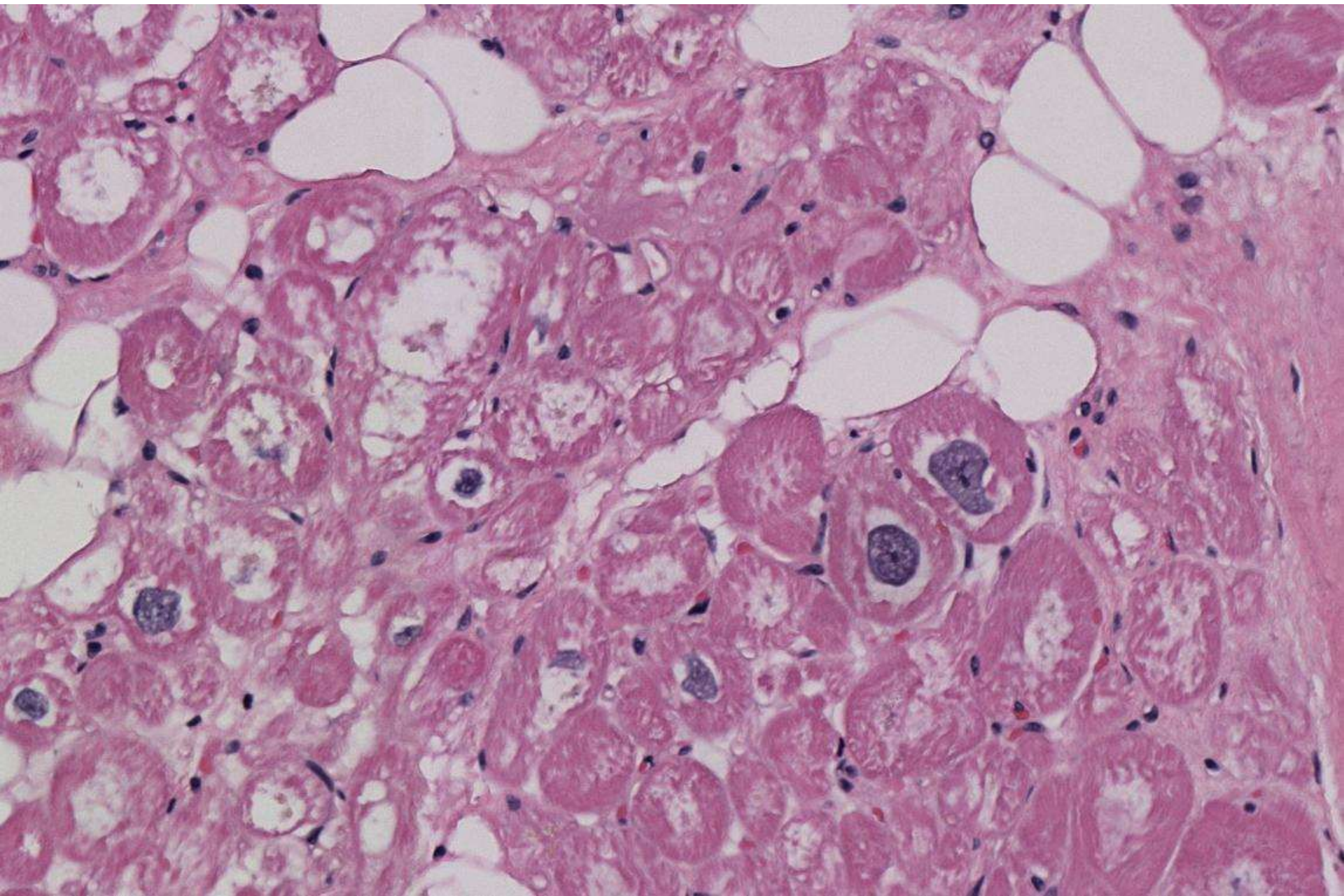


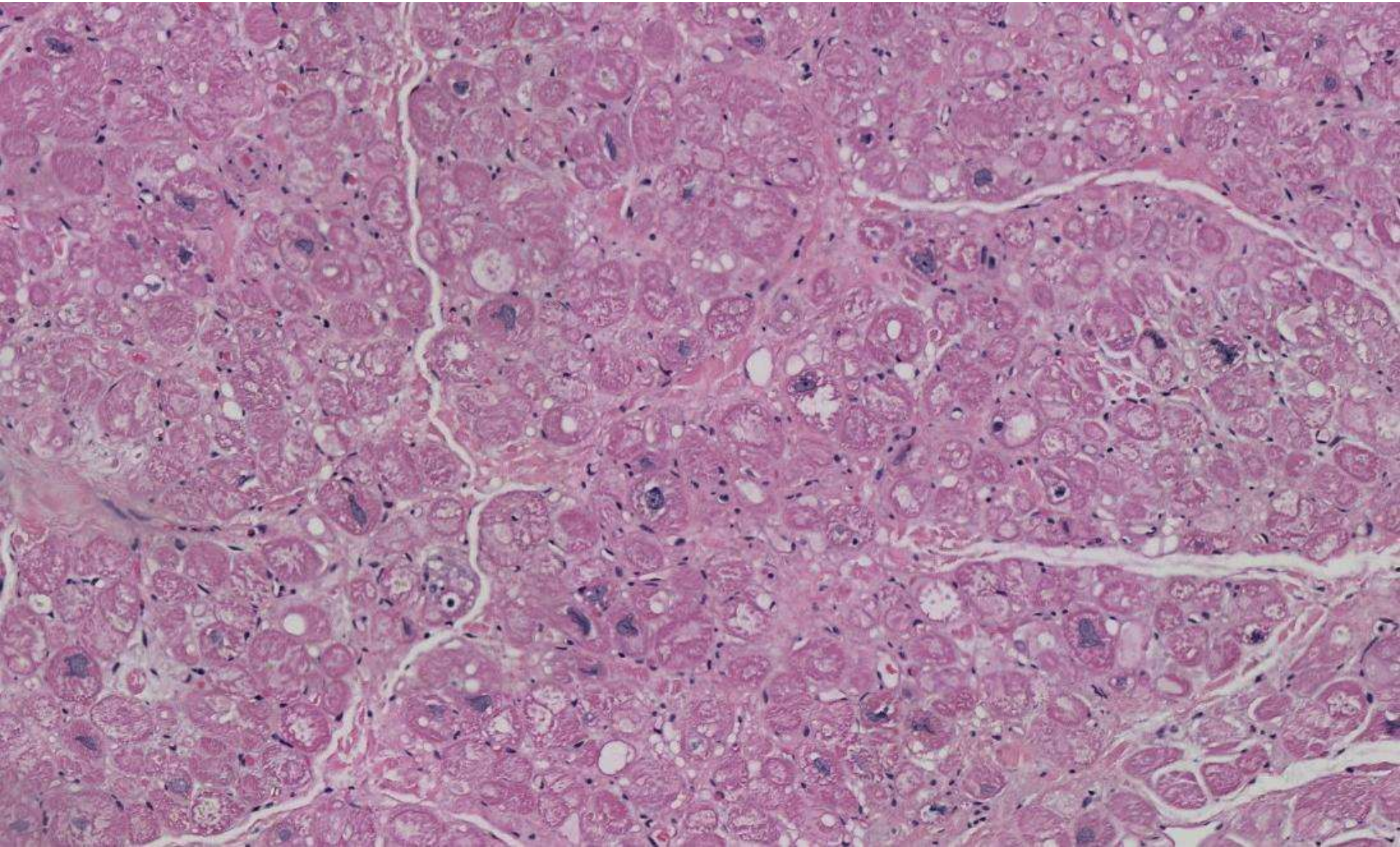


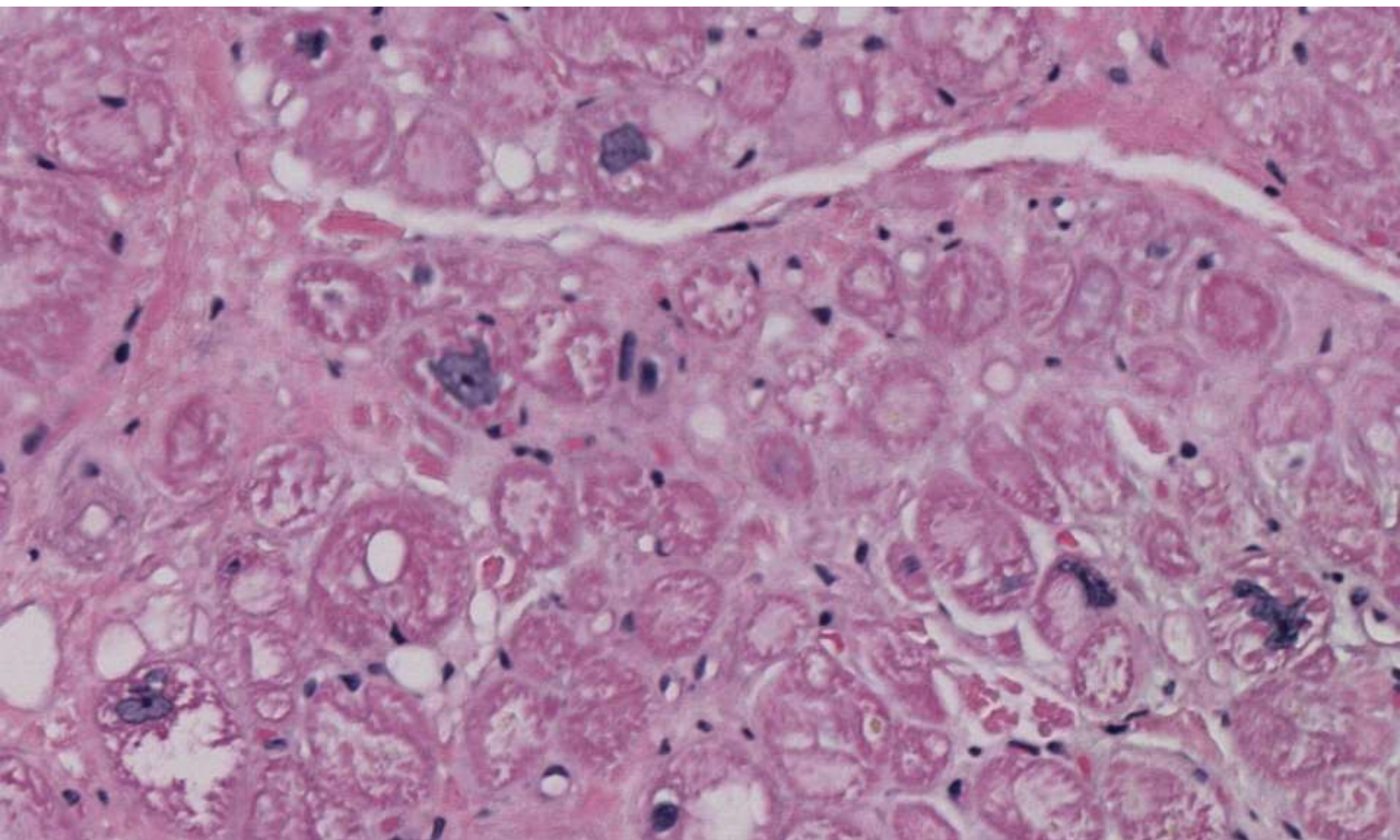








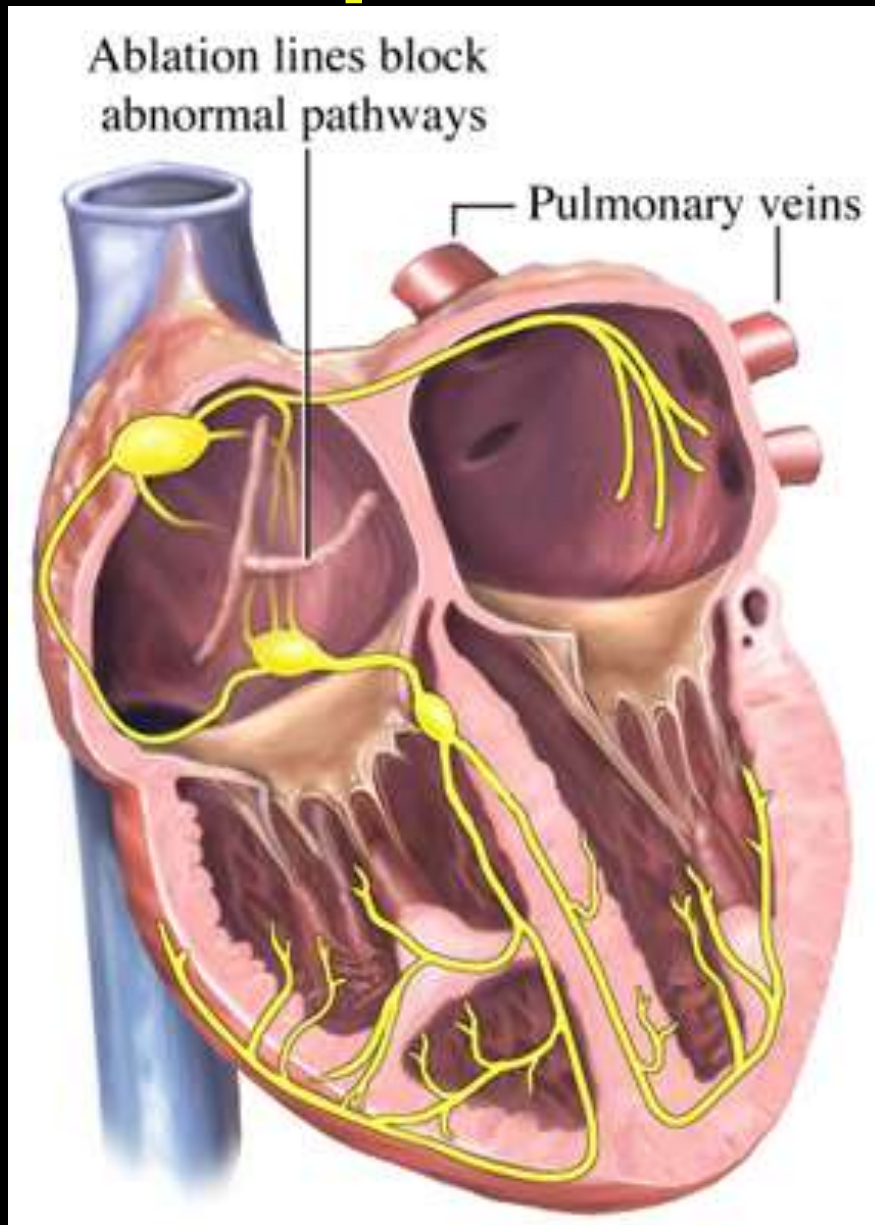




Final Dx

- **Atrial appendage, Maze procedure**
 - Myocyte hypertrophy, vacuolation, fatty infiltration
 - Secondary to h/o Afib

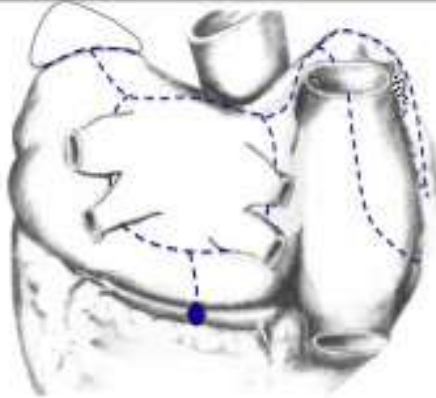
Maze procedure



Many Patterns but only one Principle

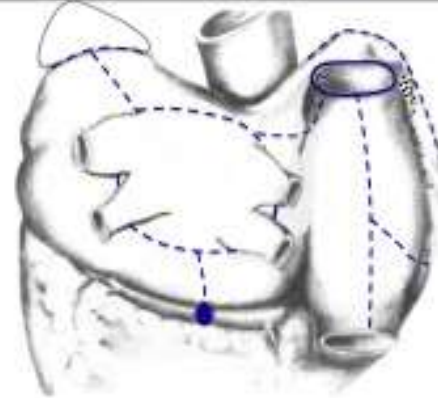
A

Maze-I Procedure



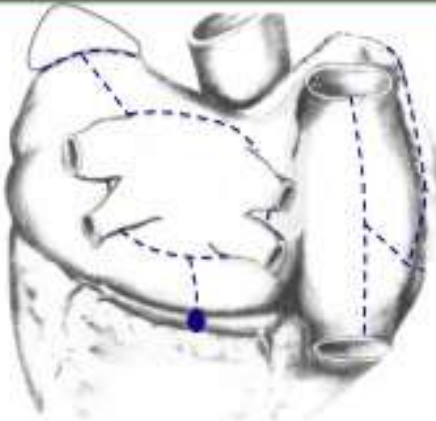
B

Maze-II Procedure



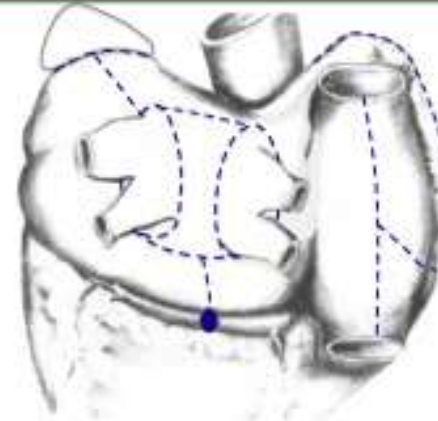
C

Maze-III Procedure



D

Maze-IV Procedure



KEY: lines of conduction blocked that preclude macro-reentry anywhere in either atrium while leaving both atria capable of activation by a sinus-generated impulse

Surgical Pathology of Atrial Appendages Removed During the Cox-Maze Procedure

A Review of 86 Cases (2004 to 2005) With Implications For Prognosis

Mathieu C. Castonguay, MD, Yinong Wang, MD,† Jacqueline L. Gerhart, MD,‡
Dylan V. Miller, MD,§ John M. Stulak, MD,|| William D. Edwards, MD,*
and Joseph J. Maleszewski, MD**

Abstract: Atrial fibrillation (AF) is the most common sustained cardiac arrhythmia. Some patients are managed surgically (Cox-maze procedure) with removal of 1 or both atrial appendages. A retrospective review was performed on surgically excised atrial appendages from 86 consecutive patients with AF (2004 to 2005), at Mayo Clinic in Rochester, MN. These were compared with atrial appendages removed from 2 autopsy control groups without a history of AF (26 without heart disease, and 20 with heart disease). Compared with the 2 control groups, appendages from patients with AF contained more myocyte vacuolization, fatty infiltration, and myocardial inflammation. Among the AF patients, left atrial appendages (LAA) were larger and more likely to show fatty infiltration, endocardial fibroelastosis, and mural thrombus than were right atrial appendages (RAA); in contrast, RAA were more likely to show myocyte hypertrophy and interstitial fibrosis than were LAA. In the LAA, myocyte hypertrophy and interstitial fibrosis were more often seen in patients with long-term AF recurrence than were those who remained in normal sinus rhythm postoperatively ($P = 0.045$ and 0.036 , respectively). Given the potential clinical relevance of these findings, it is recommended that the presence or absence of hypertrophy and fibrosis, and their extent, be incorporated into the surgical pathology report of all patients undergoing resection of an atrial appendage.

Key Words: atrial fibrillation, maze procedure, atrial appendages, arrhythmia, surgical pathology

(*Am J Surg Pathol* 2013;37:890–897)

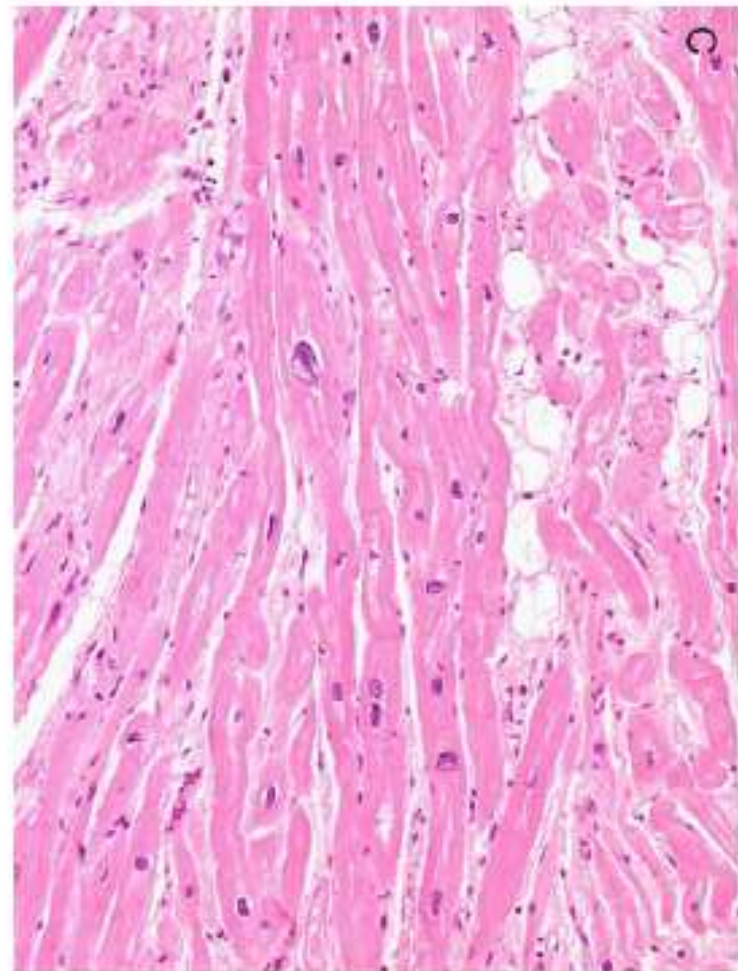


TABLE 3. Histopathologic Features in Patients With AF

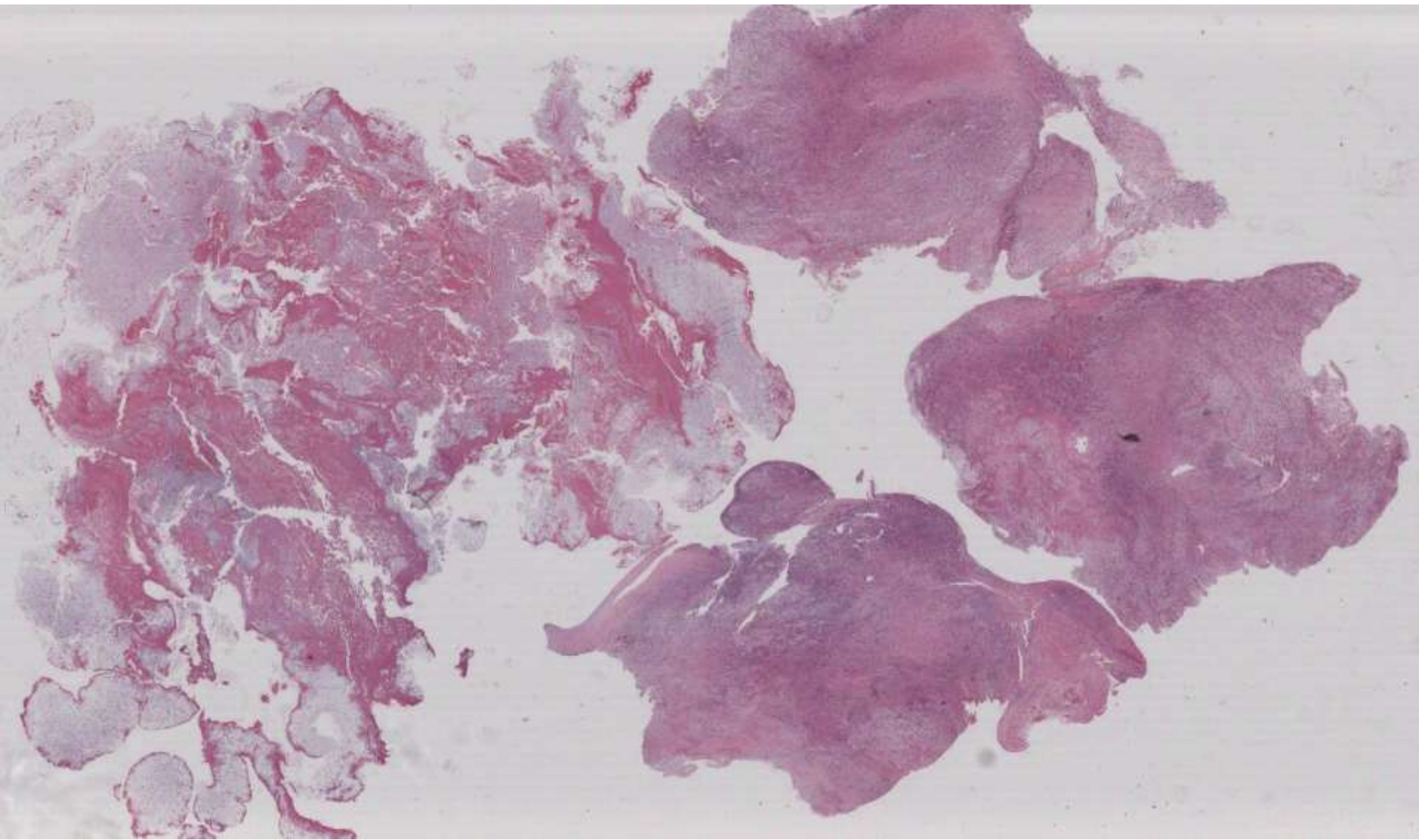
	RAA (n = 74)	LAA (n = 69)	<i>P</i>
Myocyte hypertrophy, moderate or marked	37	21	0.0173
Myocardial interstitial fibrosis	62	45	0.0029
Myocardial fatty infiltration	35	50	0.0329
EFE	39	48	0.039
Mural thrombus	2	9	0.0204
Myocyte vacuolization	31	27	>0.05
Inflammation			
Epicardial	53	46	>0.05
Myocardial	20	18	>0.05
Endocardial	3	3	>0.05
Amyloid	10	8	>0.05
Myocyte iron	1	1	>0.05

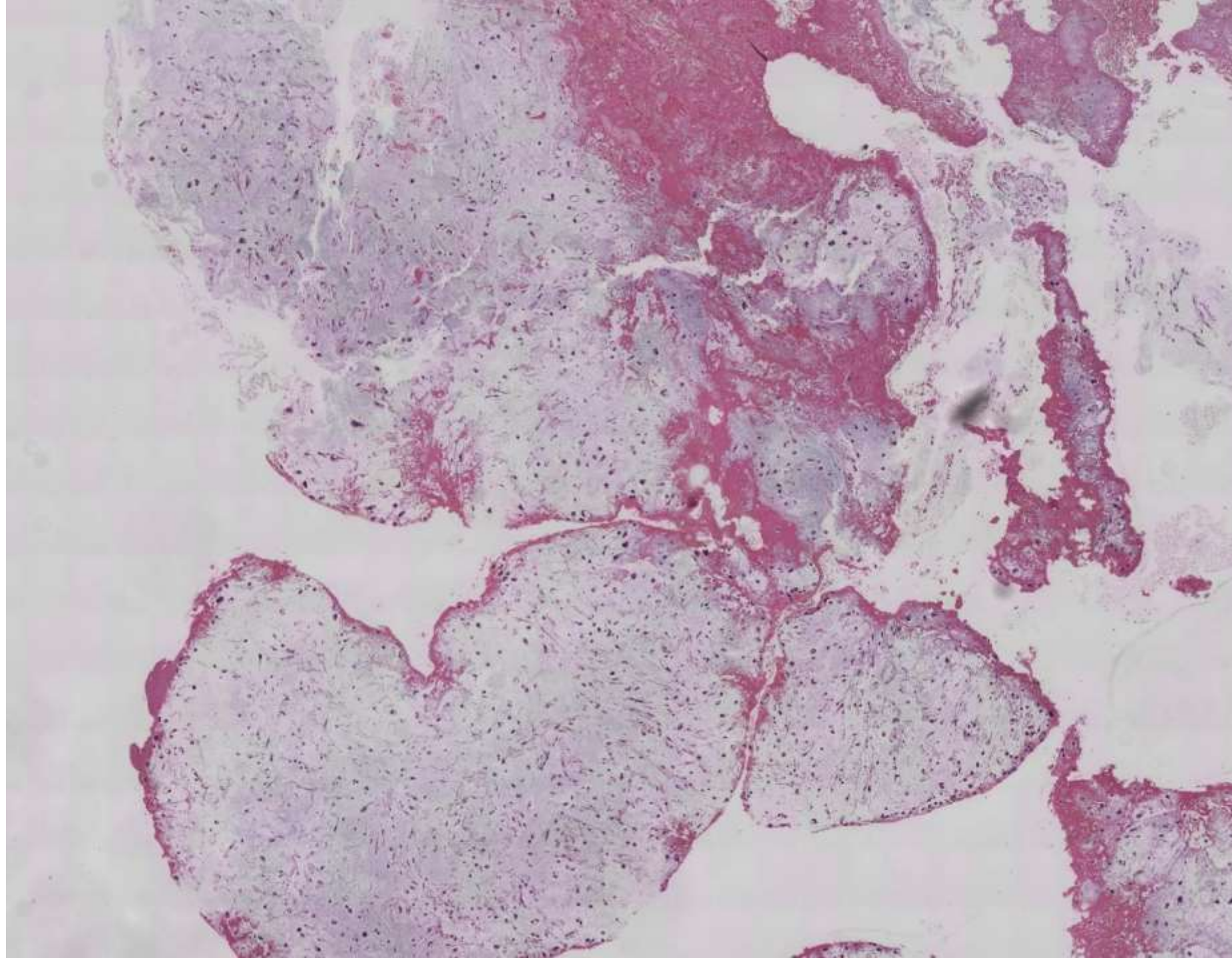
20-1004 A&B

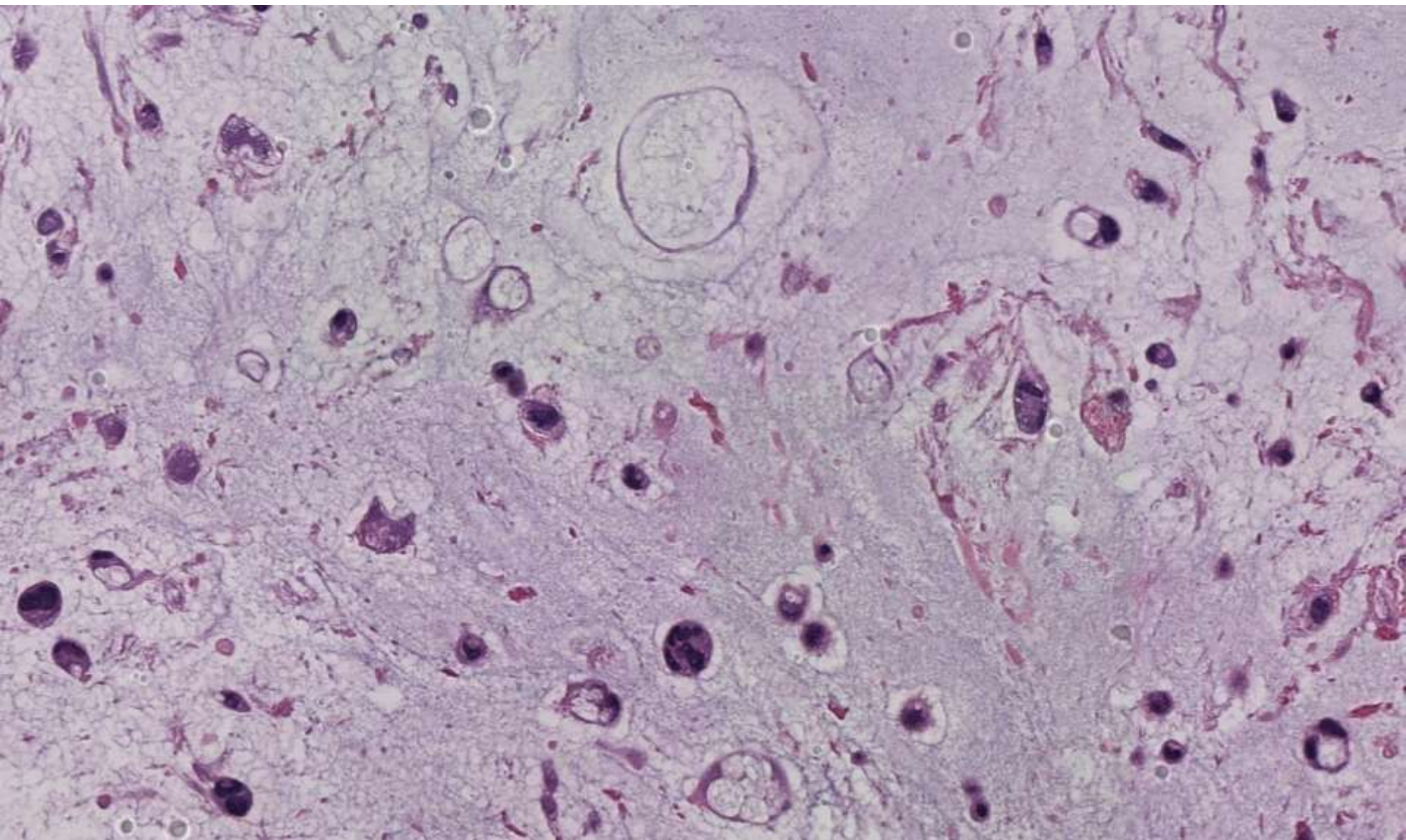
scanned slides available!

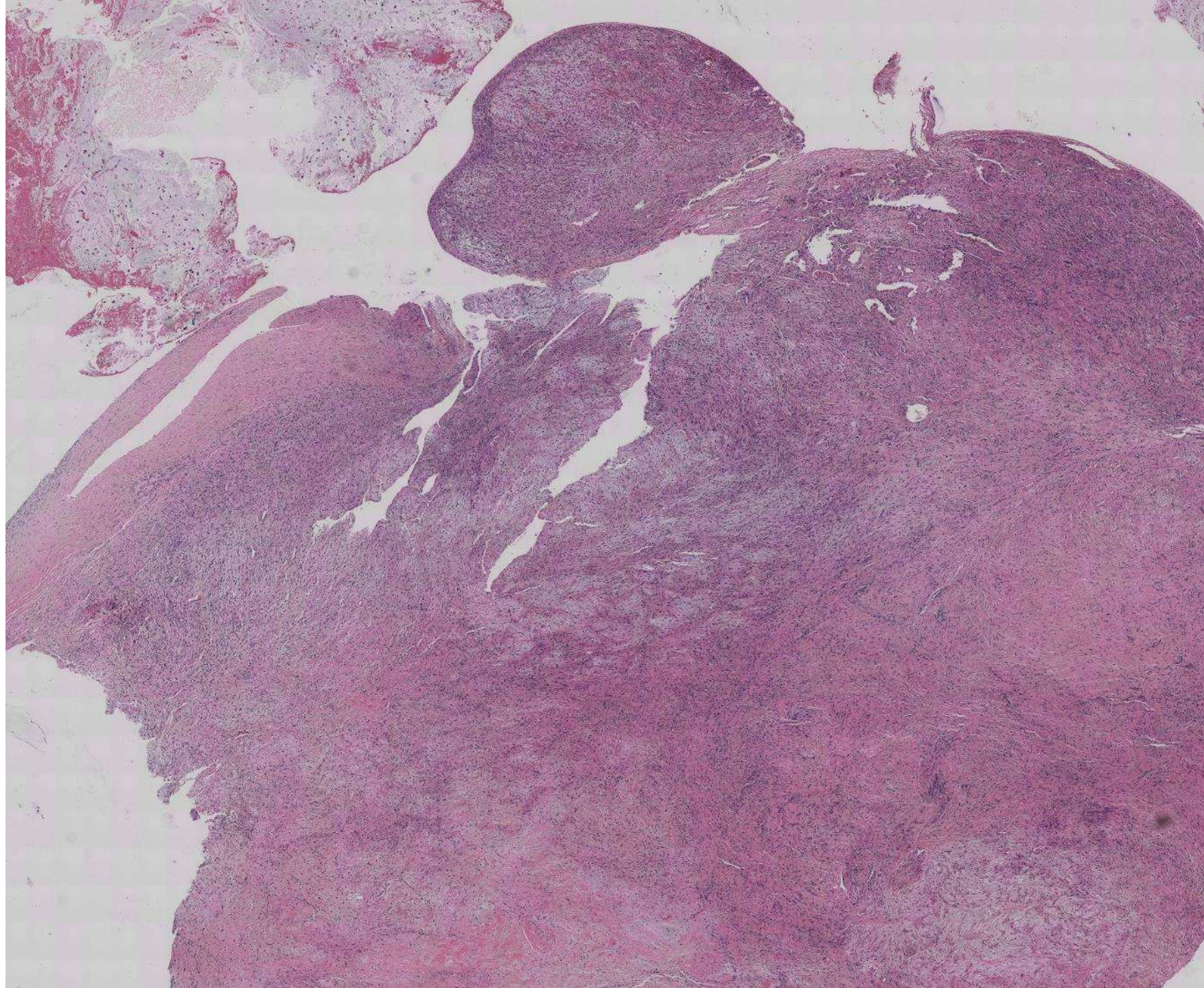
Ankur Sangoi; El Camino Hospital

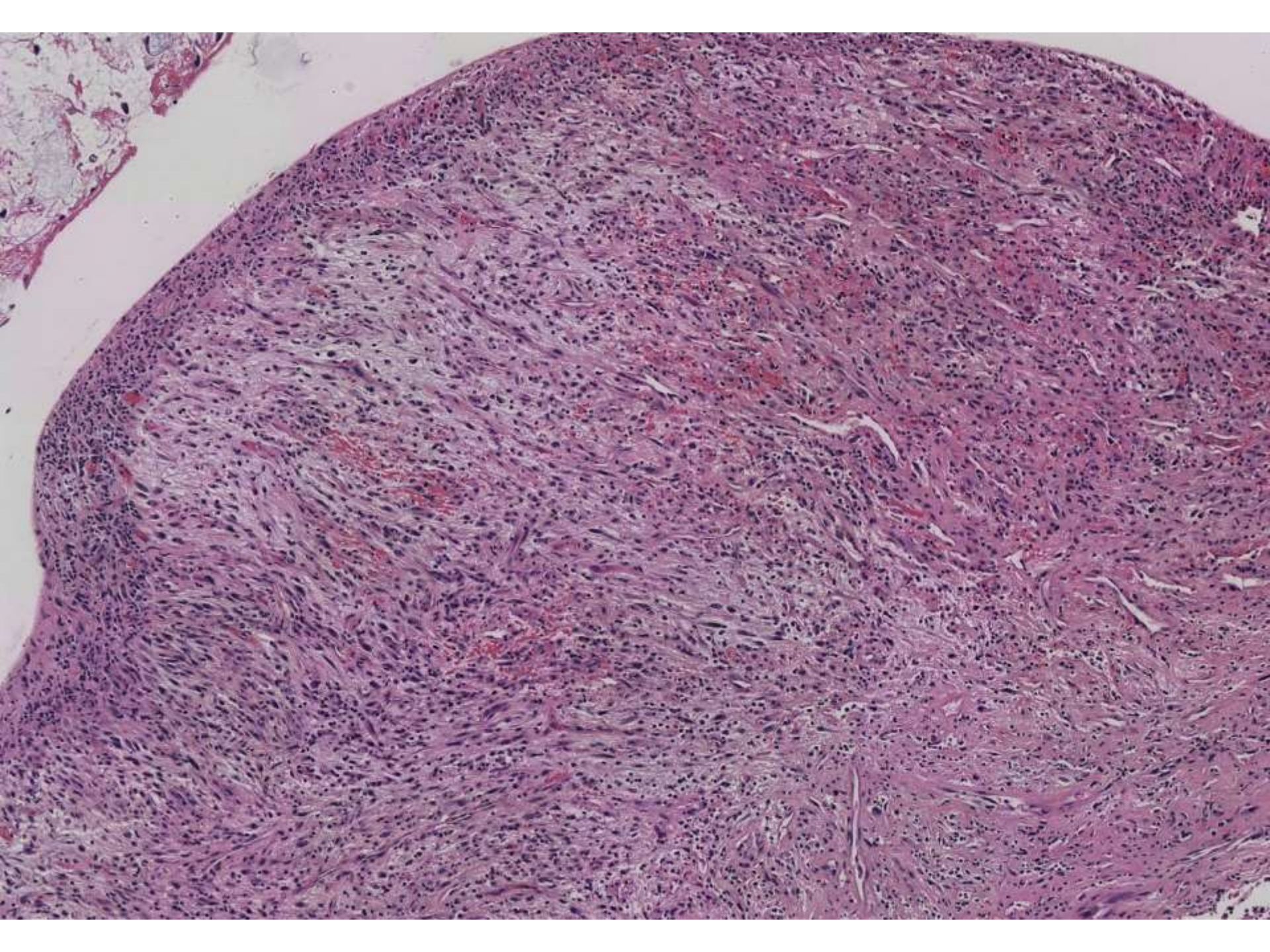
67-year-old M with left atrial mass, excised.

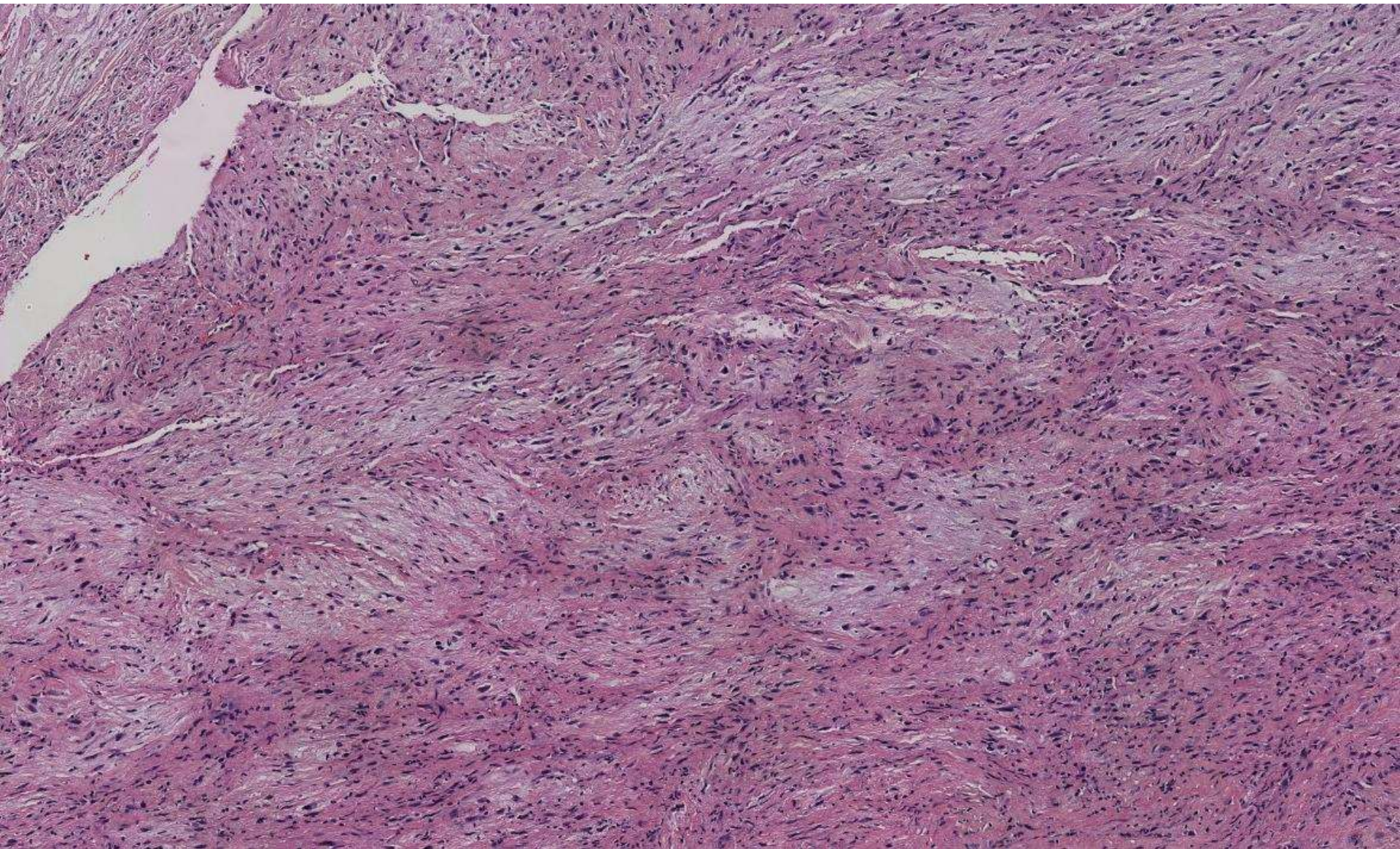


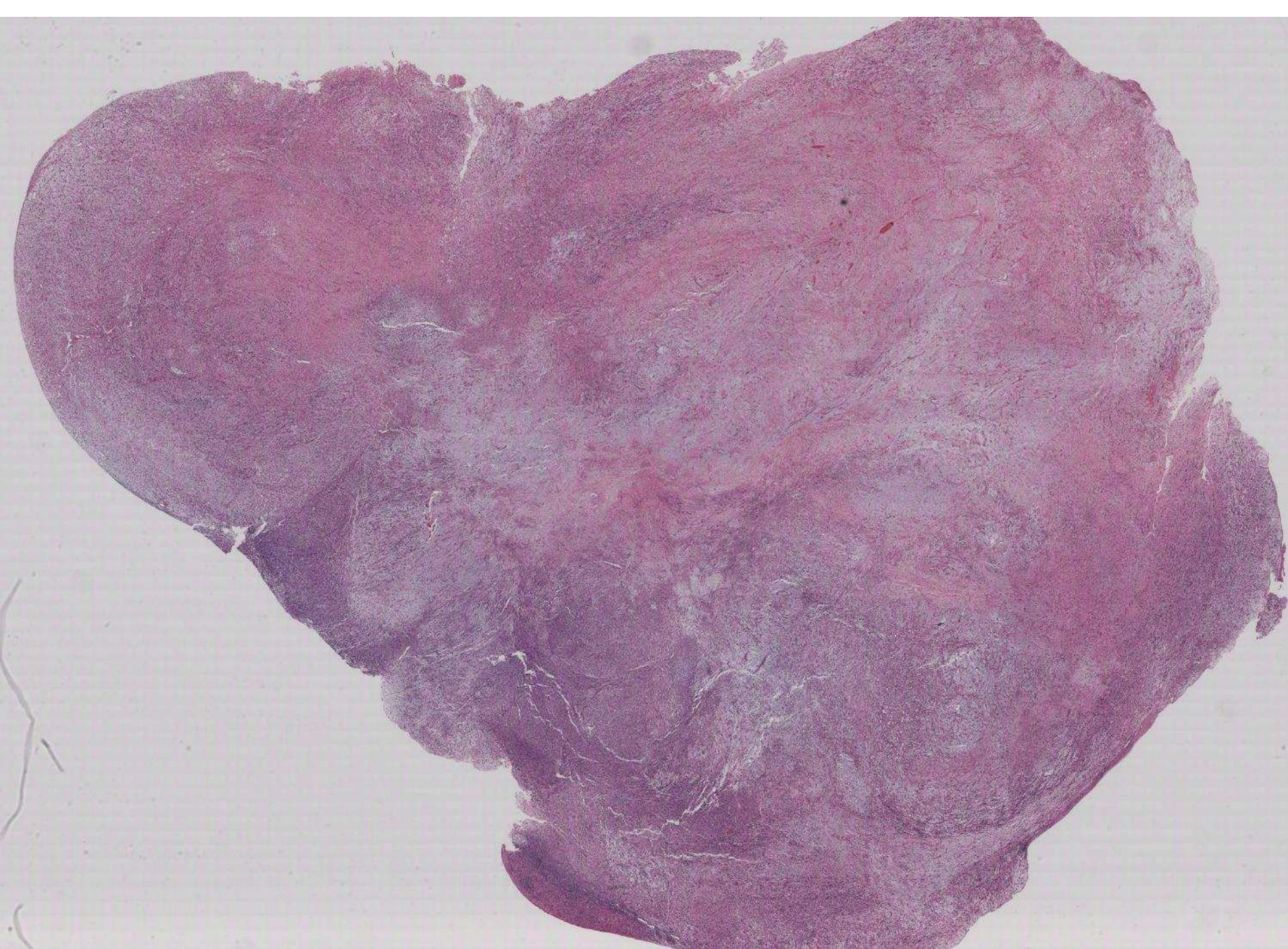


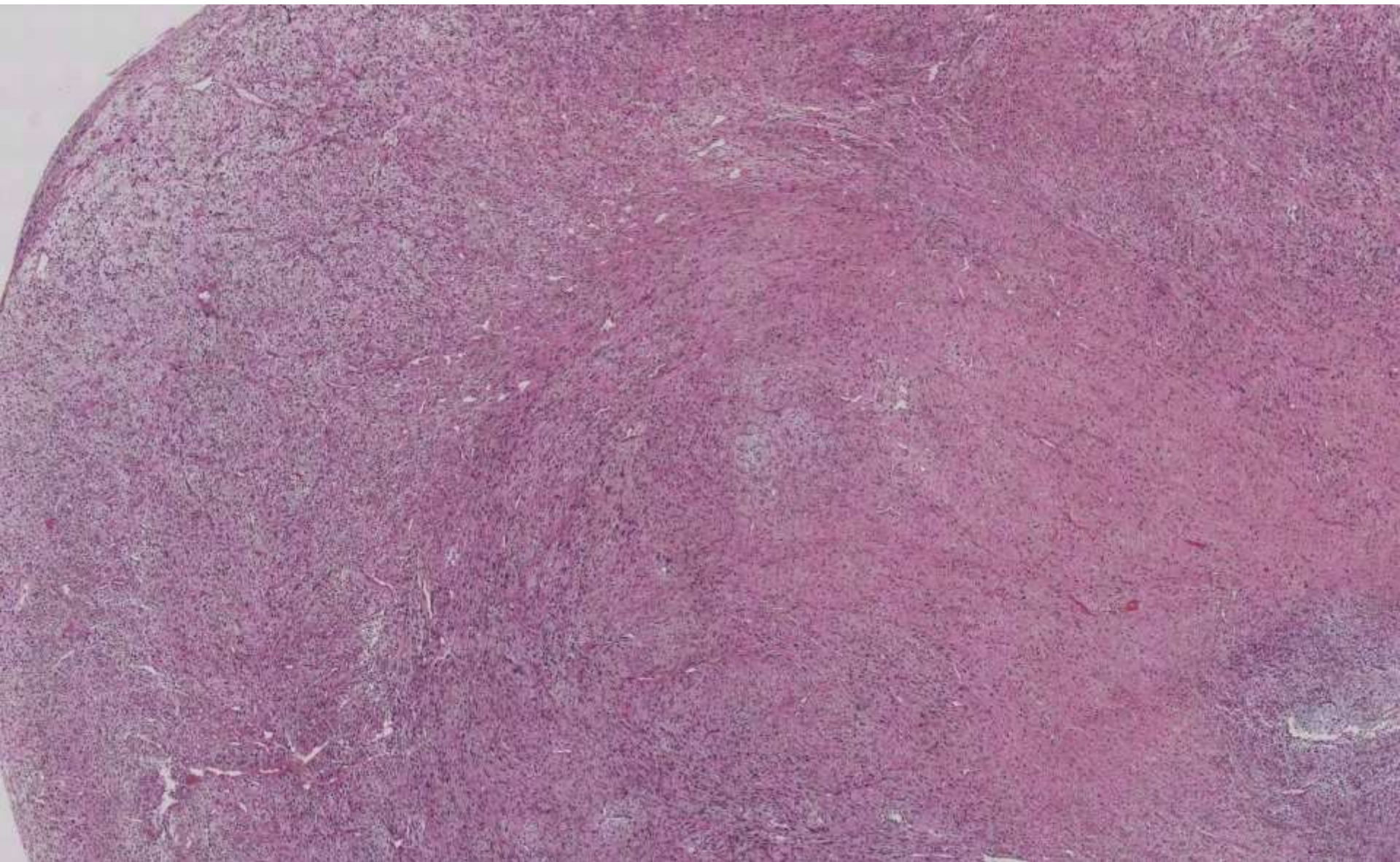


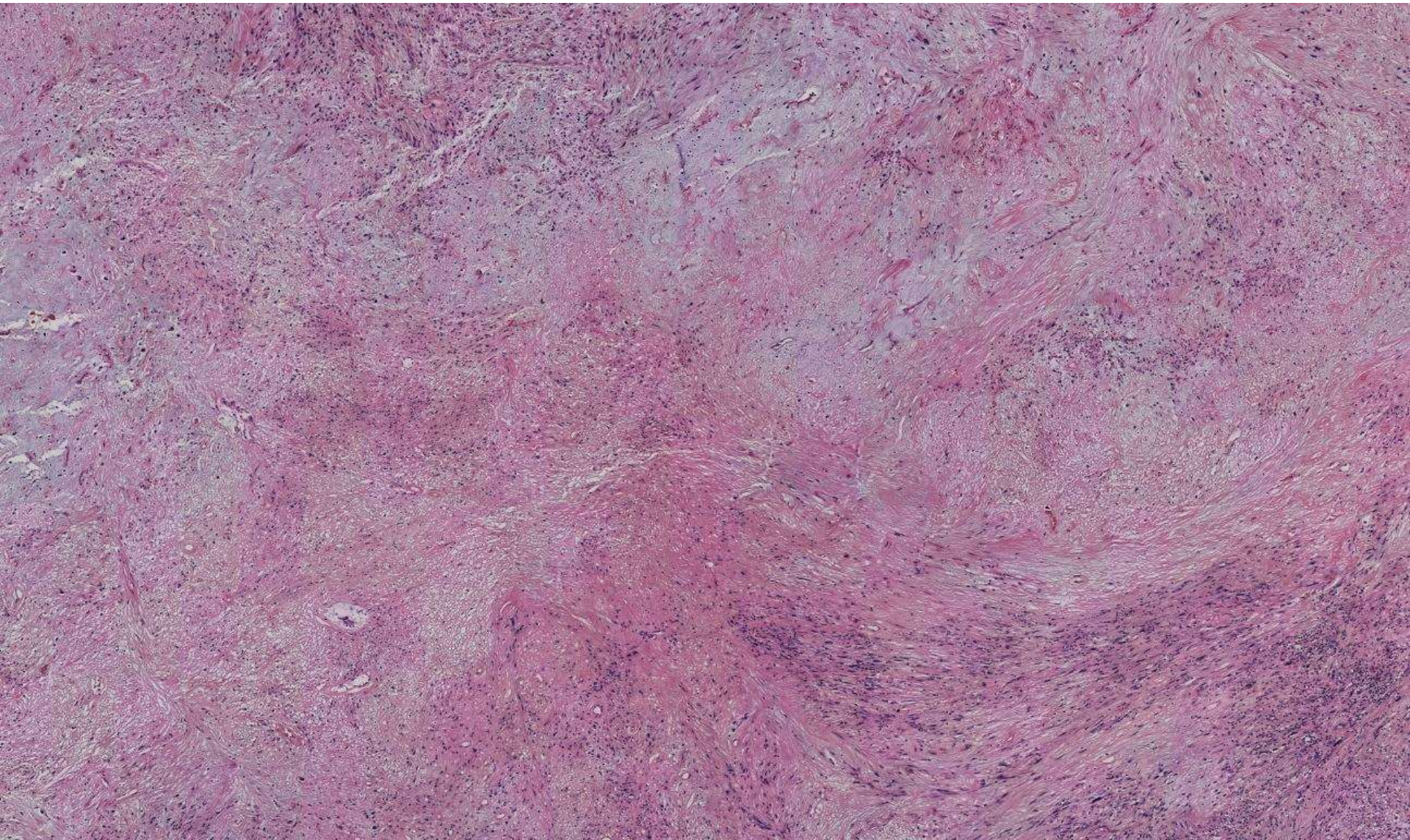


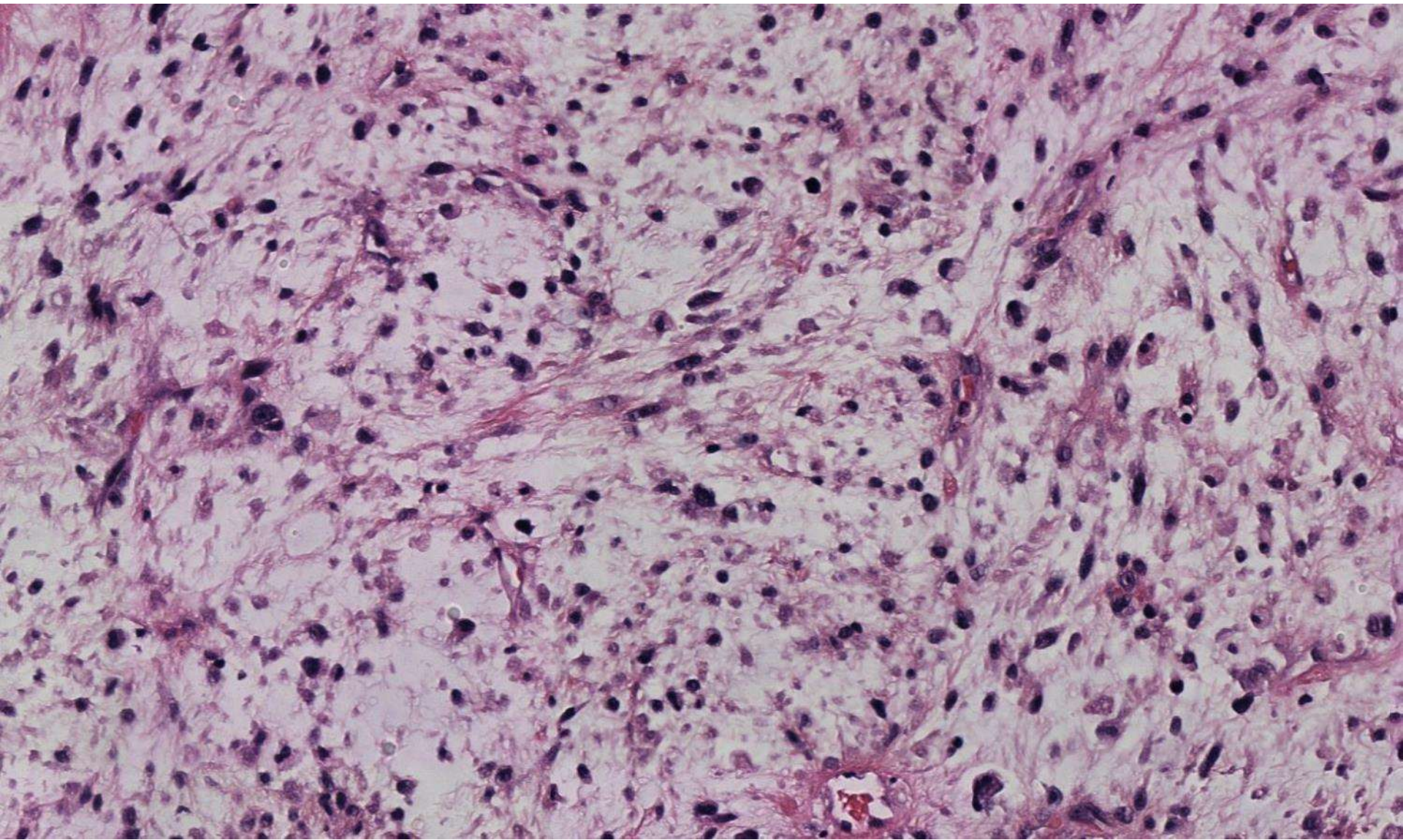


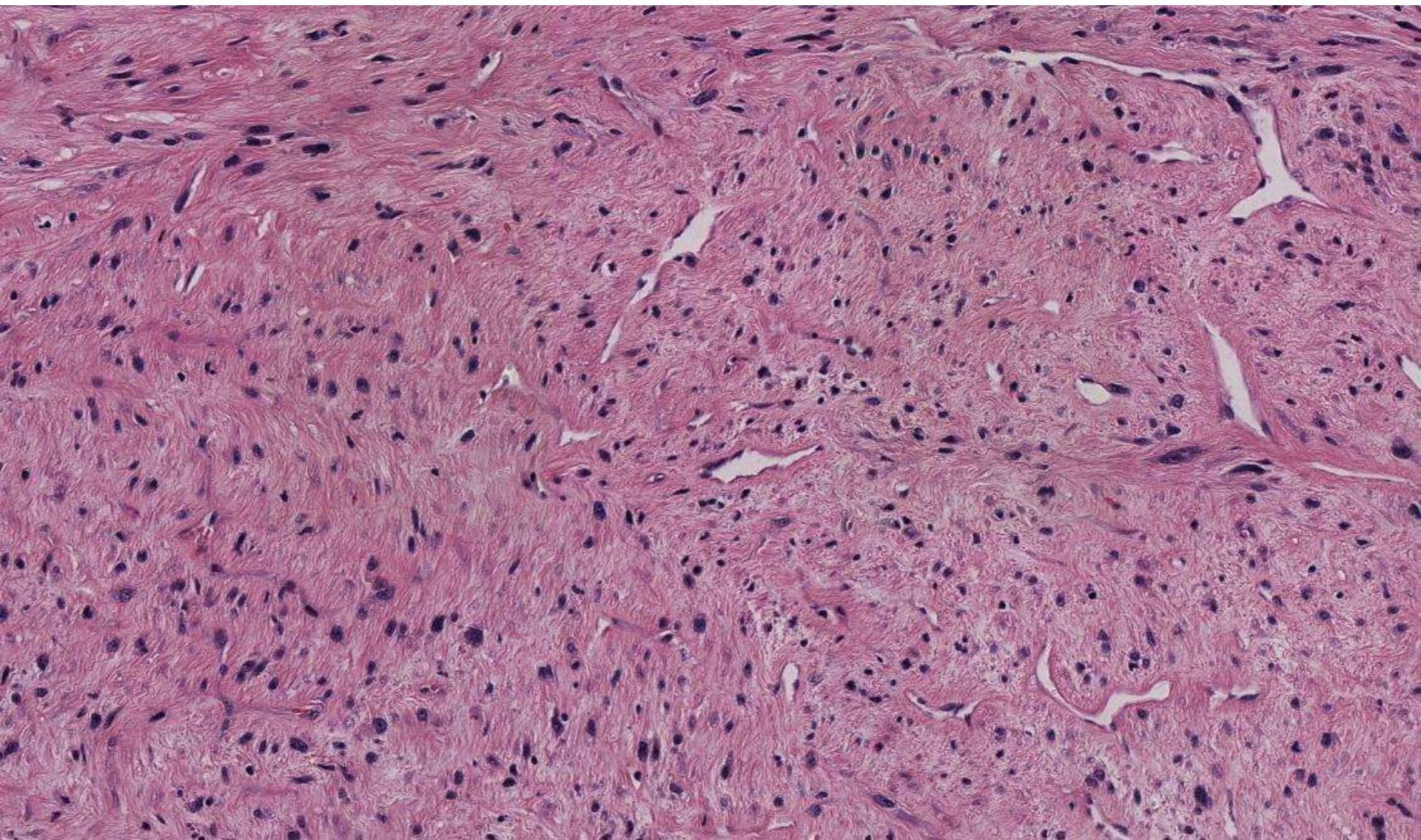


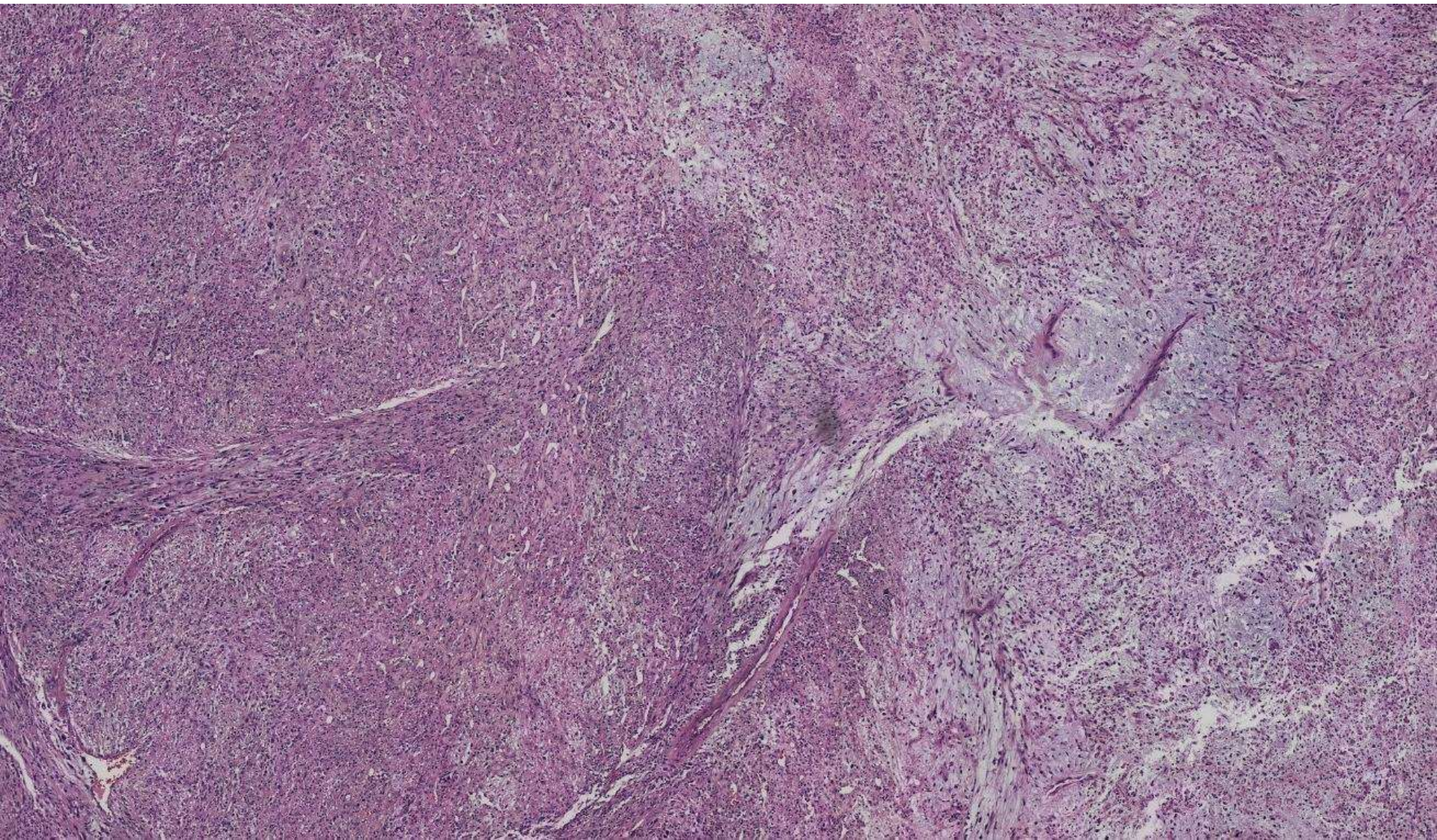


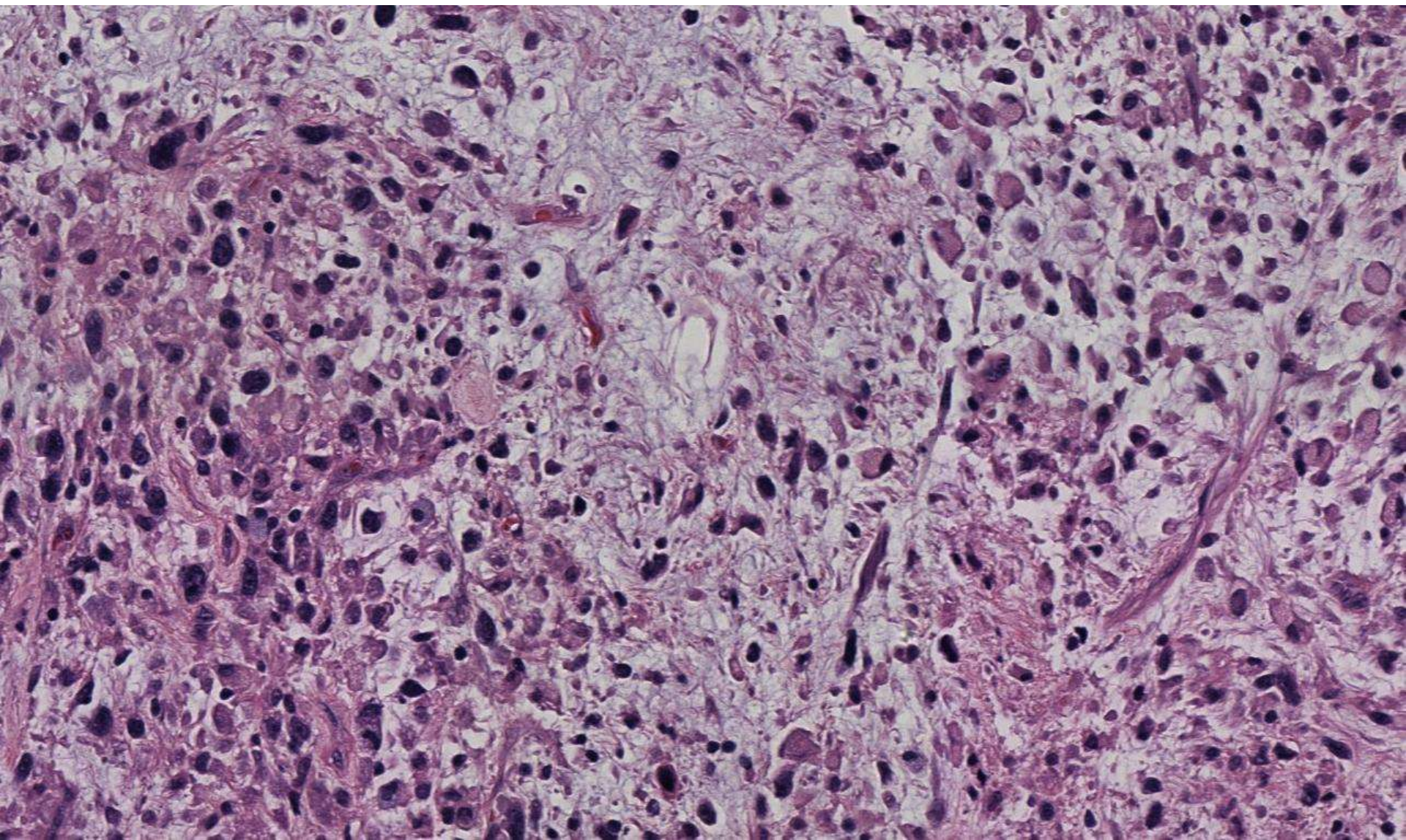


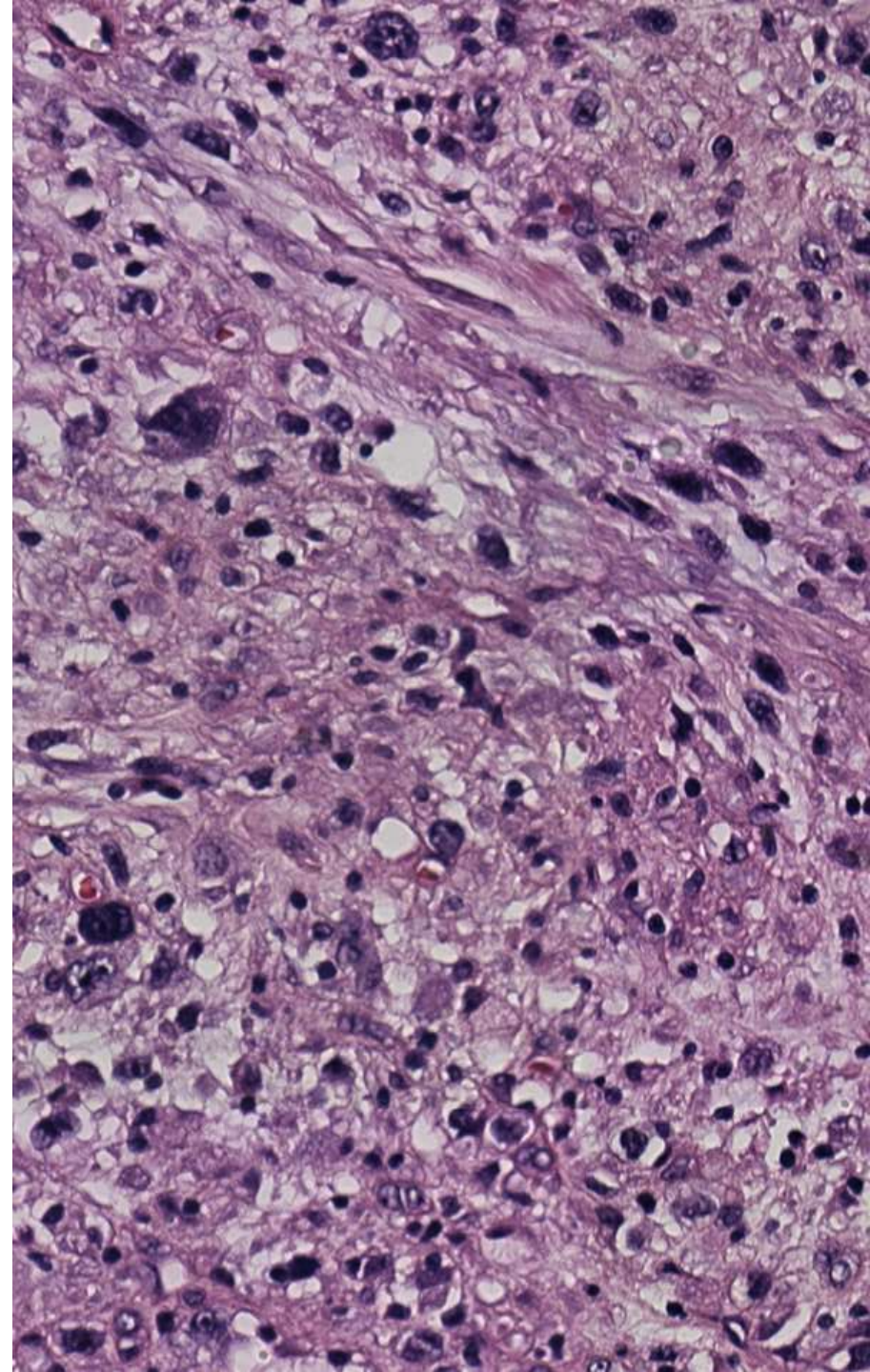
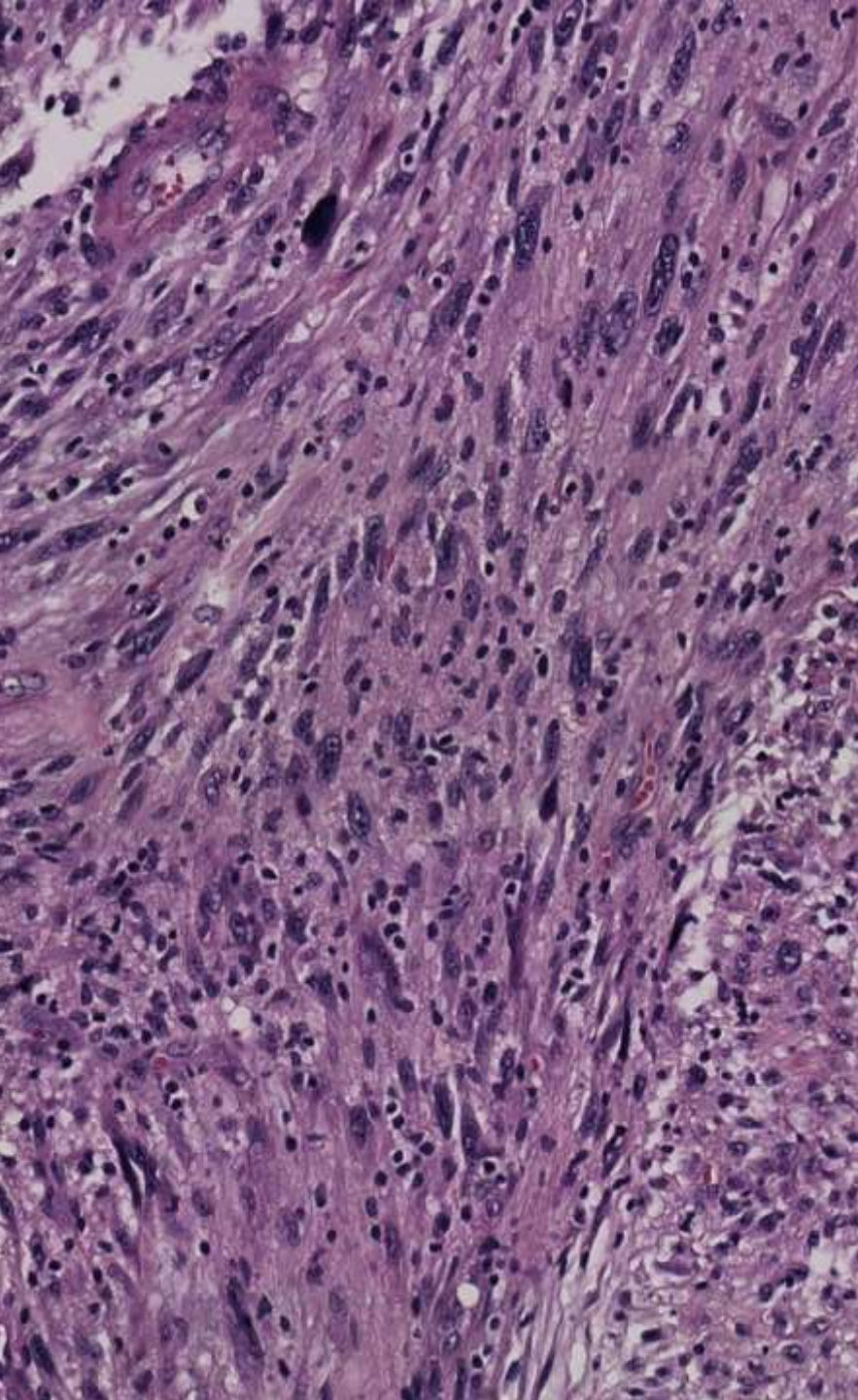








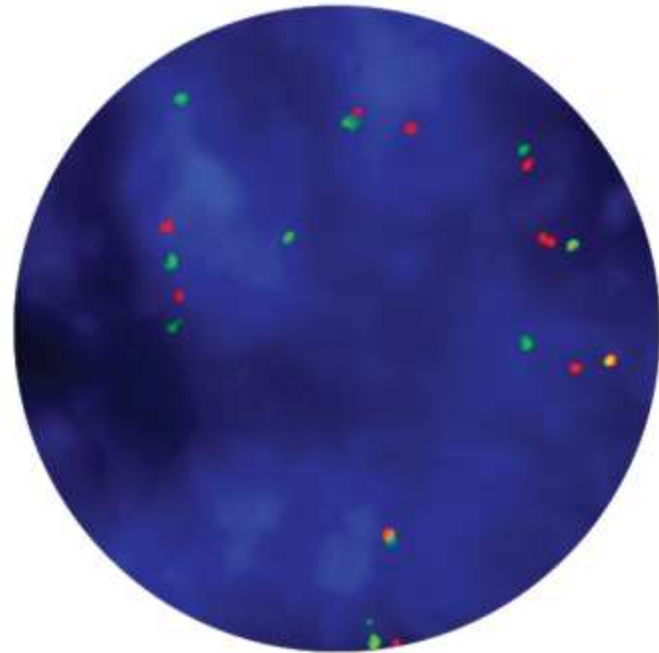
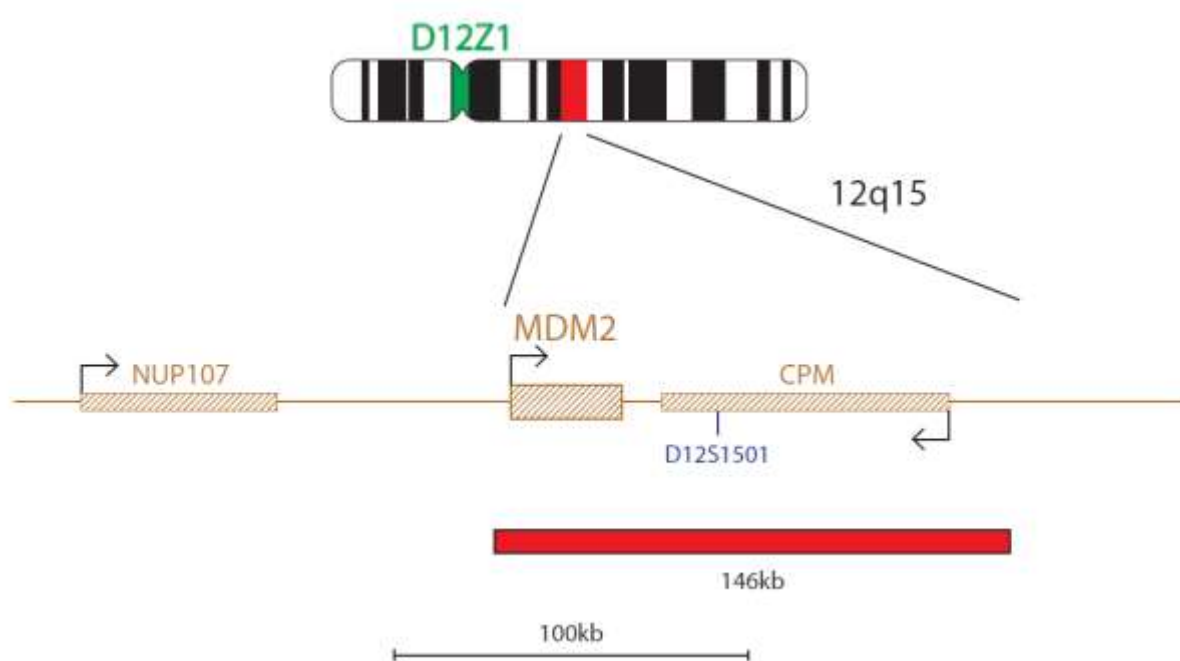




IHC summary

- Patchy positive: desmin
- Negative: caldesmon, myogenin, myoD1, SMA, EMA, ERG, CD31, S100, SOX10, calretinin, ALK

MDM2 amplification



Intimal sarcoma

- **“undiff pleomorphic sarcoma” arising from intima or associated with great vessel**
 - Presentation: Sx of obstruction/compression
 - Grim prognosis
 - Often post-mortem Dx
- **Wide range of histology**
- **Most cases show MDM overexpression**

DDx

- **Angiosarcoma**
→ CD31+
- **Alveolar rhabdomyosarcoma**
→ Desmin/myogenin/myoD1+
- **Synovial sarcoma**
→ SSX IHC or SSX molecular
- **Metastatic melanoma**
→ S100/SOX10+
- **Leiomyosarcoma**
→ desmin/caldesmon/SMA+
- **Pleomorphic undifferentiated sarcoma**
→ Negative for MDM2

Intimal Sarcoma Is the Most Frequent Primary Cardiac Sarcoma

Clinicopathologic and Molecular Retrospective Analysis of 100 Primary Cardiac Sarcomas

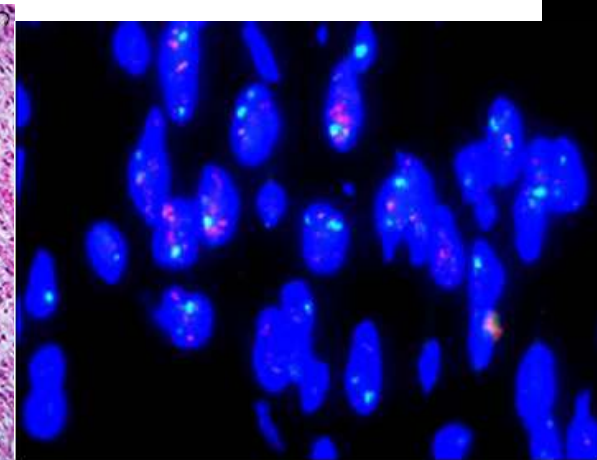
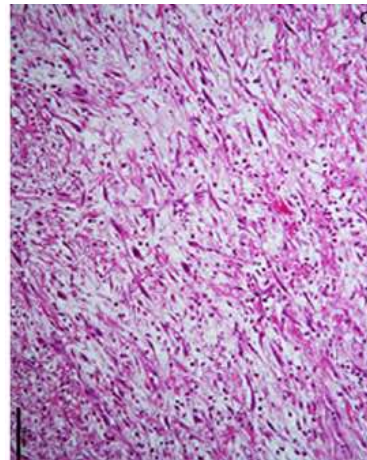
Agnès Neuville, MD, PhD,†‡ Françoise Collin, MD,§ Patrick Bruneval, MD,|| Marie Parrens, MD,*¶ Françoise Thivolet, MD,# Anne Gomez-Brouchet, MD, PhD,** Philippe Terrier, MD,†† Vincent Thomas de Montpreville, MD,‡‡ François Le Gall, MD,§§ Isabelle Hostein, PhD,‡ Pauline Lagarde, MSc,*†‡ Frédéric Chibon, PhD,†‡ and Jean-Michel Coindre, MD*†‡*

Abstract: We report novel molecular and pathologic features of sarcomas involving the heart. Intimal sarcoma appears as the most frequent primary cardiac sarcoma within the largest described series of 100 primary cardiac sarcomas. Immunohistochemical analysis, fluorescence in situ hybridization, real-time polymerase chain reaction, and array-comparative genomic hybridization were performed on materials from 65 women and 35 men, aged 18 to 82 years (mean 50 y), retrieved from the French Departments of Pathology, between 1977 and early 2013. Right and left heart was involved in 44 and 56 cases, respectively. There were 42 intimal sarcomas, 26 angiosarcomas, 22 undifferentiated sarcomas, 7 synovial sarcomas, 2 leiomyosarcomas, and 1 peripheral neuroectodermal tumor. All but 1 angiosarcomas originated from the right heart, whereas 83% of the intimal sarcomas and 72% of the undifferentiated sarcomas were from the left heart. *MDM2* overexpression was immunohistochemically observed in all intimal sarcomas, as well as in 10 of the 22 undifferentiated sarcomas and in 5 of the 26 angiosarcomas. *MDM2* amplification was only demonstrated in intimal sarcomas. Genomic analysis showed a complex profile, with recurrent 12q13-14 amplicon involving *MDM2*, 4q12 amplicon involving

KIT and *PDGFRA*, 7p12 gain involving *EGFR*, and 9p21 deletion targeting *CDKN2A*. Immunohistochemical detection of *MDM2* overexpression can easily detect intimal sarcoma, provided that molecular aberration is proved. As resections are limited to the left atrium, this histologic subtype could benefit from therapies targeting *PDGFRA* or *MDM2*.

Key Words: cardiac sarcoma, intimal sarcoma, *MDM2* amplification

(*Am J Surg Pathol* 2014;38:461–469)

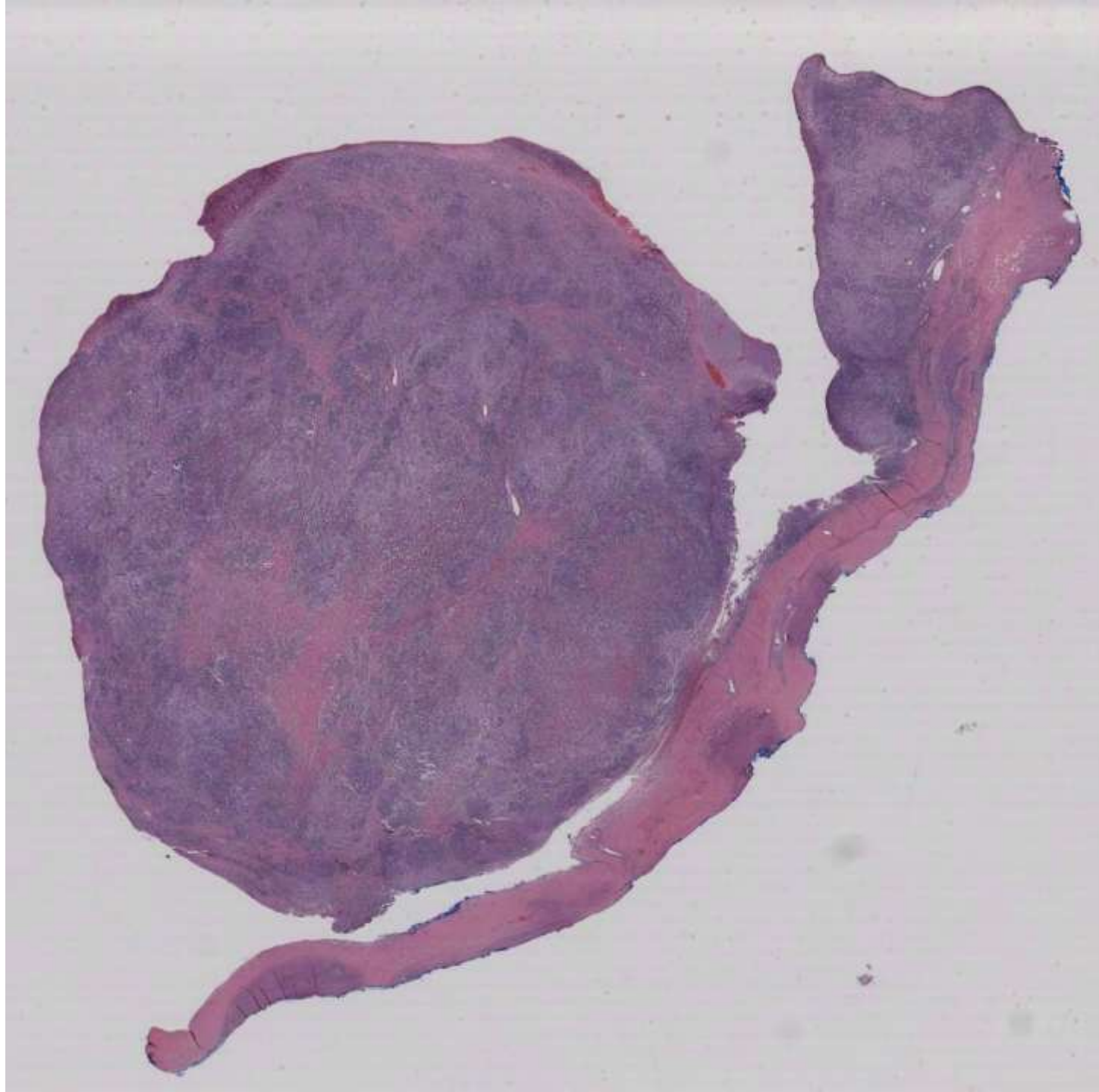


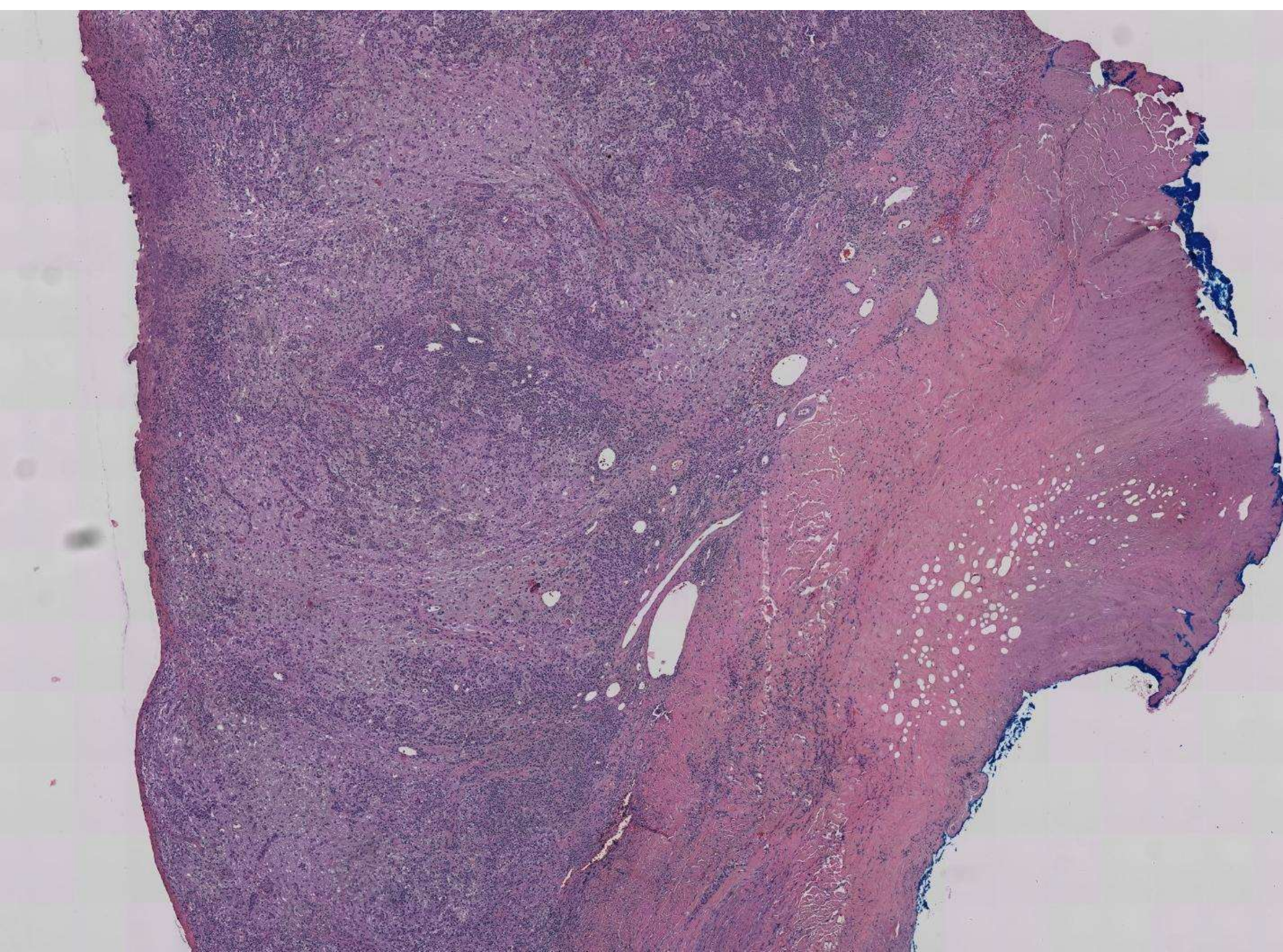
20-1005

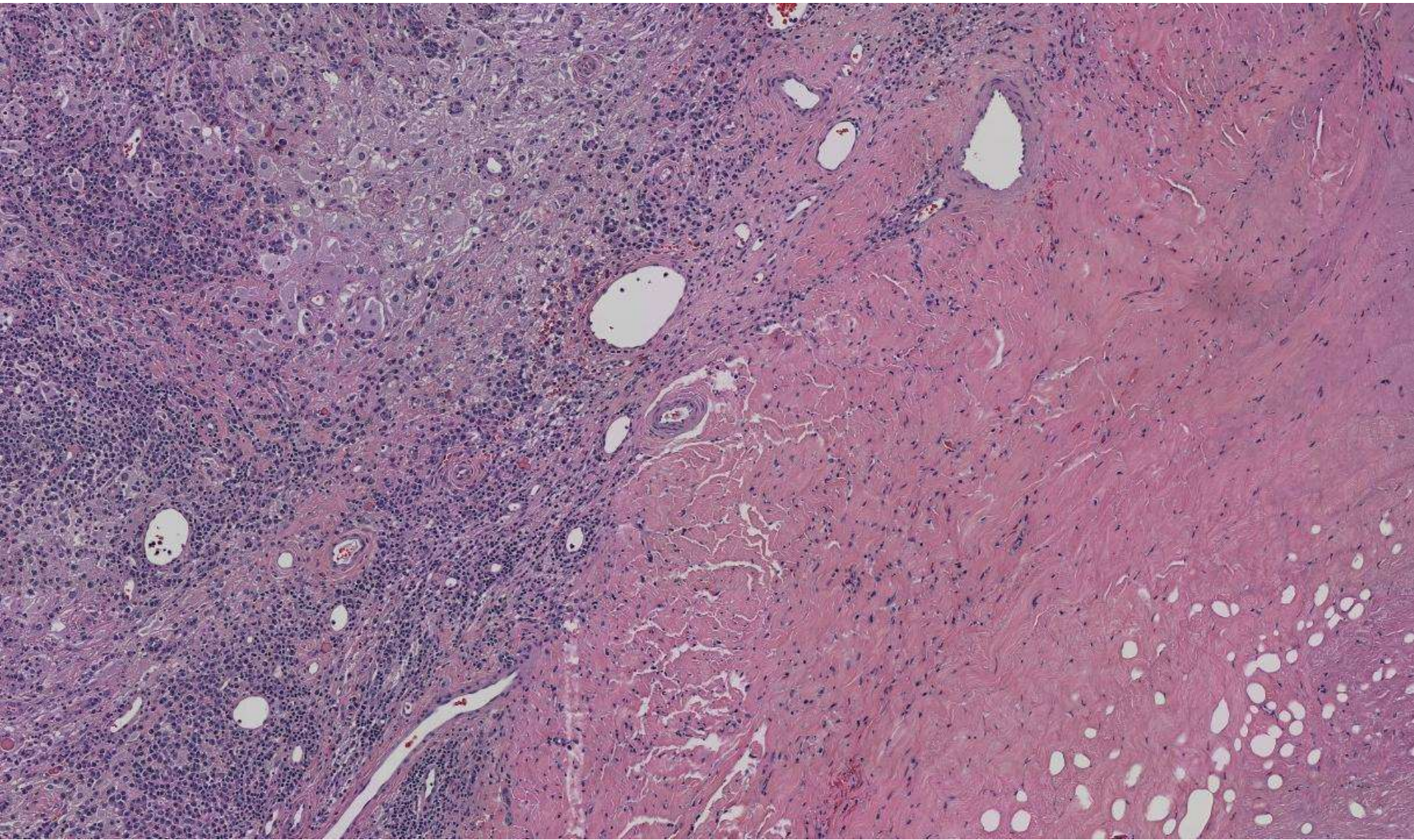
scanned slide available!

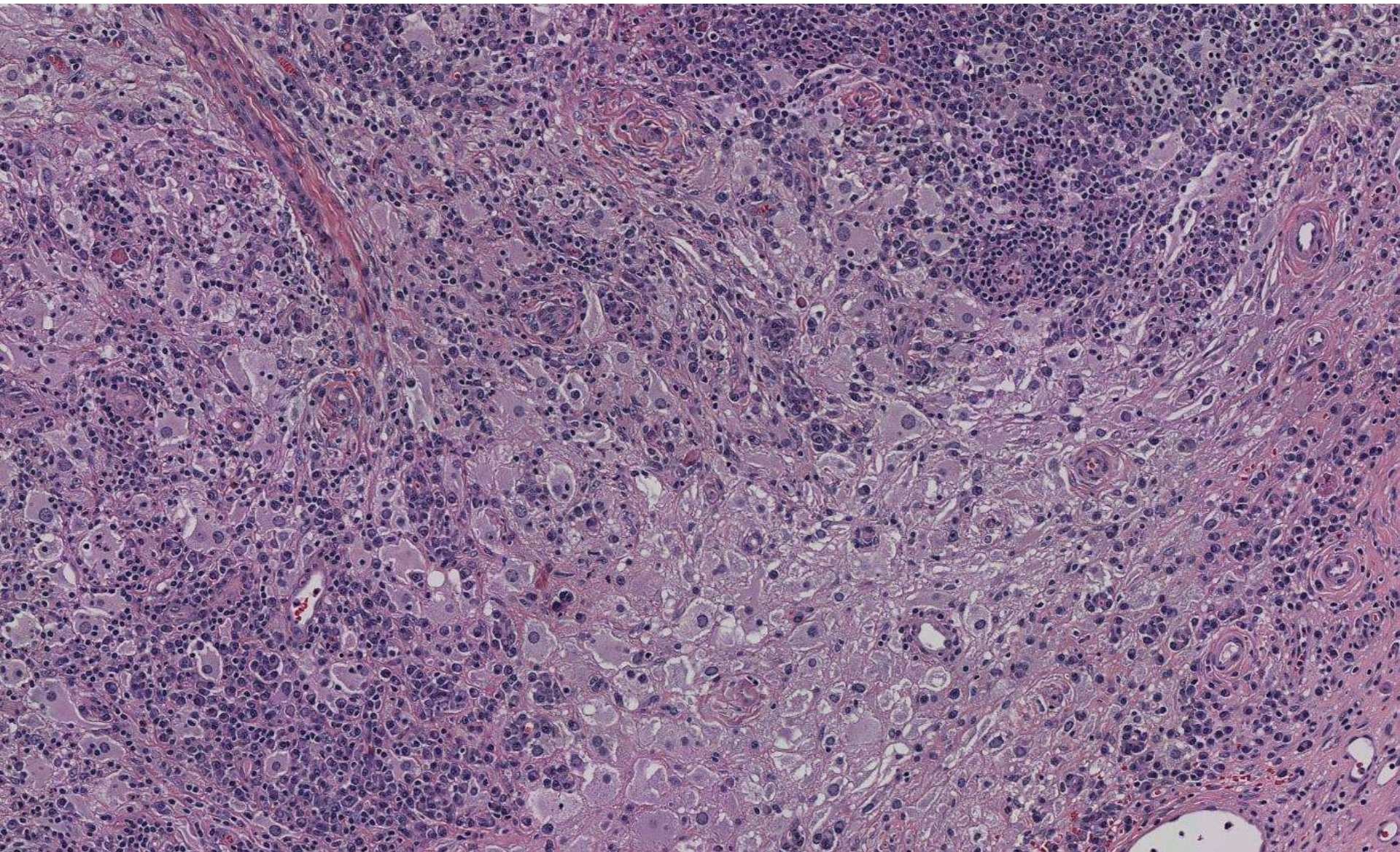
Mahendra Ranchod; Good Samaritan Hospital

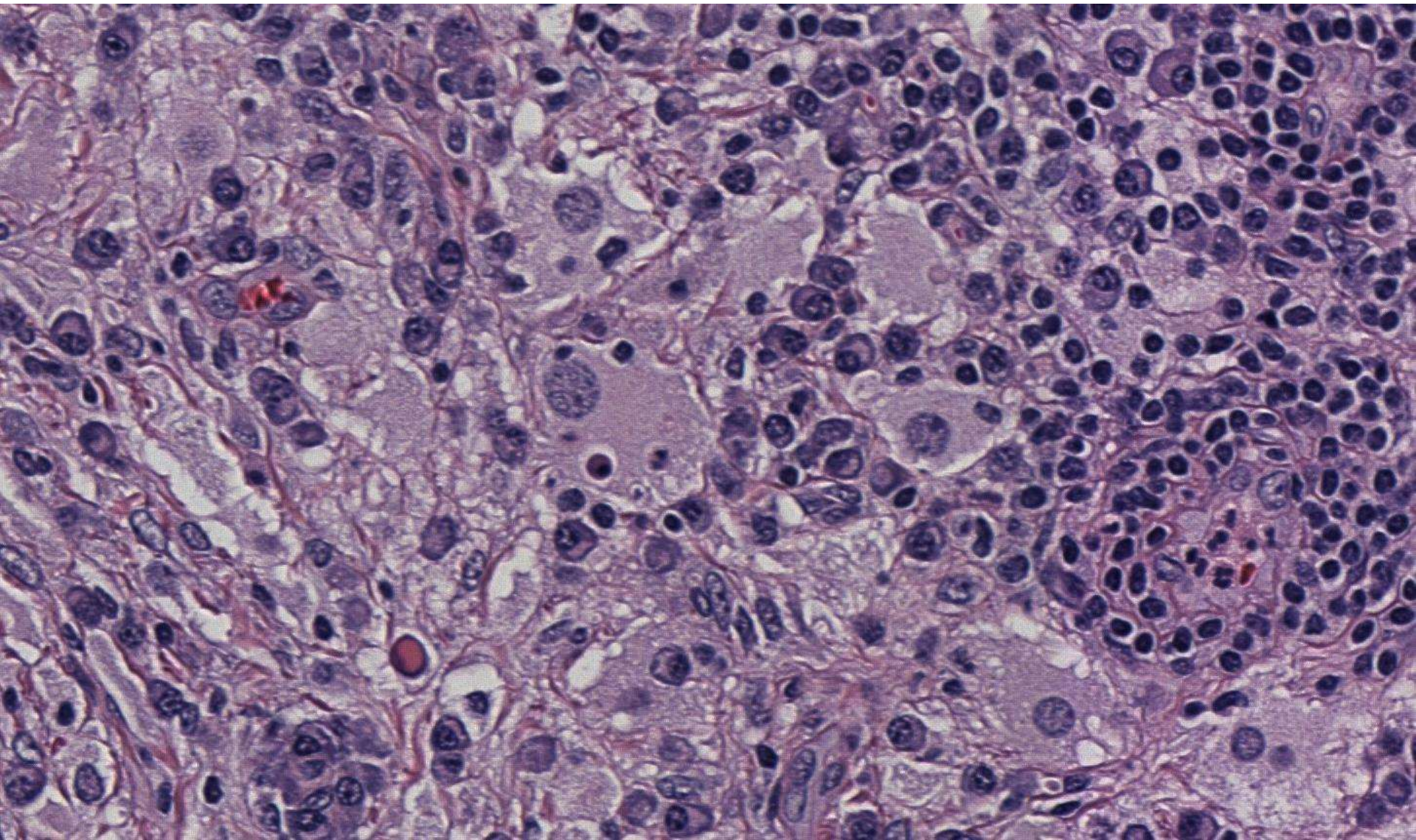
43-year-old F presented with epilepsy. MRI showed 2cm mass in the dural of the right frontal area.

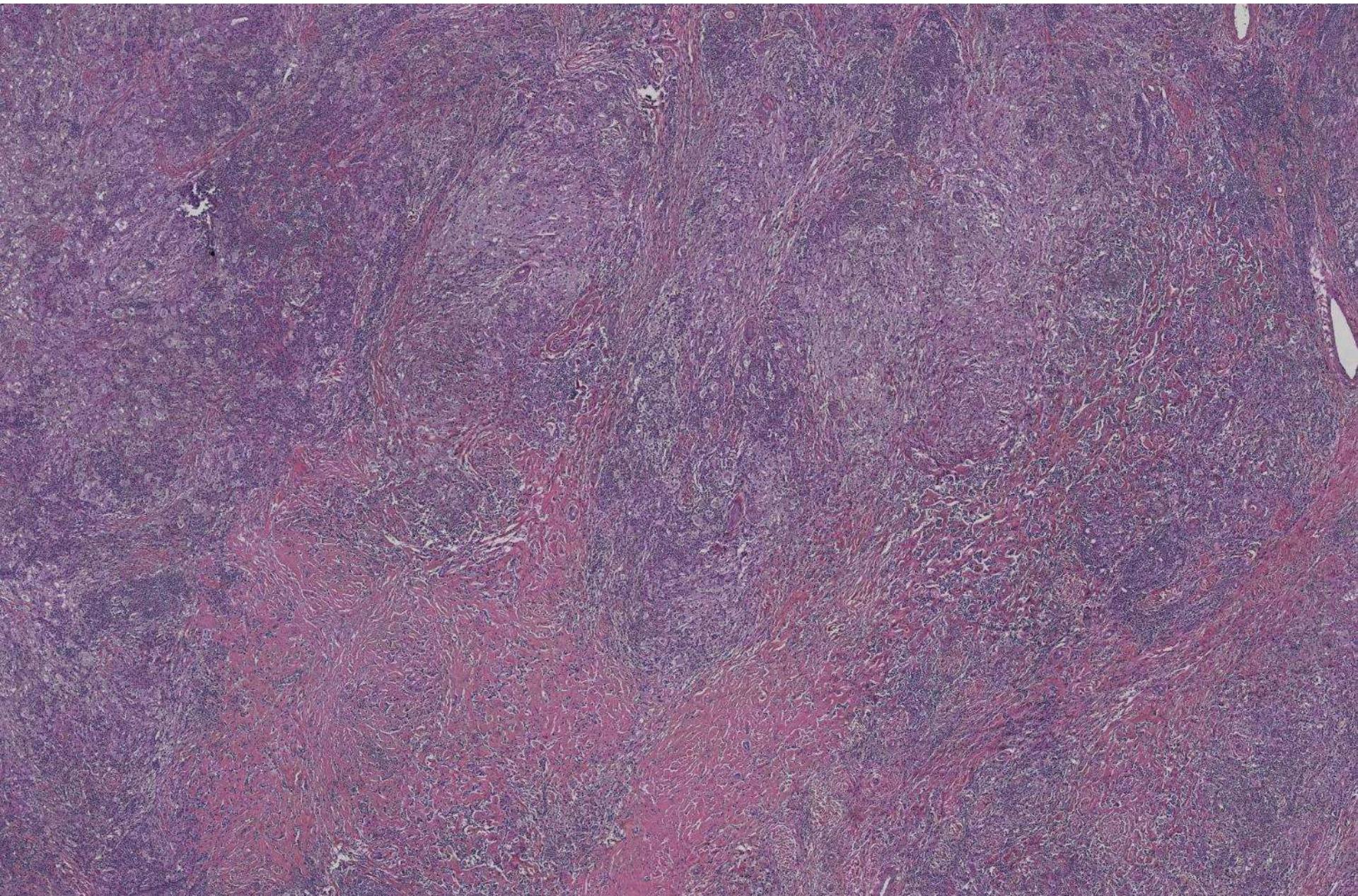


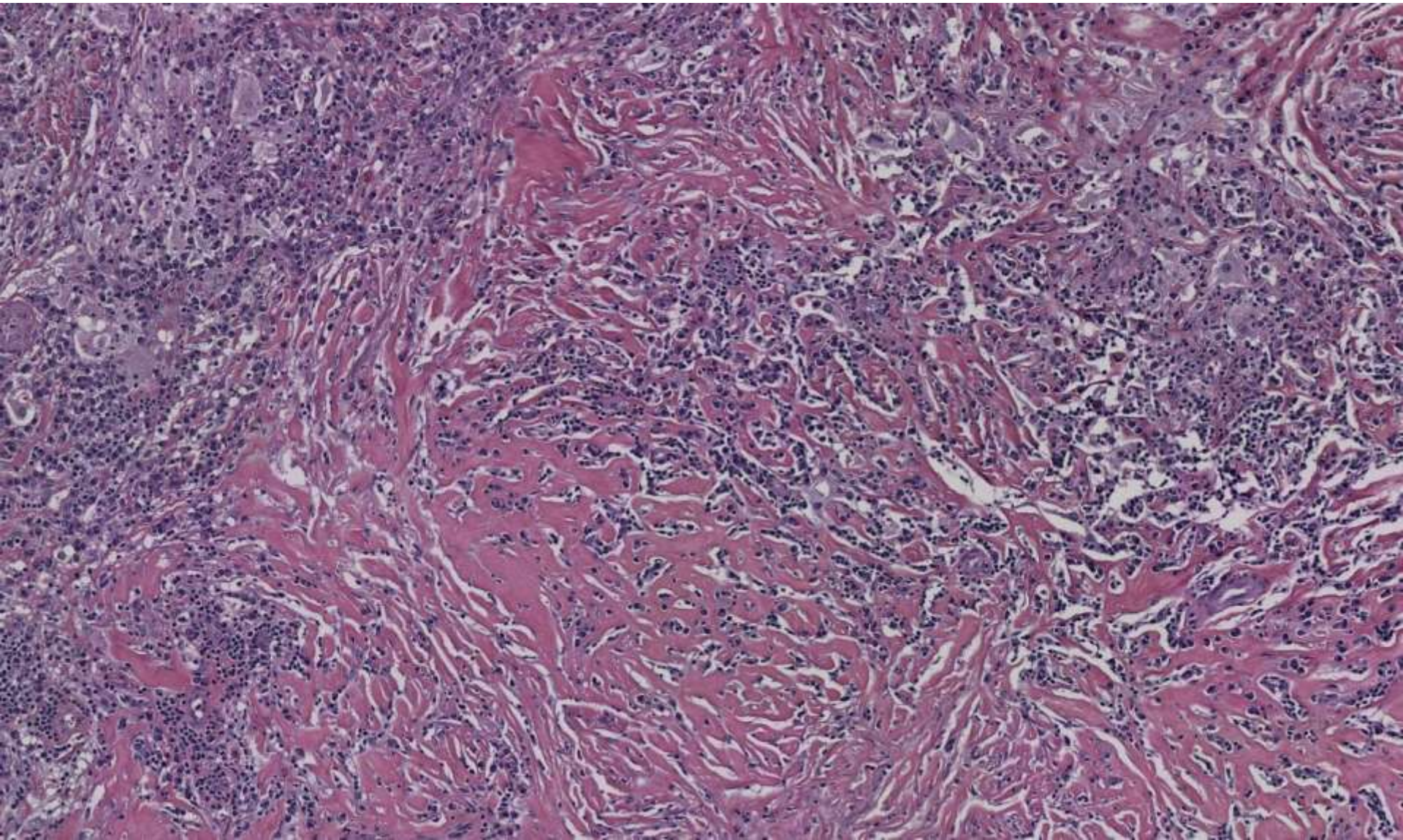


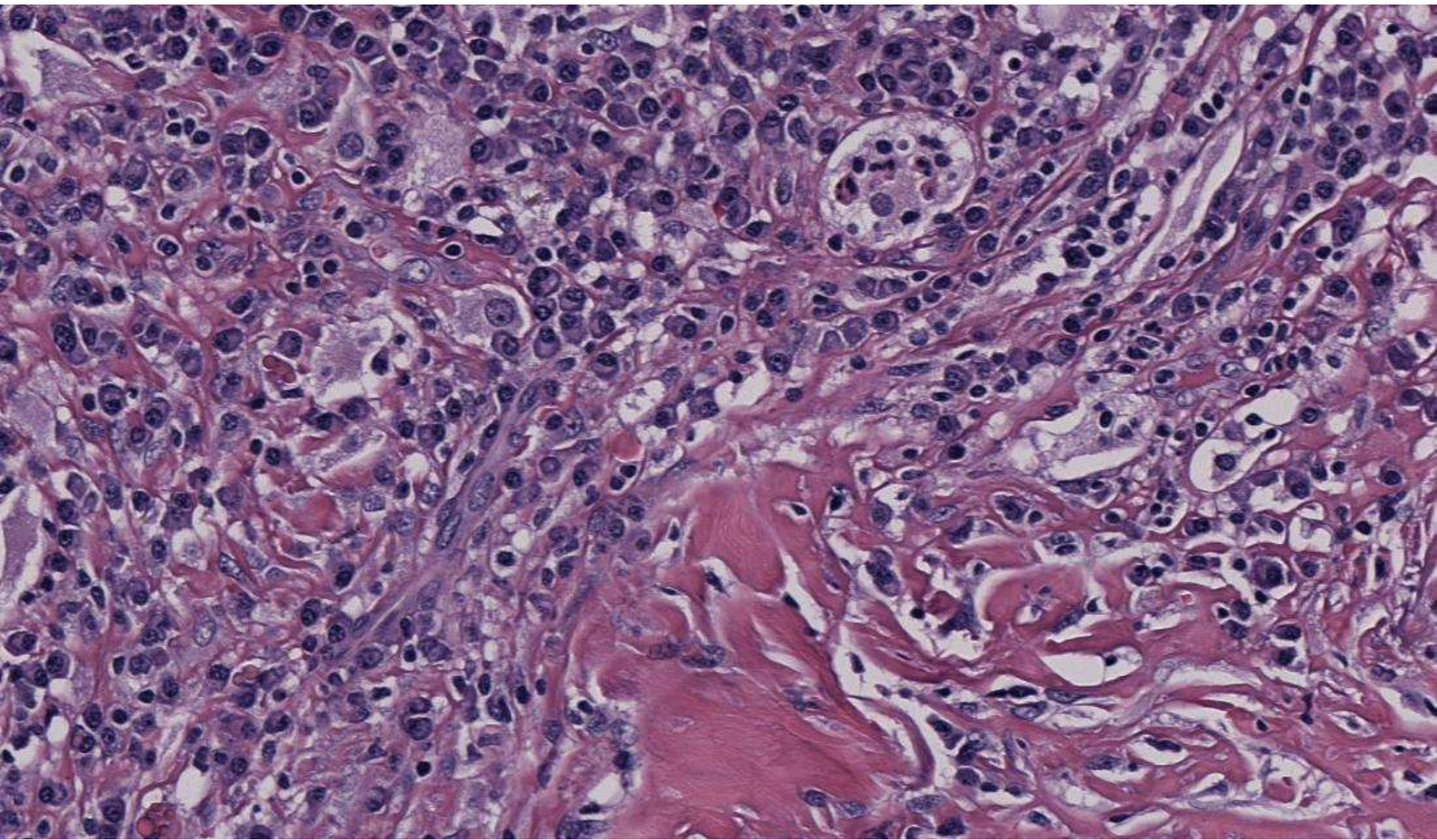


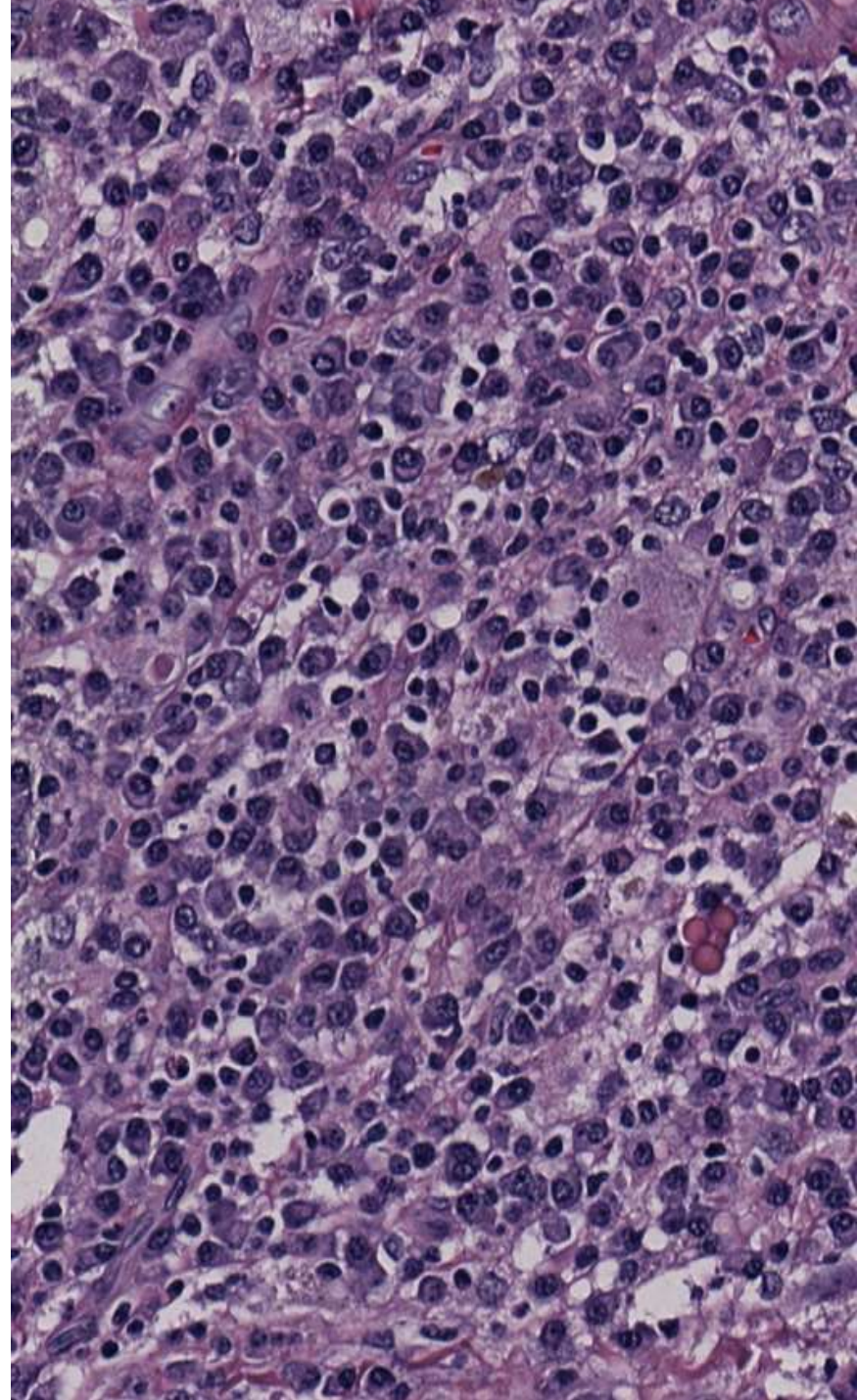
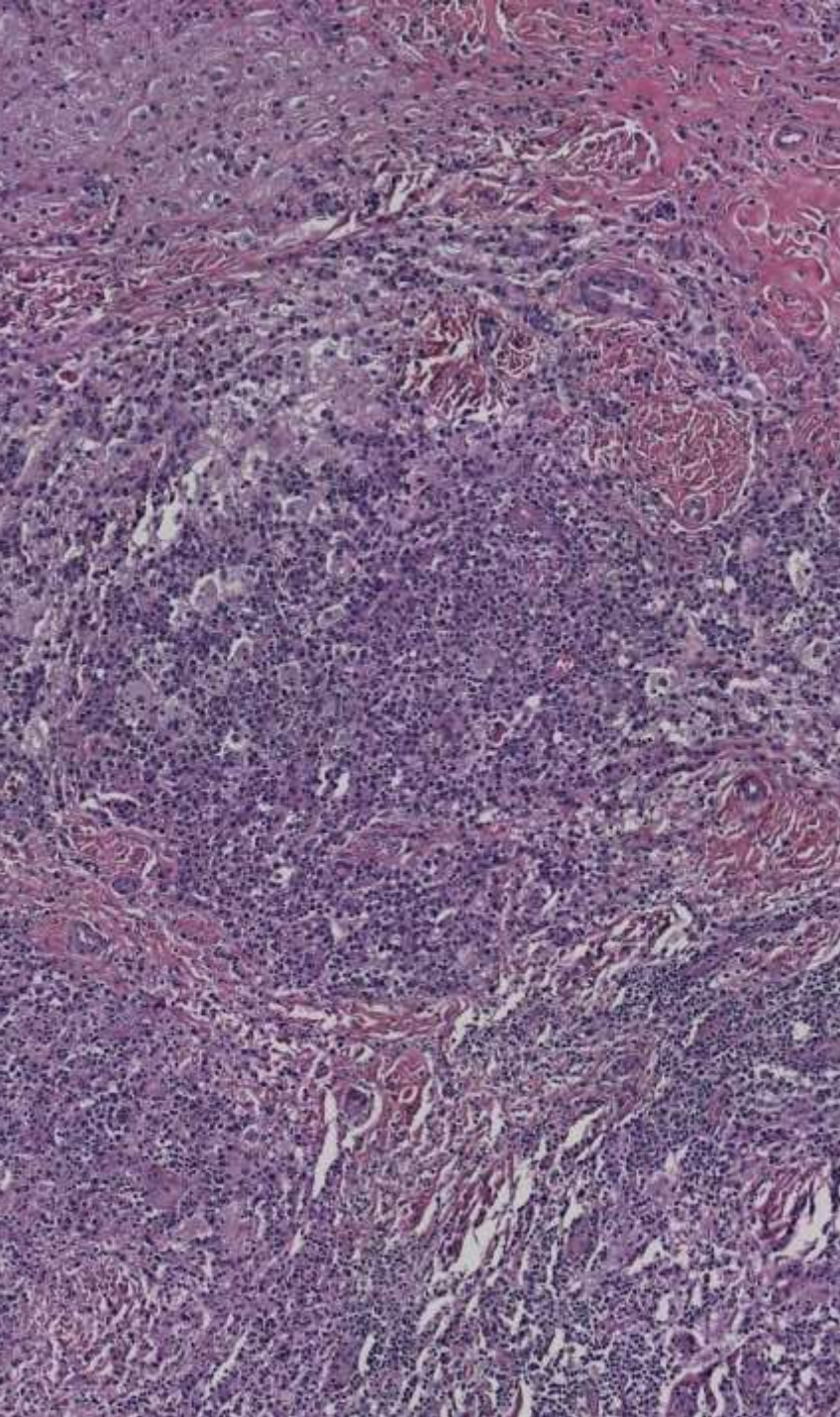


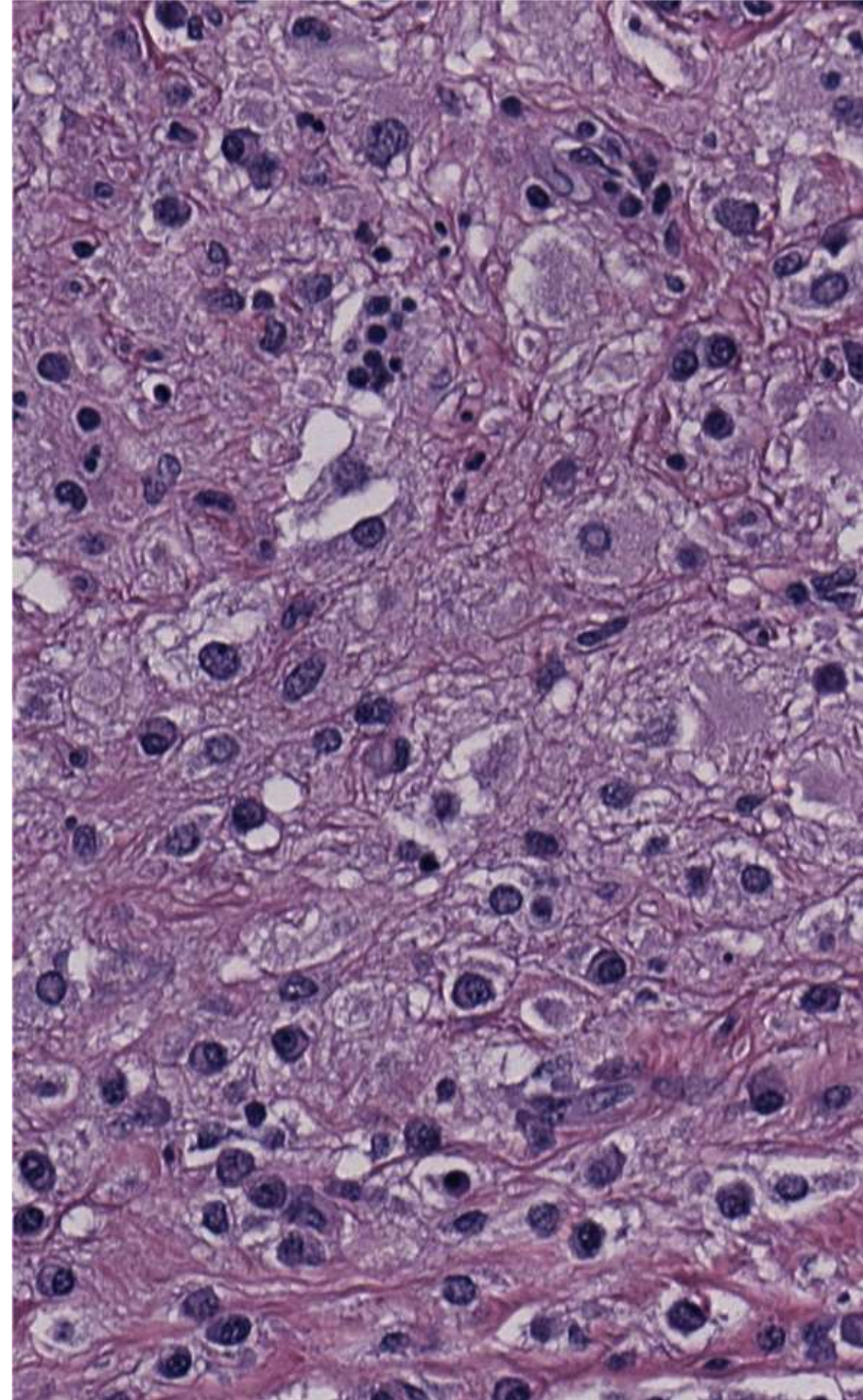
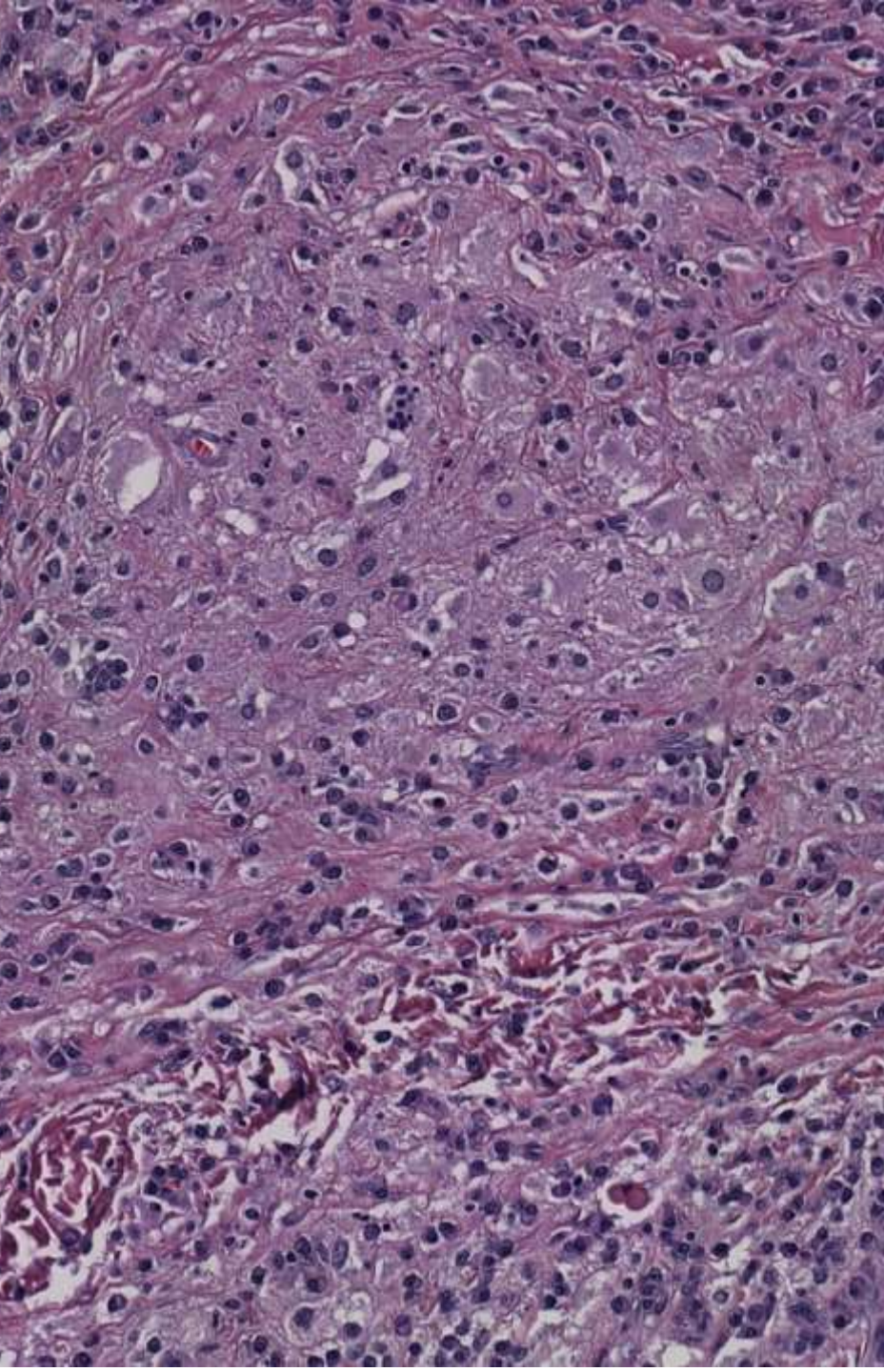


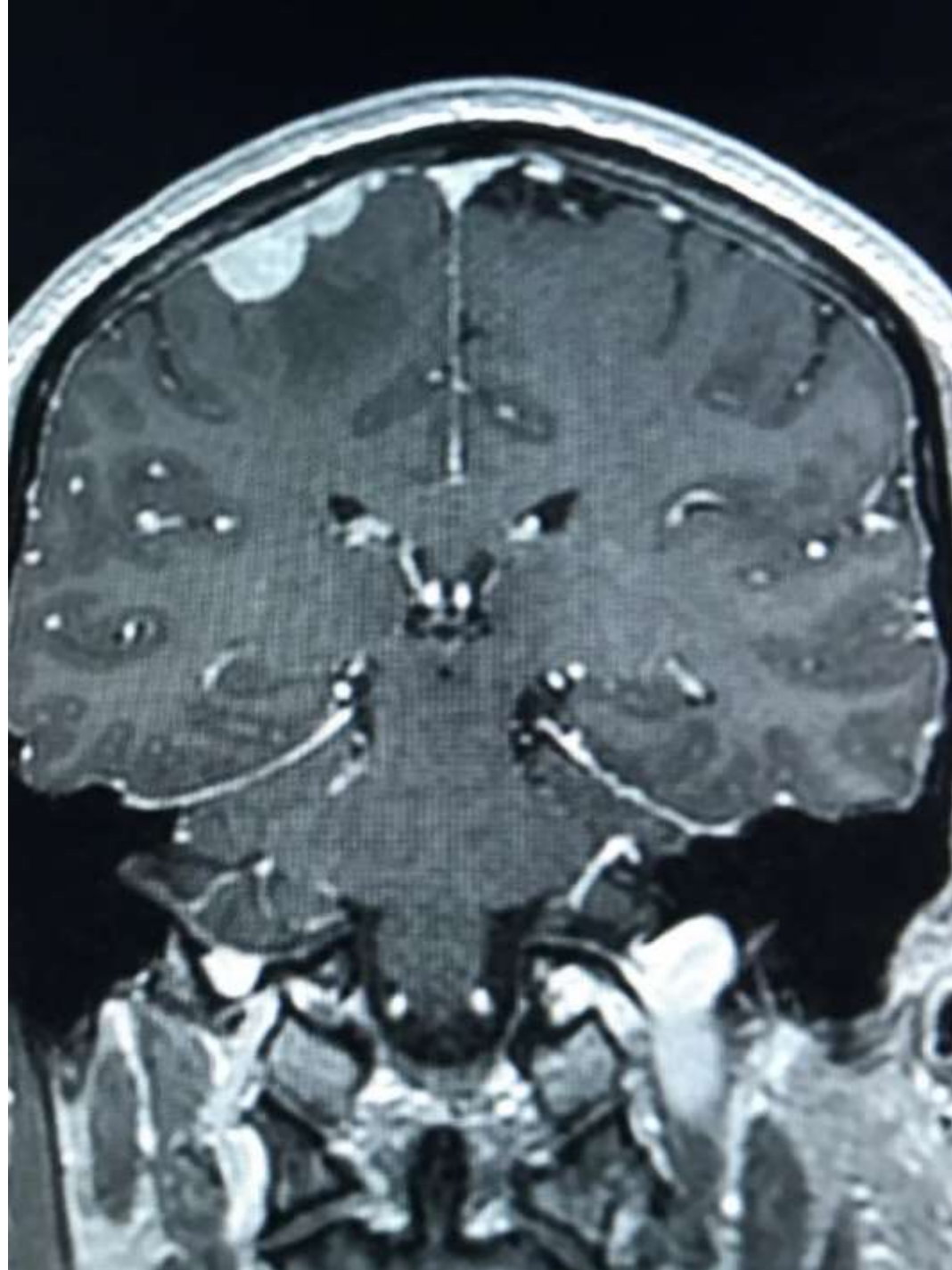




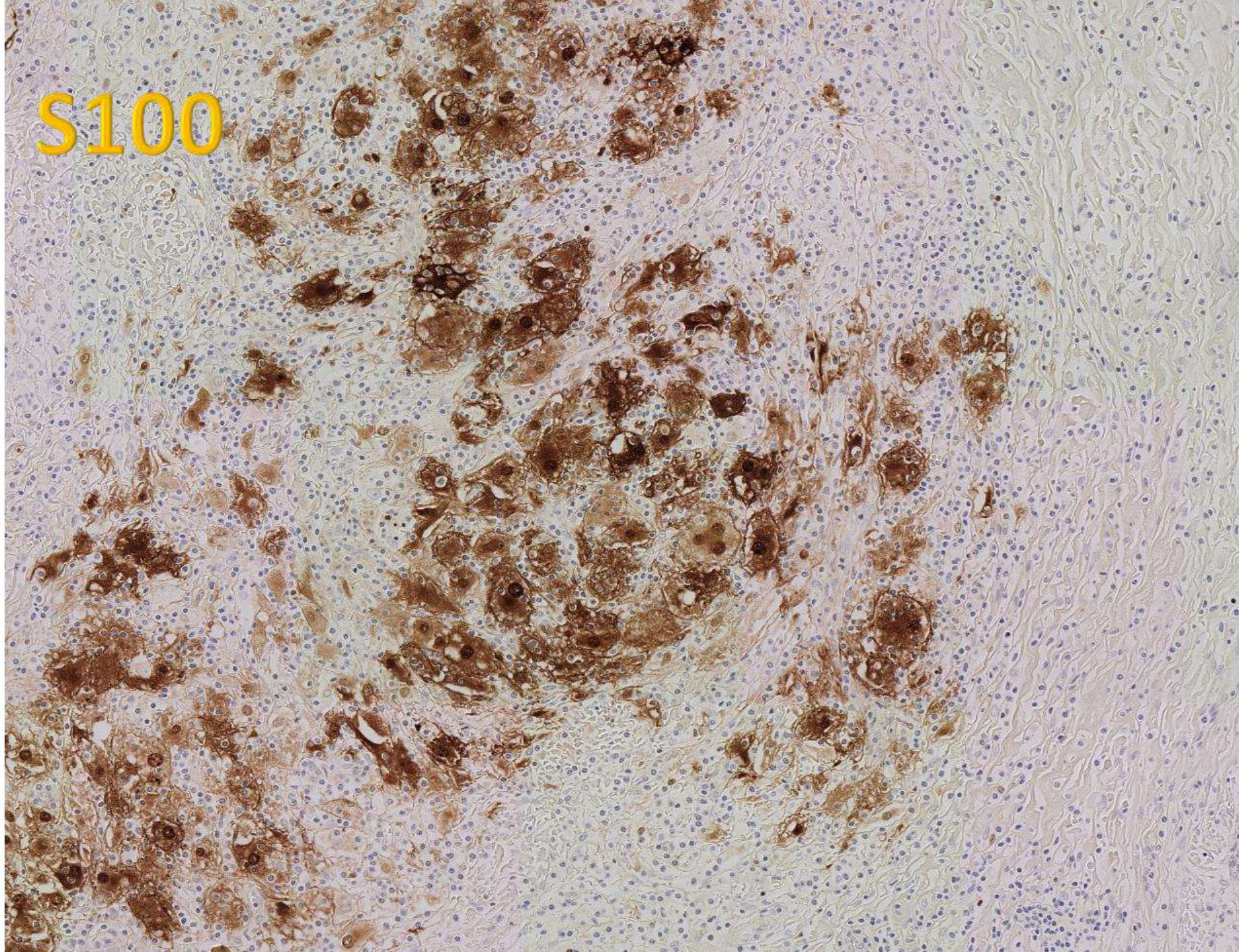


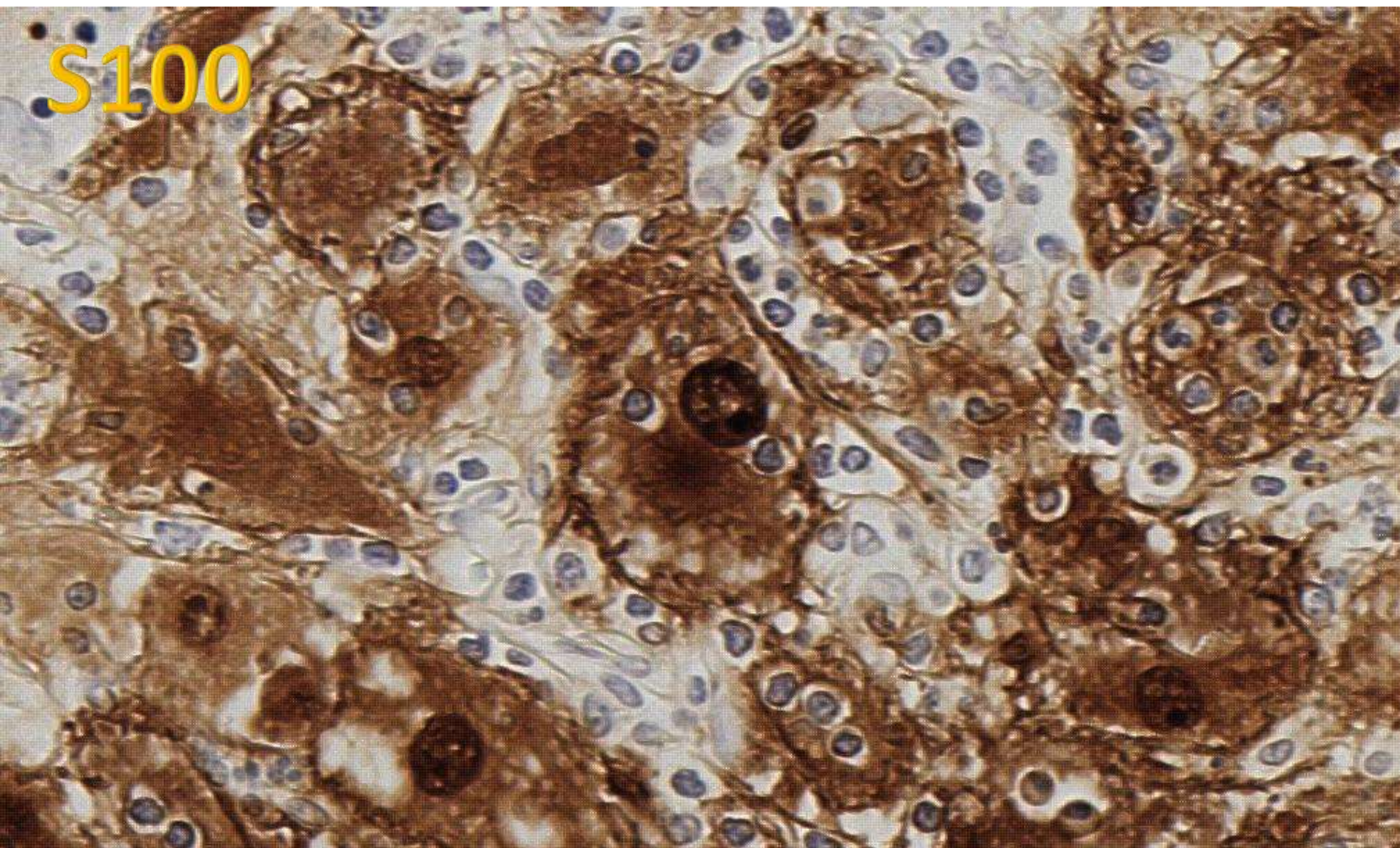






S100





S100

Rosai-Dorfman Disease

Clinical (slide 1)

Lymphadenopathy (fever, night sweats)

40% extranodal

Isolated, regional

Multiple sites

Associated with other diseases

Autoimmune disorders

Other malignancies (lymphoma)

Rosai-Dorfman Disease

Extranodal sites (slide 2)

Skin

Intracranial and intraspinal – usually dural based

Soft tissue

Intraorbital

Upper aerodigestive tract

Pulmonary (interstitial or nodular)

Genitourinary

G.I. tract

Bone

Rosai-Dorfman Disease

Pathology (slide 3)

- **Characteristic histiocytes with emperipolesis**
- **Plasma cells**
 - **R-D changes present in at least 10% of the lesion**
- **IHC**
 - **S100 +**
 - **CD68 +**
 - **CD1a -**

Rosai-Dorfman Disease

Diagnostic challenges (slide 4)

You have to include this in your DD

- **Especially in unusual anatomic locations**
- **When plasma cells are abundant obscuring the histiocytes**
- **When there are microabscesses (? infection)**
- **When there is abundant fibrosis with a storiform pattern suggesting a fibrohistiocytic neoplasm**

Rosai-Dorfman Disease

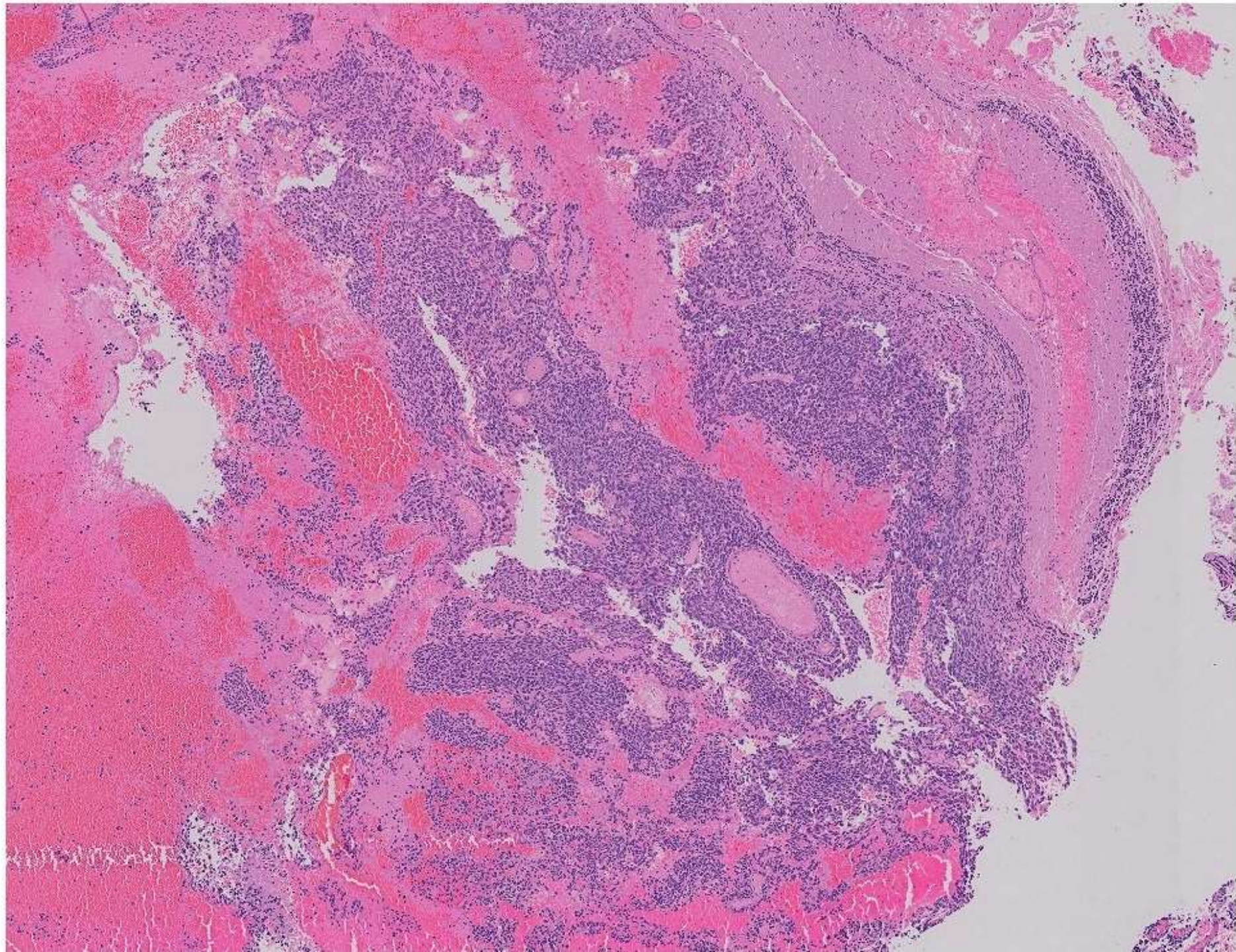
Management (slide 5)

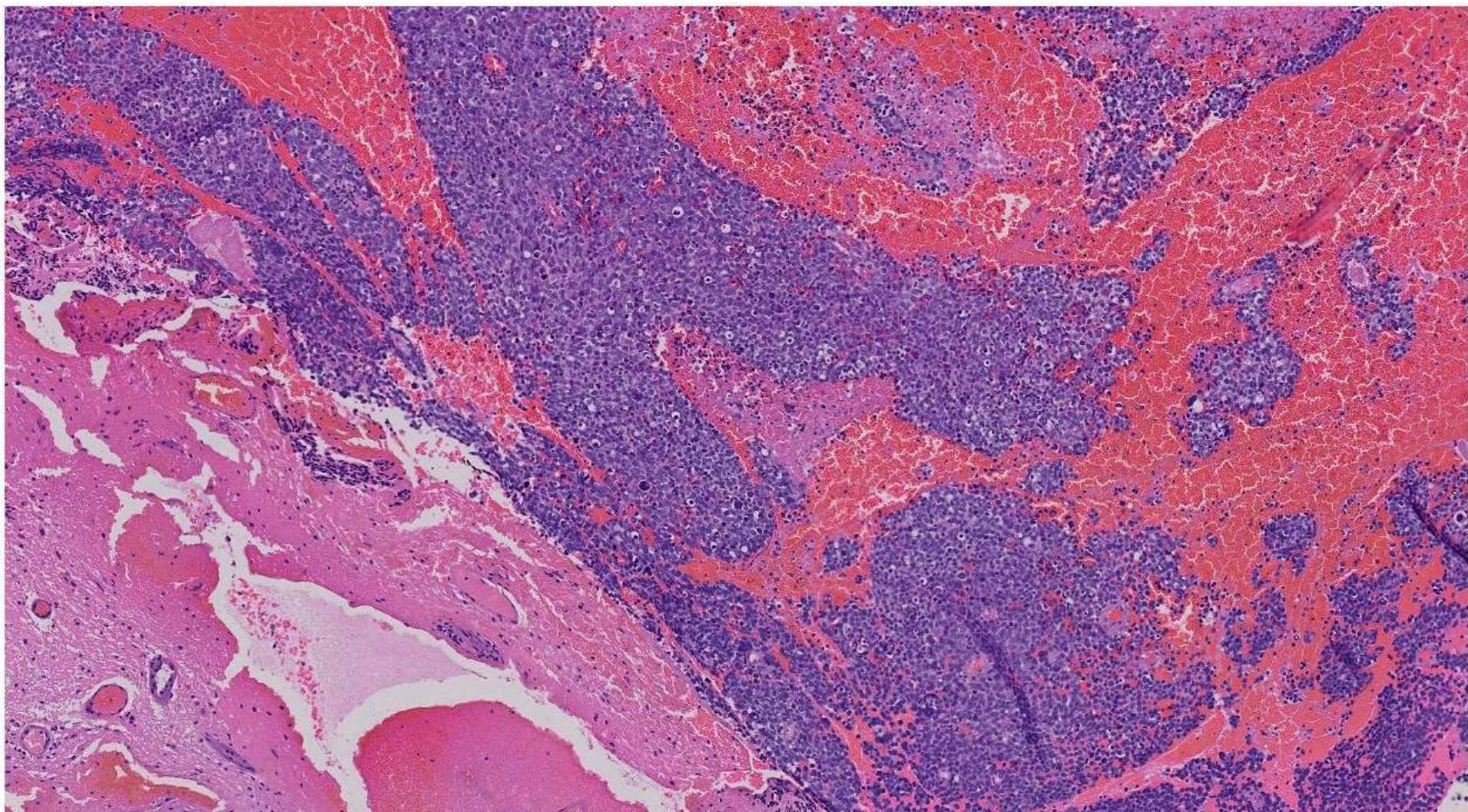
- **Observation**
- **Surgical excision**
- **Steroids**
- **Radiation**
- **Chemotherapy**
- **Immunomodulatory agents**

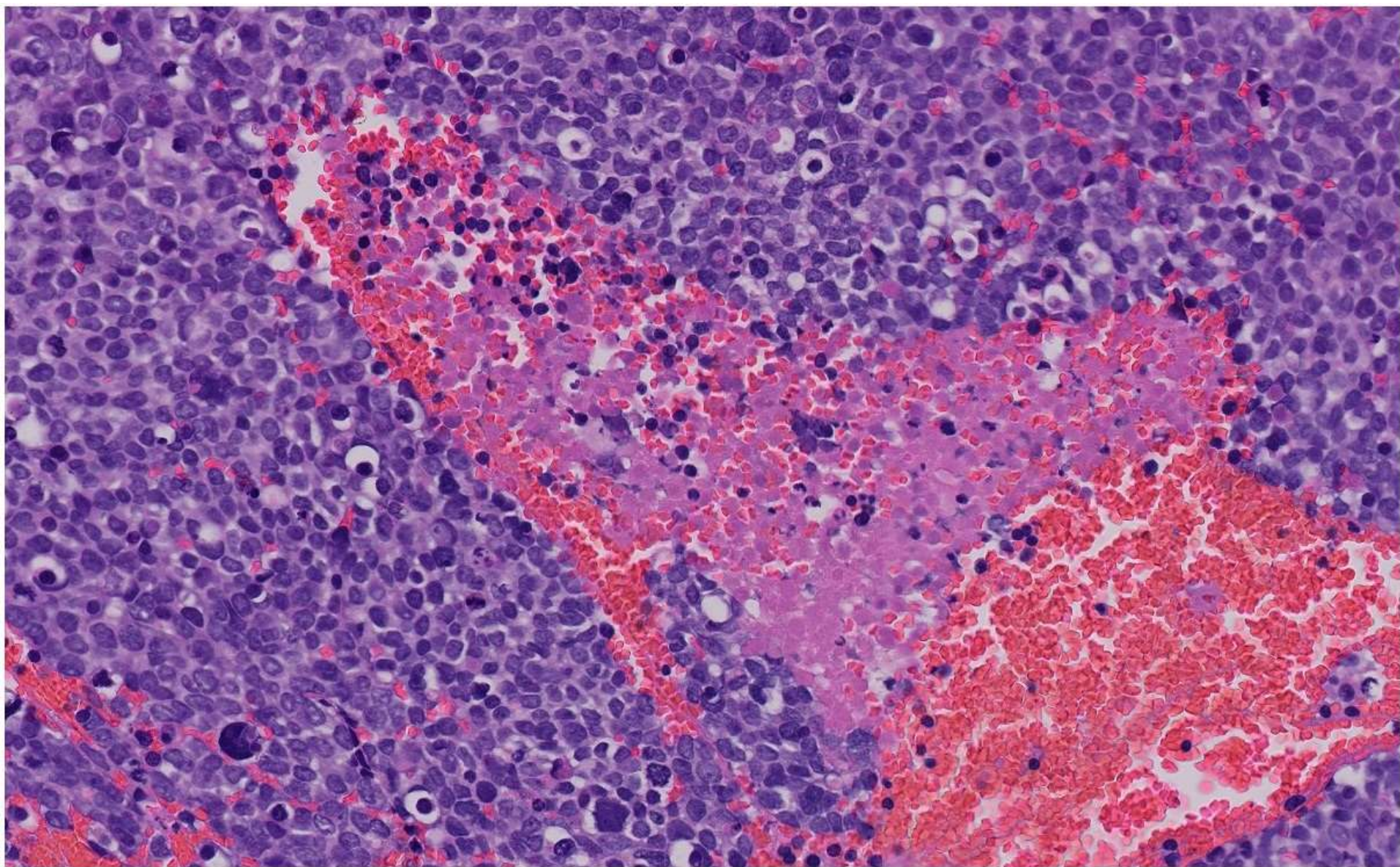
20-1006

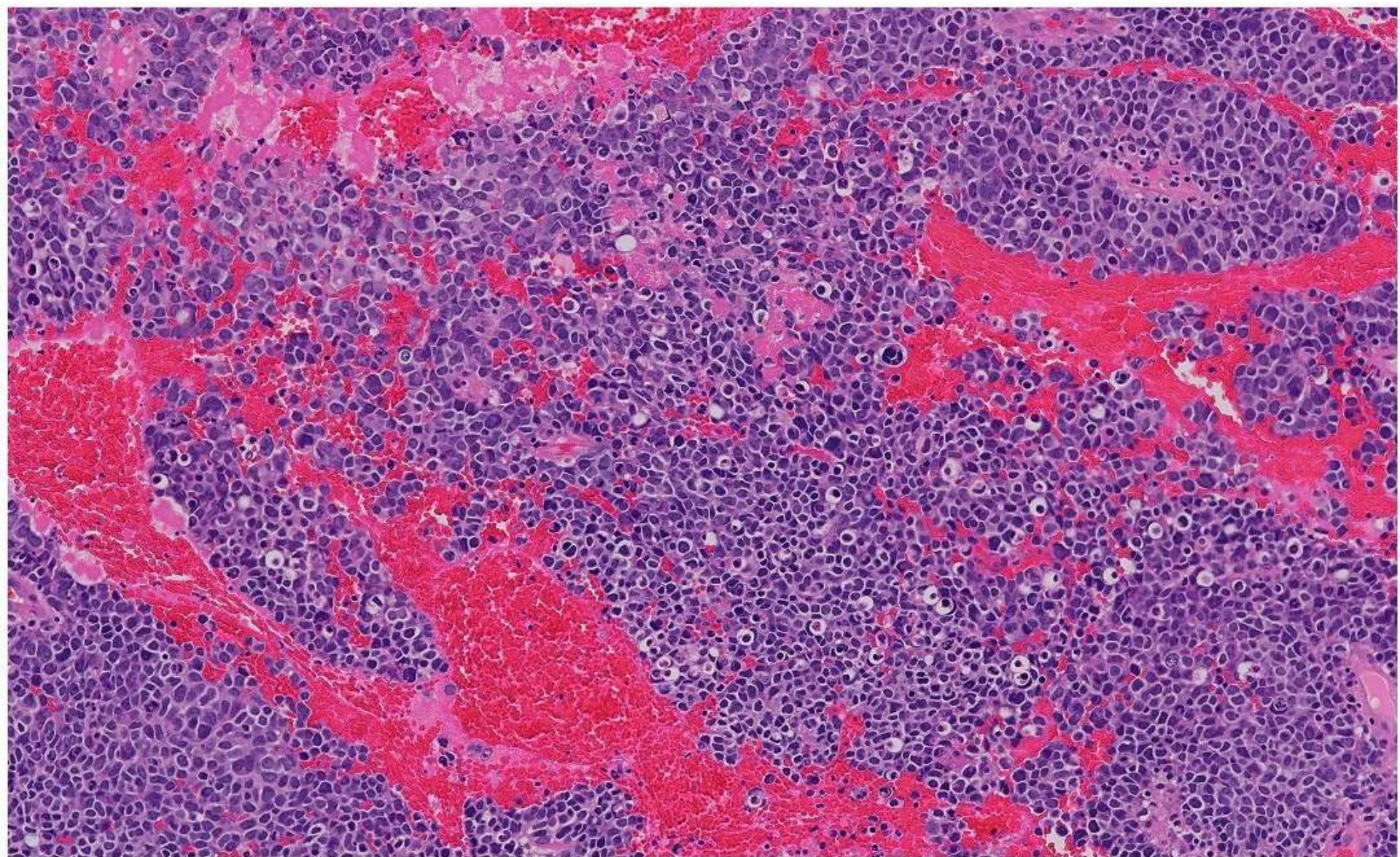
Angus Toland/Hannes Vogel; Stanford

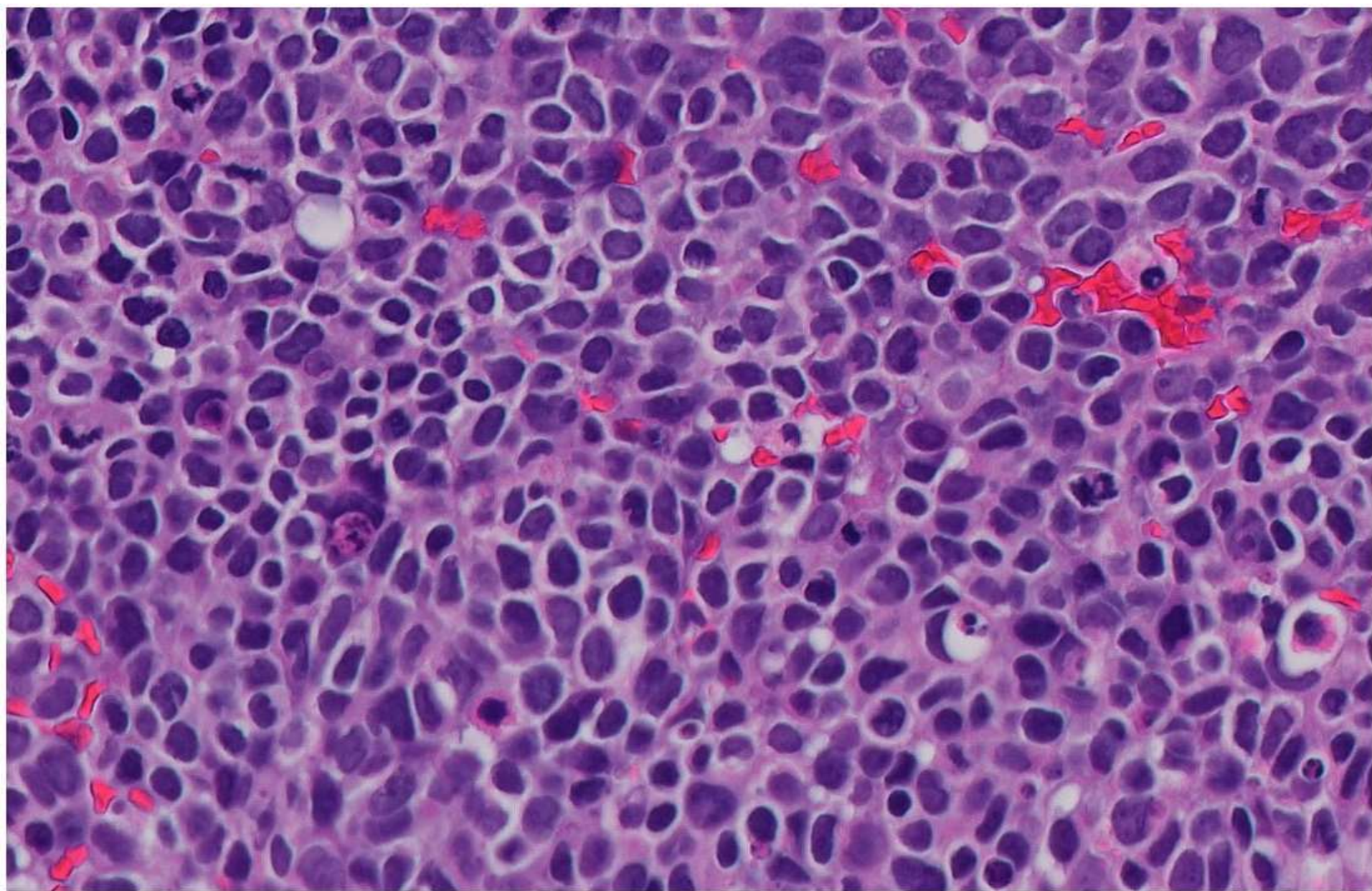
62-year-old M presenting with dizziness and altered mental status changes. MRI demonstrates 5x4x3.7cm mass with nodular heterogenous enhancement in the right cerebellum.





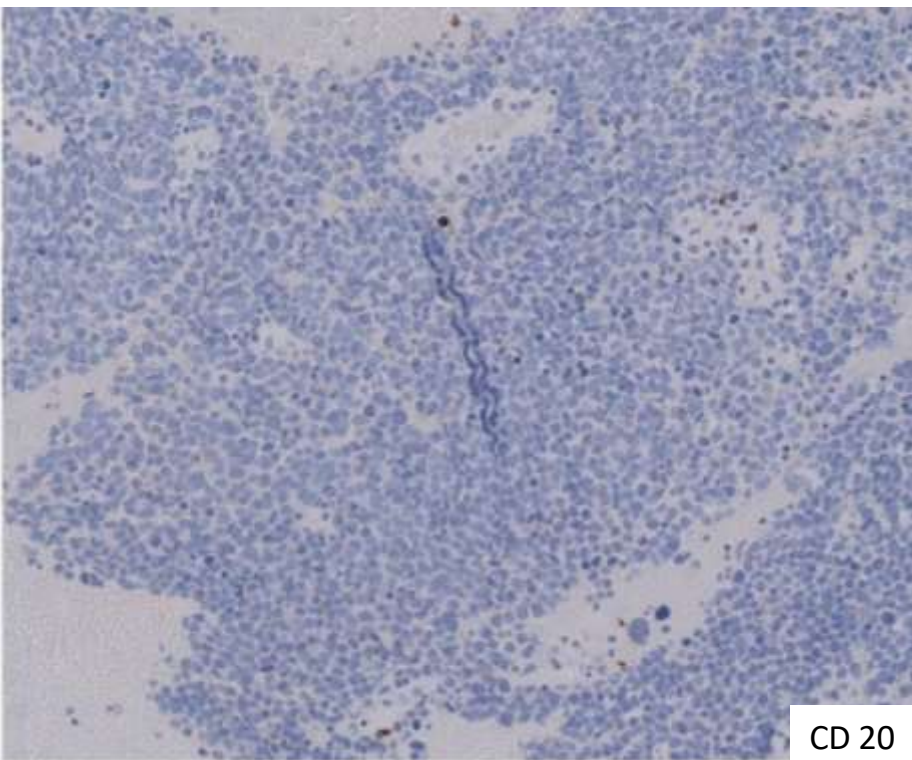




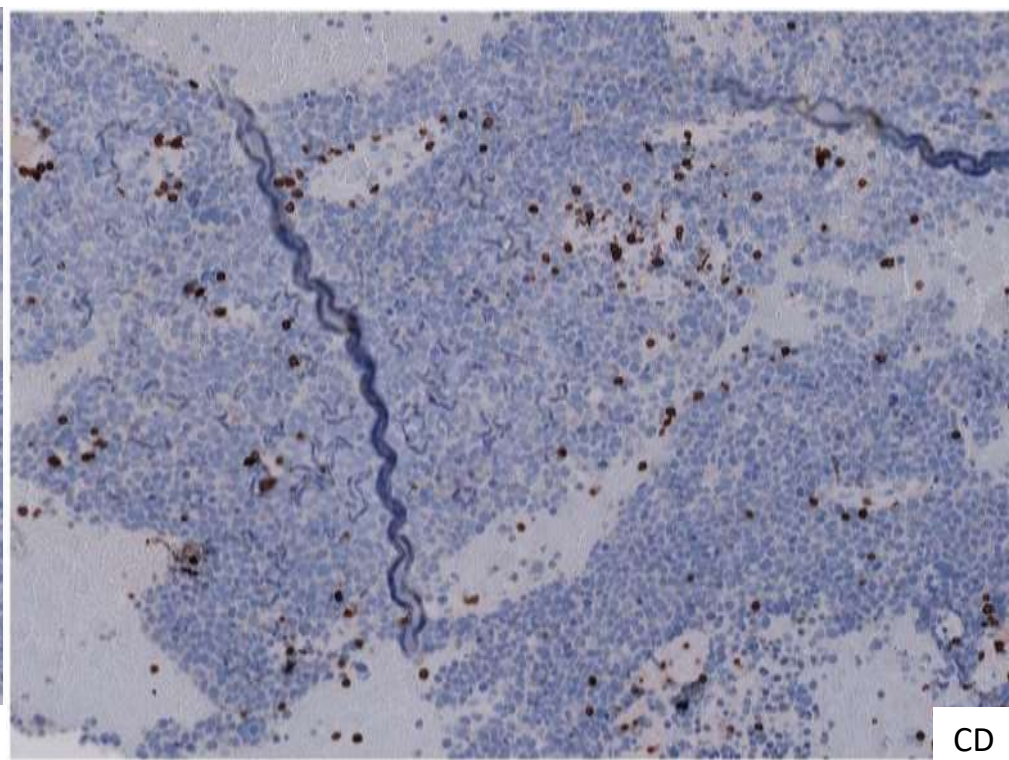


Differential Diagnosis

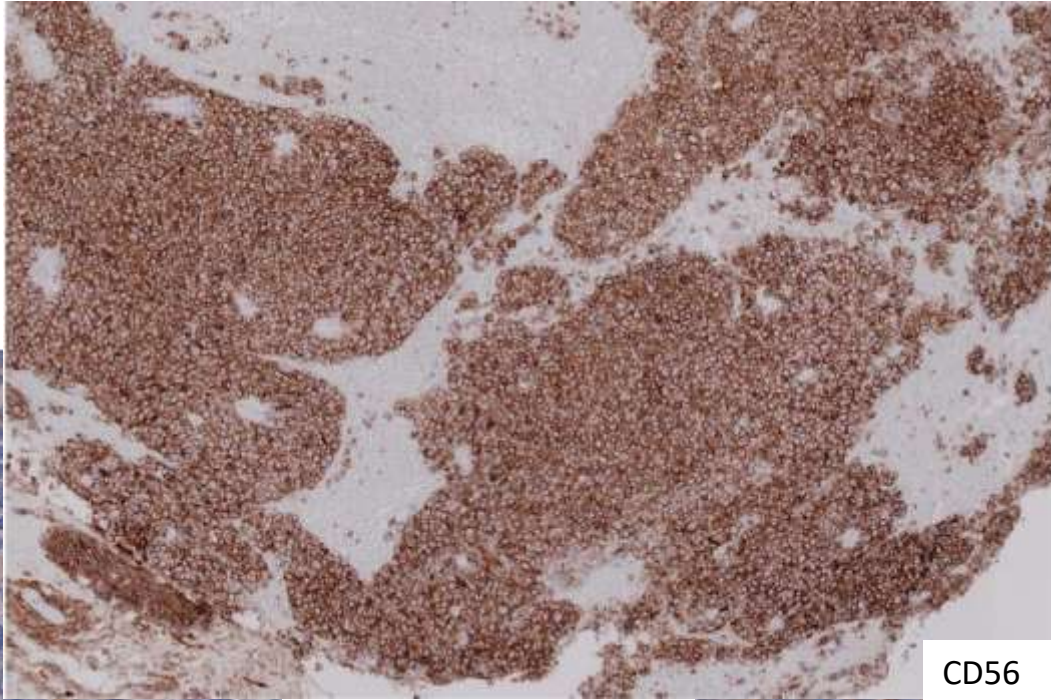
- High-grade lymphoma
- Metastatic melanoma
- Metastatic carcinoma
- Poorly-differentiated sarcoma
- Medulloblastoma/other embryonal tumor



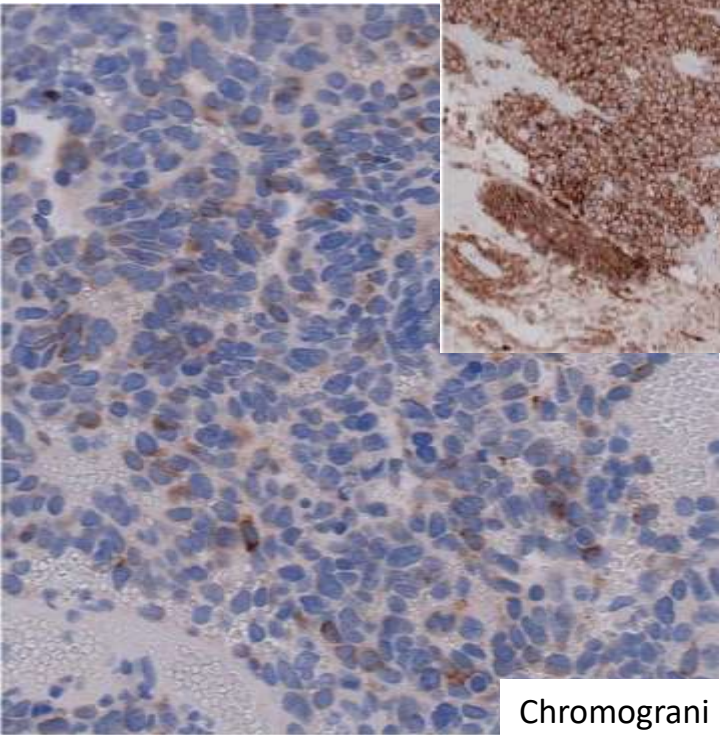
CD 20



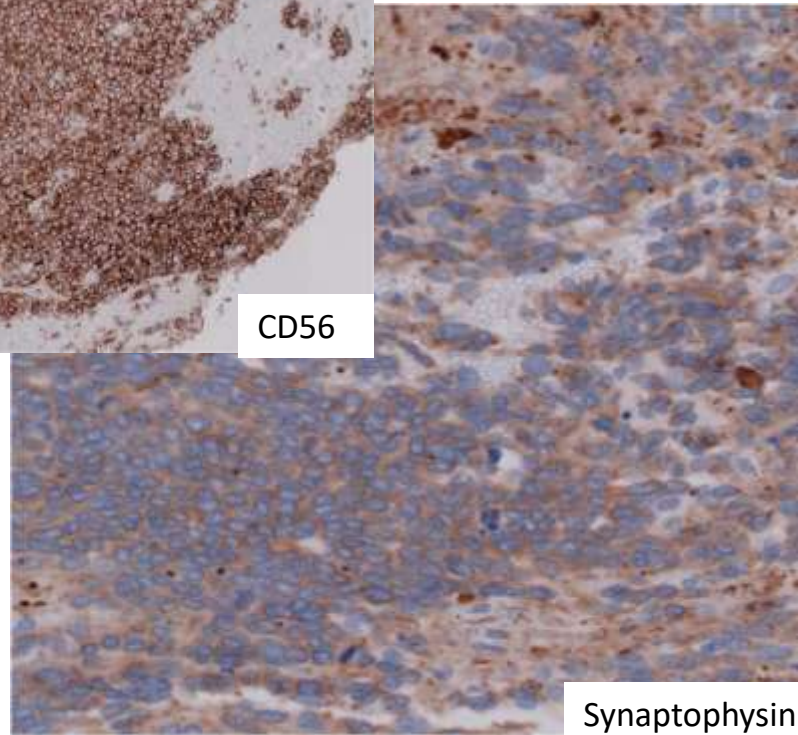
CD
3



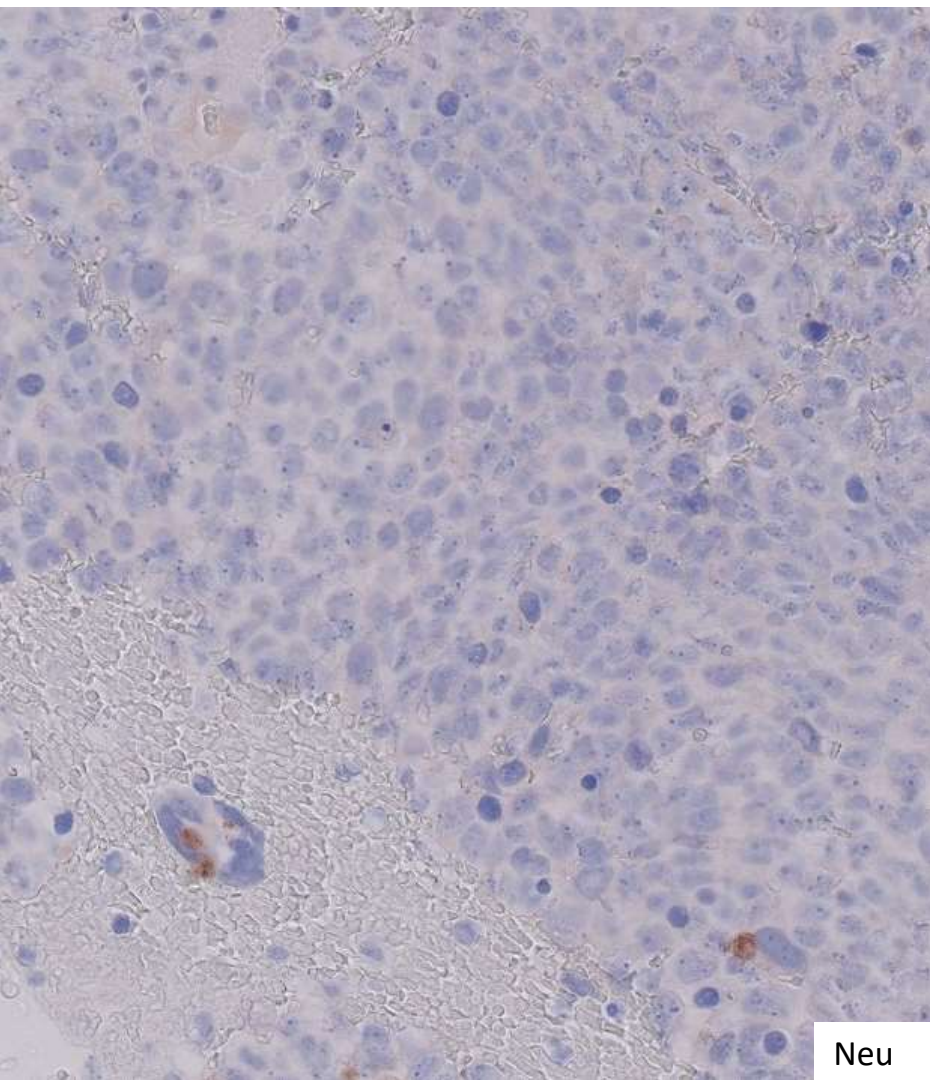
CD56



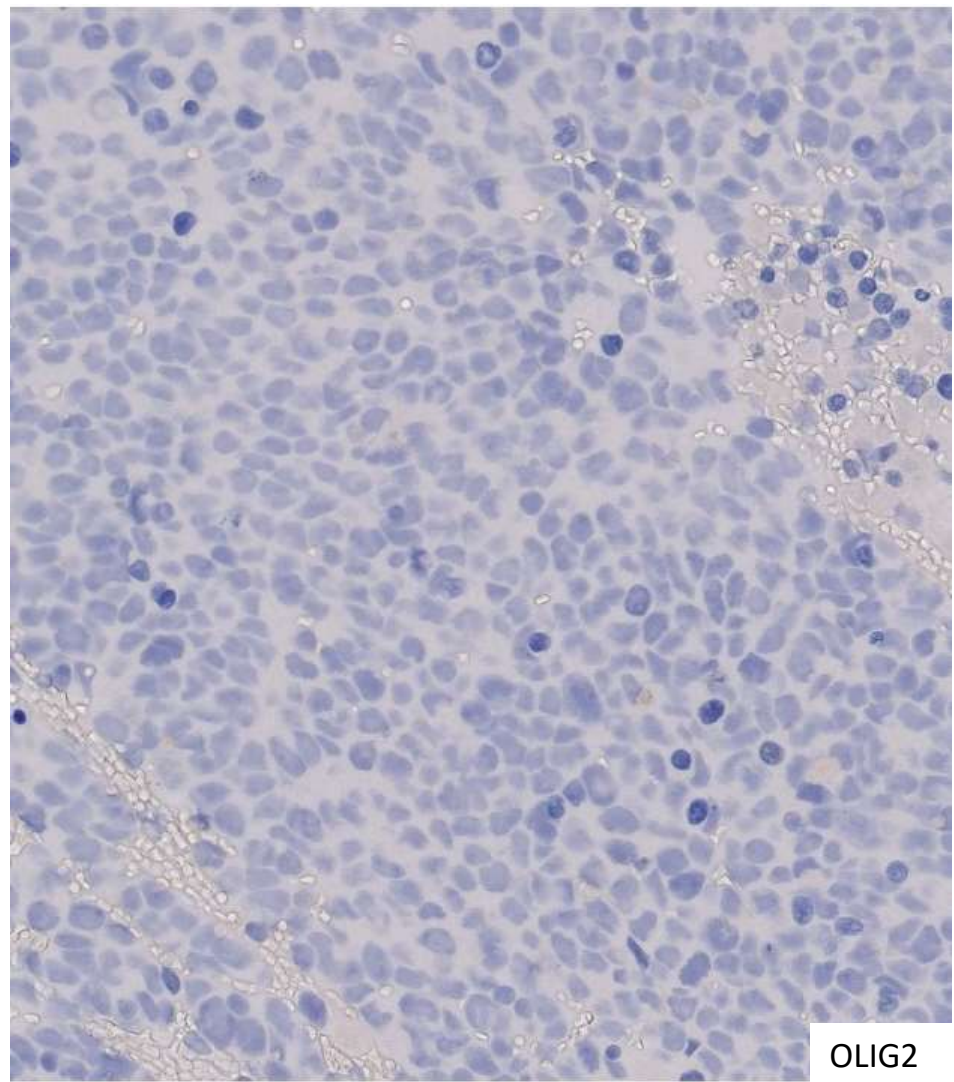
Chromogranin



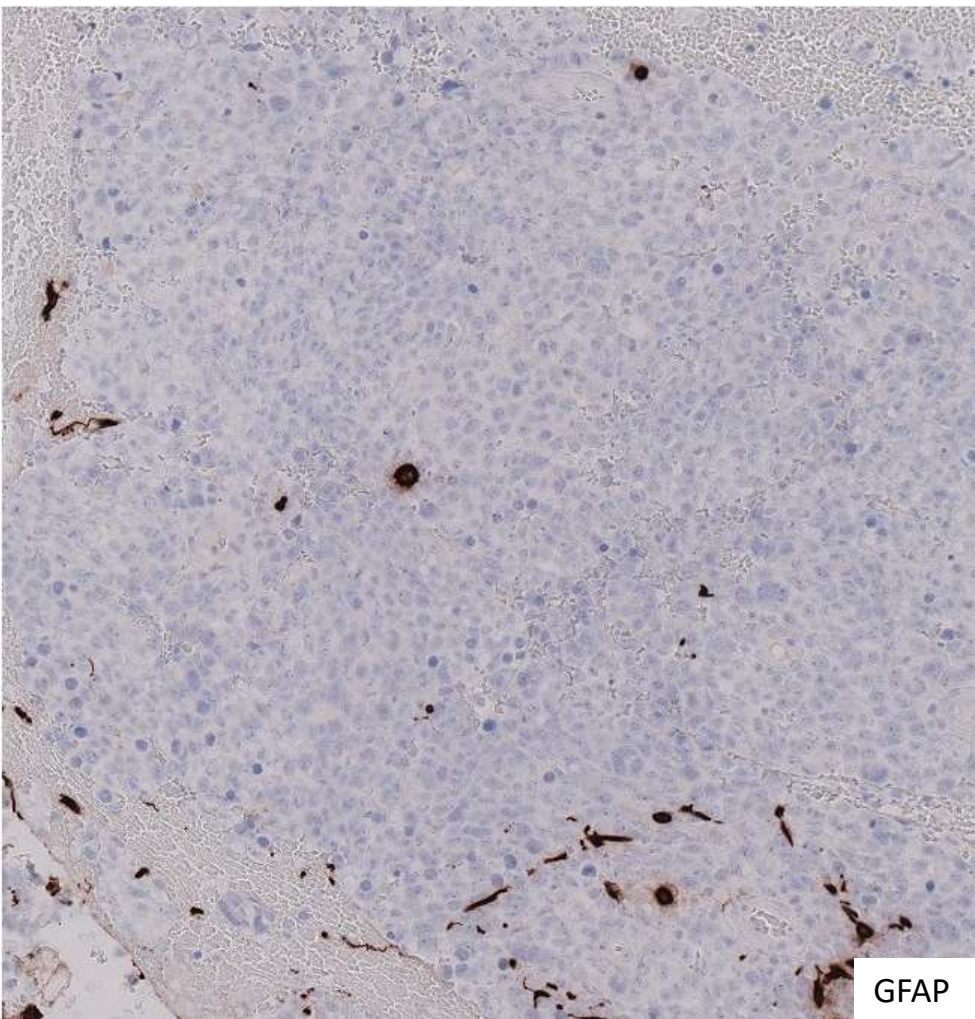
Synaptophysin



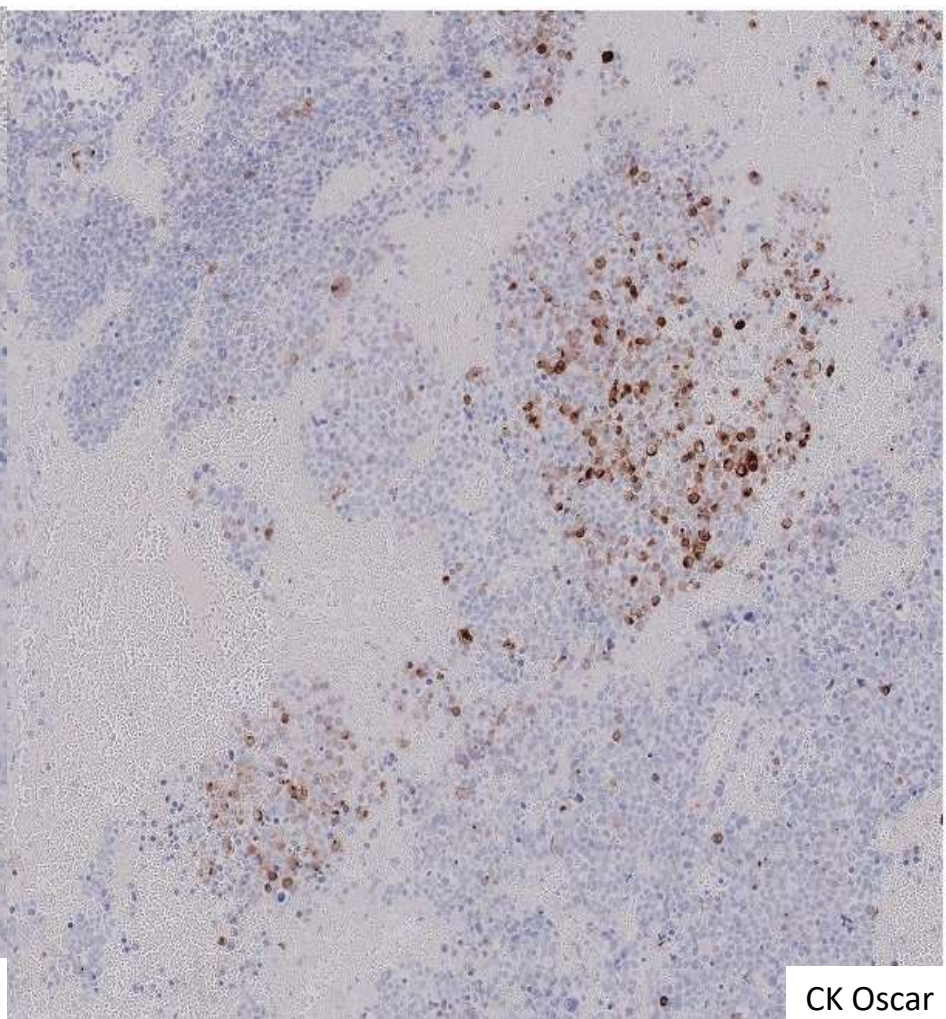
Neu
N



OLIG2



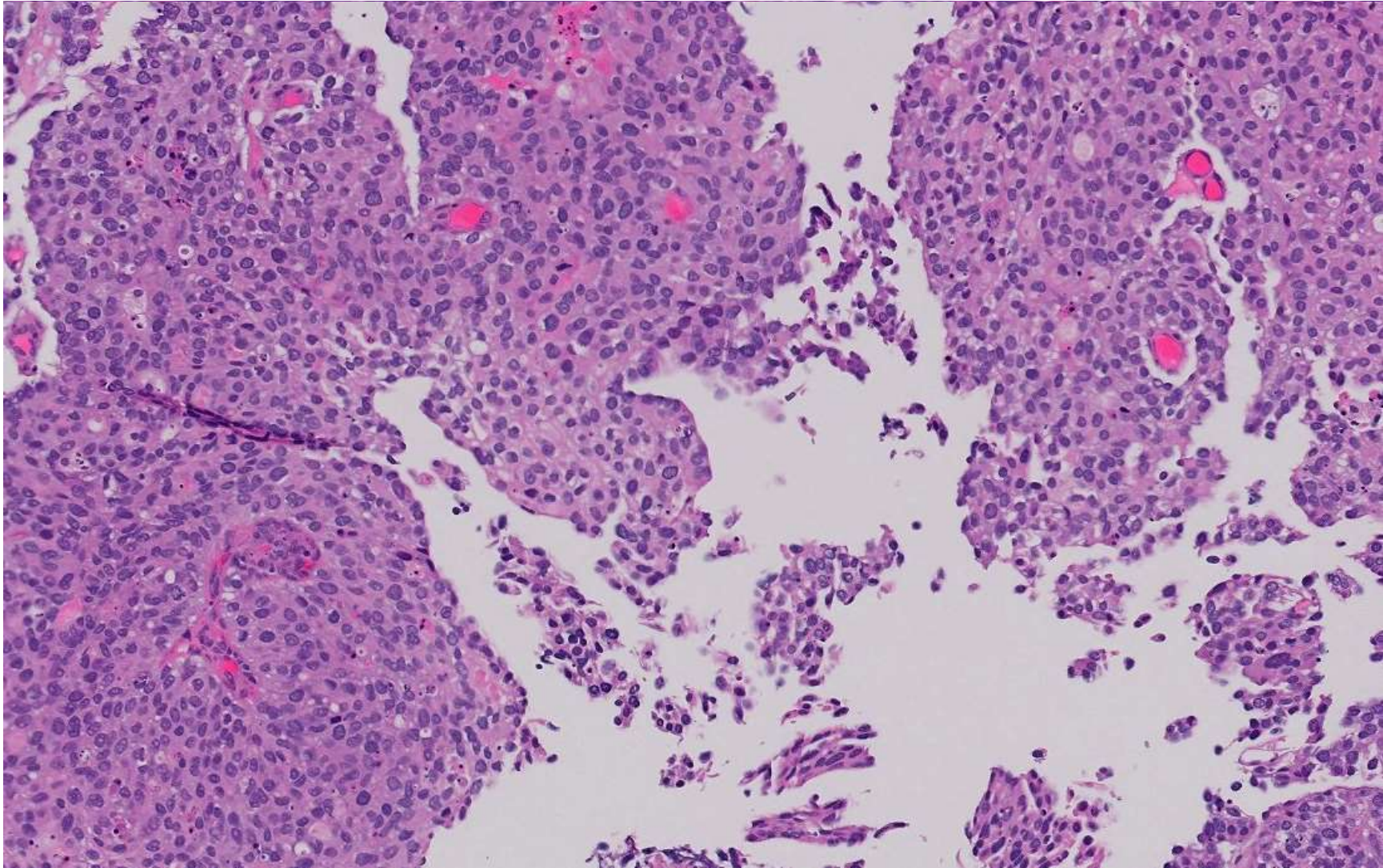
GFAP

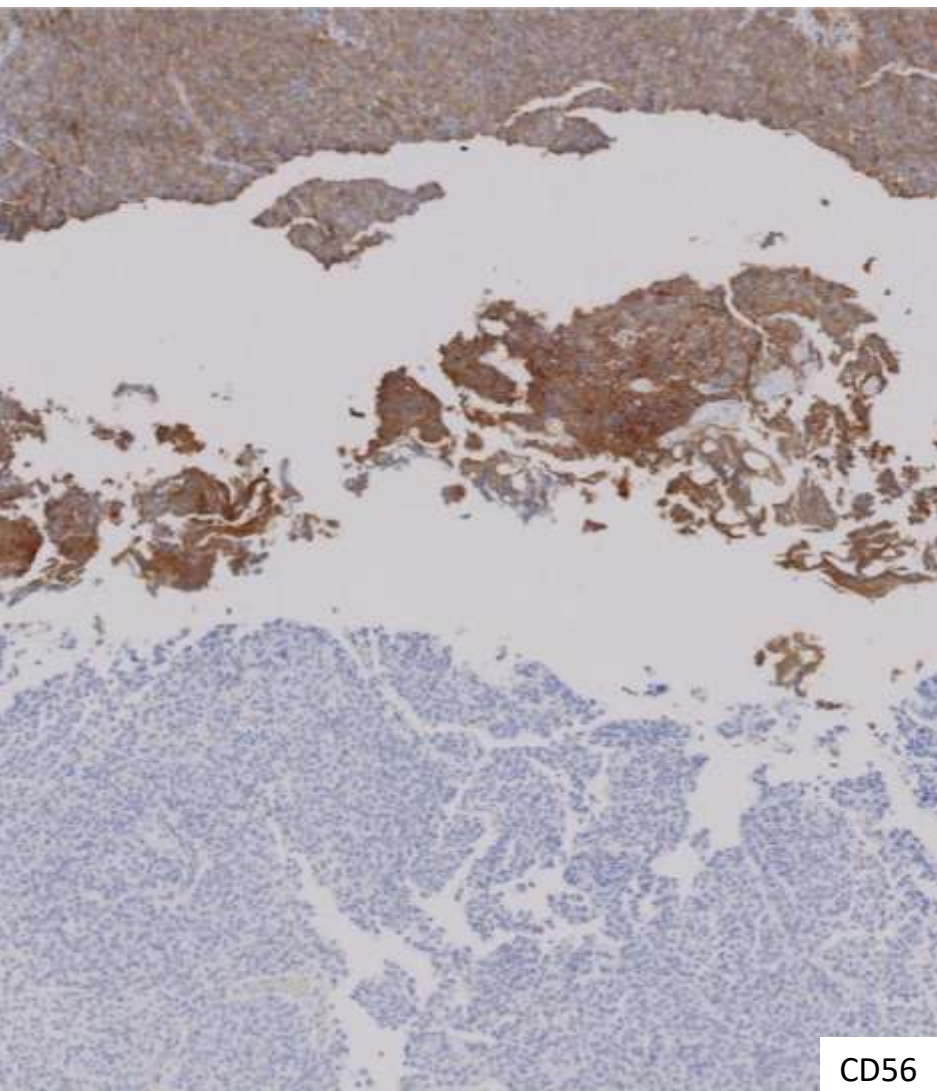


CK Oscar

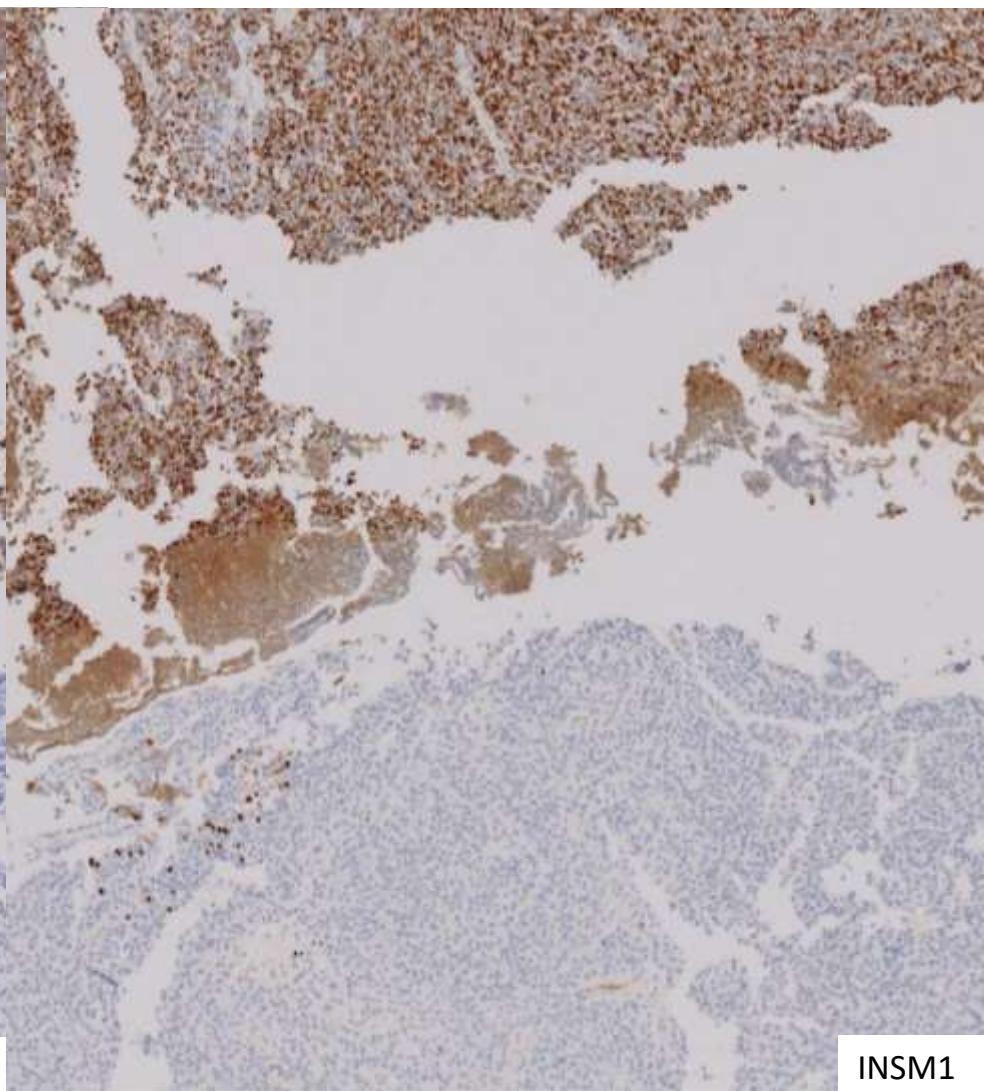
Metastatic neuroendocrine carcinoma

- Negative for:
 - TTF-1
 - Sox10/S100/Melan A/HMB45
 - CK mix
 - GATA3
 - CD99
- Prior biopsy reviewed as a consult





CD56



INSM1

Small Cell Carcinoma of the Urinary Bladder

- <1% of all bladder carcinomas
- Frequently present at advanced stage; worse prognosis than urothelial carcinoma at higher stages
- Often mixed histology with other carcinoma subtypes (invasive urothelial and urothelial CIS)
- Express neuroendocrine markers: synaptophysin, chromogranin, CD56, (INSM1)
 - Weakly express cytokeratins: pan-CK (89%; 8/9), CK7 (47%; 9/19), HMWCK (60%; 3/5), and CAM5.2 (100%; 6/6)

Table 2 Immunohistochemical features of bladder SmCC

Antibody	Source	Dilution	No. cases tested	No. positive cases
Synaptophysin	Leica Biosystems	1:600	56	41 (73%)
Chromogranin A	Millipore	1:4000	55	26 (47%)
CD56	Life Technologies	1:100	41	39 (95%)
NSE	Cell Marque	1:3	4	4 (100%)
CAM5.2	BD Biosciences	1:50	6	6 (100%)
AE1/AE3	Dako	1:100	9	8 (89%)
CK5/6	Dako	1:50	25	9 (36%)
CK7	Dako	1:100	19	17 (89%)
CK14	BioGenex	1:50	25	0 (0%)
CK20	Dako	1:4000	17	0 (0%)
CK903	Dako	1:100	5	3 (60%)
GATA-3	Santa Cruz	1:100	30	1 (3%)
Uroplakin II	Biocare	1:100	22	1 (5%)
p63	Santa Cruz	1:1000	6	1 (17%)
Thrombomodulin	Dako	1:10	2	0 (0%)
RB1	Millipore	1:30	23	2 (9%)



Original contribution

Small cell carcinoma of the urinary bladder: a clinicopathological and immunohistochemical analysis of 81 cases☆☆☆

Gang Wang MD, PhD^a, Li Xiao MD^a, Miao Zhang MD, PhD^a, Ashish M. Kamat MD^b, Arlene Siefker-Radtke MD^c, Colin P. Dinney MD^b, Bogdan Czerniak MD, PhD^a, Charles C. Guo MD^{a,*}

^aDepartment of Pathology, The University of Texas MD Anderson Cancer Center, Houston, TX, 77030, USA

^bDepartment of Urology, The University of Texas MD Anderson Cancer Center, Houston, TX, 77030, USA

^cDepartment of Genitourinary Medical Oncology, The University of Texas MD Anderson Cancer Center, Houston, TX, 77030, USA

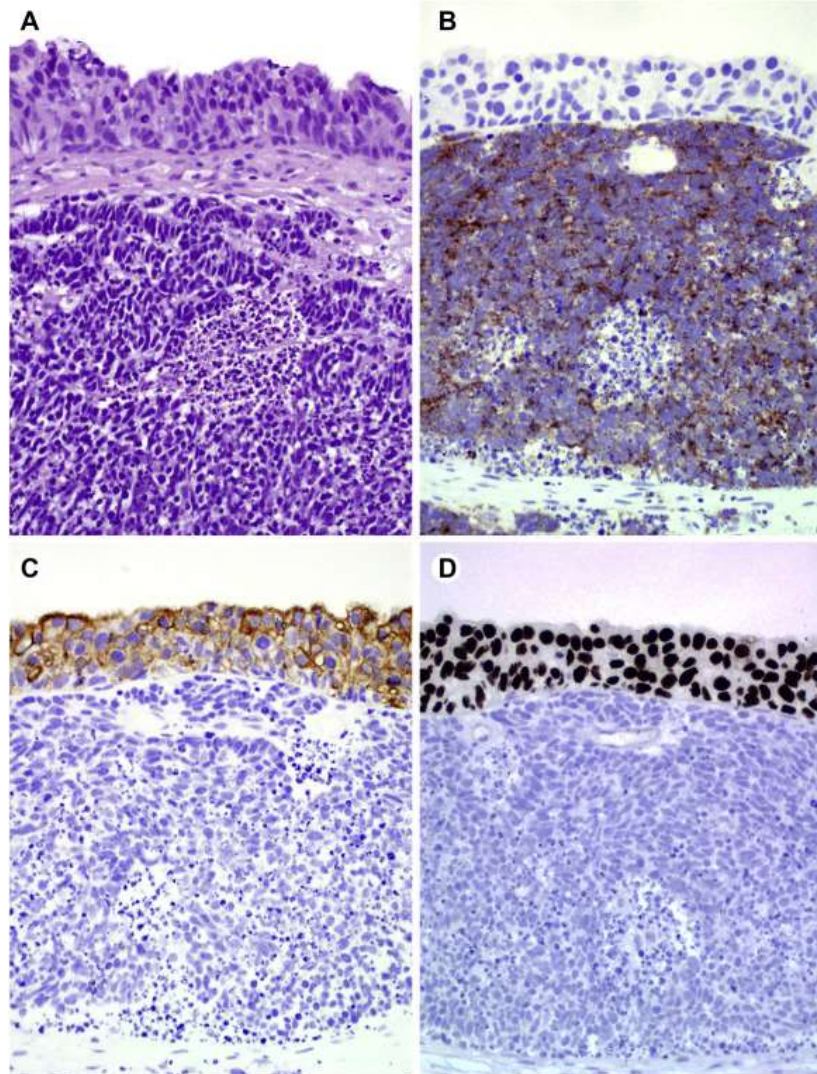
Received 11 January 2018; revised 25 April 2018; accepted 4 May 2018

Keywords:

Bladder cancer;
Small cell carcinoma;
Urothelial carcinoma;
Neuroendocrine
differentiation;
Immunohistochemistry;
Retinoblastoma gene

Summary Small cell carcinoma (SmCC) of the bladder is a rare disease. We retrospectively studied a large series of bladder SmCC from a single institution. The patients included 69 men and 12 women with a mean age of 68 years. Most bladder SmCCs were presented at advanced stage, with tumors invading the muscularis propria and beyond (n = 77). SmCC was pure in 27 cases and mixed with other histologic types in 54 cases, including urothelial carcinoma (UC) (n = 32), UC in situ (n = 26), glandular (n = 14), micropapillary (n = 4), sarcomatoid (n = 4), squamous (n = 3), and plasmacytoid (n = 1) features. Most SmCCs expressed neuroendocrine markers synaptophysin (41/56), chromogranin (26/55), and CD56 (39/41); however, they did not express UC luminal markers CK20 (0/17), GATA3 (1/30), and uroplakin II (1/22). Some SmCCs showed focal expression of CK5/6 (9/25), a marker for the basal molecular subtype. Furthermore, expression of the retinoblastoma 1 (*RB1*) gene protein was lost in most of the bladder SmCCs (2/23). The patients' survival was significantly associated with cancer stage but did not show a significant difference between mixed and pure SmCCs. Compared with conventional UC at similar stages, SmCC had a worse prognosis only when patients developed metastatic diseases. In conclusion, bladder SmCC is an aggressive disease that is frequently present at an advanced stage. A fraction of SmCCs show a basal molecular subtype, which may underlie its good response to chemotherapy. Inactivation of the *RB1* gene may be implicated in the oncogenesis of bladder SmCC.

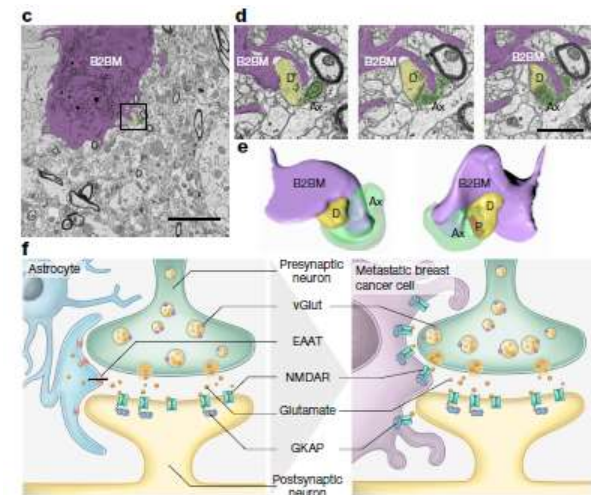
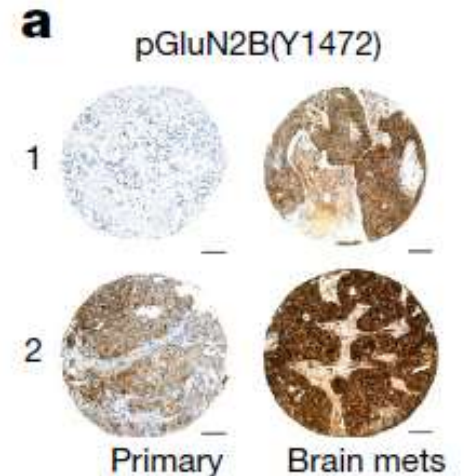
© 2018 Elsevier Inc. All rights reserved.



Synaptic proximity enables NMDAR signalling to promote brain metastasis

Qiqun Zeng^{1,2}, Iacovos P. Michael^{1,2}, Peng Zhang³, Sadegh Saghafeina^{1,2,4,5}, Graham Knott⁶, Wei Jiao⁷, Brian D. McCabe⁷, José A. Galván⁸, Hugh P. C. Robinson⁹, Inti Zlobec⁸, Giovanni Ciriello^{2,4,5} & Douglas Hanahan^{1,2*}

Metastasis—the disseminated growth of tumours in distant organs—underlies cancer mortality. Breast-to-brain metastasis (B2BM) is a common and disruptive form of cancer and is prevalent in the aggressive basal-like subtype, but is also found at varying frequencies in all cancer subtypes. Previous studies revealed parameters of breast cancer metastasis to the brain, but its preference for this site remains an enigma. Here we show that B2BM cells co-opt a neuronal signalling pathway that was recently implicated in invasive tumour growth, involving activation by glutamate ligands of N-methyl-D-aspartate receptors (NMDARs), which is key in model systems for metastatic colonization of the brain and is associated with poor prognosis. Whereas NMDAR activation is autocrine in some primary tumour types, human and mouse B2BM cells express receptors but secrete insufficient glutamate to induce signalling, which is instead achieved by the formation of pseudo-tripartite synapses between cancer cells and glutamatergic neurons, presenting a rationale for brain metastasis.



Wang G, Xiao L, Zhang M, Kamat AM, Siefker-Radtke A, Dinney CP, Czerniak B, Guo CC. Small cell carcinoma of the urinary bladder: a clinicopathological and immunohistochemical analysis of 81 cases. *Hum Pathol*. 2018 Sep;79:57-65. doi: 10.1016/j.humpath.2018.05.005. Epub 2018 May 12. PMID: 29763719; PMCID: PMC6133751.

Xiao GQ, Barrett MM, Yang Q, Unger PD. Clinicopathologic and Immunohistochemical Study of Combined Small Cell Carcinoma and Urothelial Carcinoma Molecular Subtype. *Pathol Oncol Res*. 2019 Jul;25(3):889-895. doi: 10.1007/s12253-017-0369-1. Epub 2017 Dec 16. PMID: 29249035.

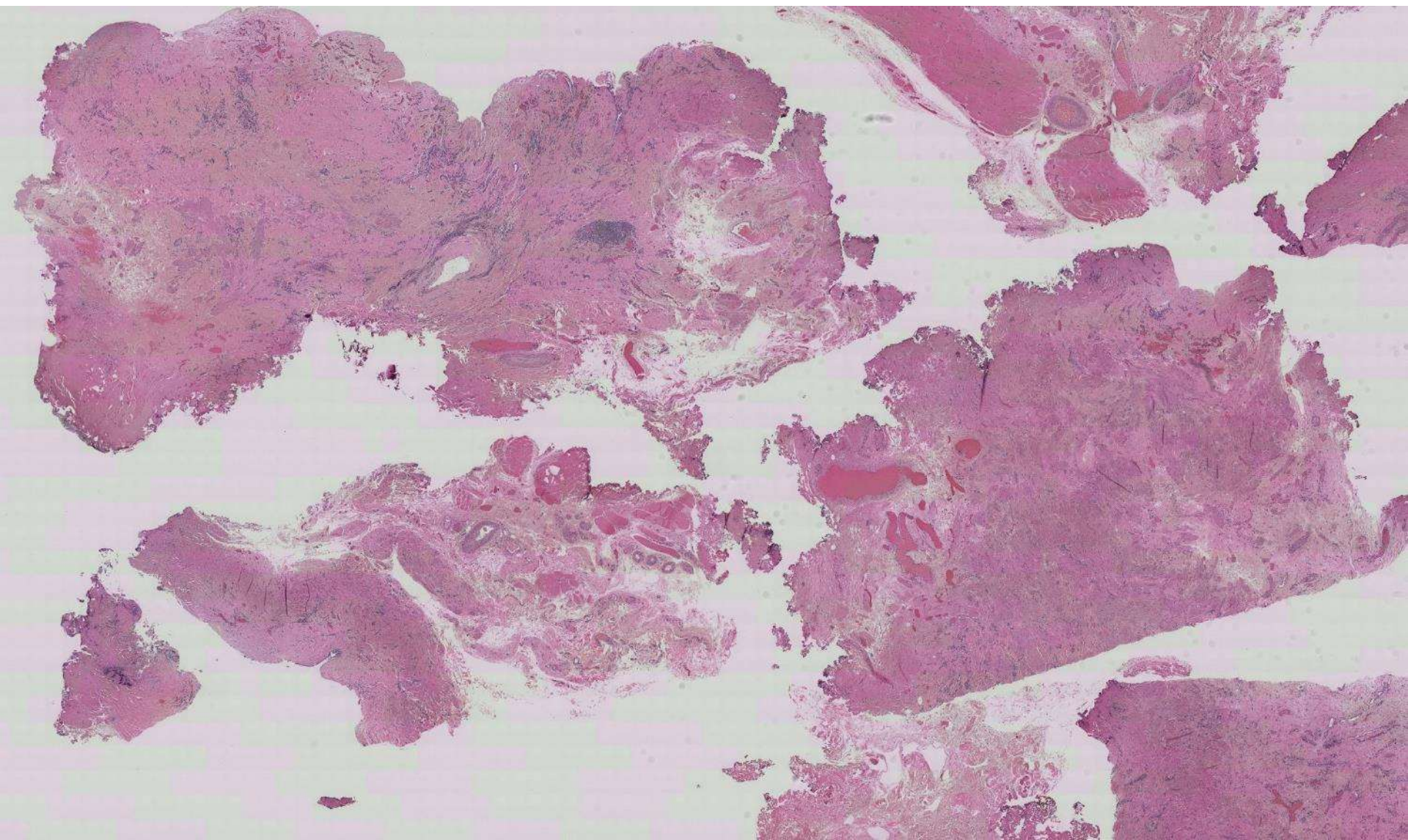
Zeng Q, Michael IP, Zhang P, Saghafeinia S, Knott G, Jiao W, McCabe BD, Galván JA, Robinson HPC, Zlobec I, Ciriello G, Hanahan D. Synaptic proximity enables NMDAR signalling to promote brain metastasis. *Nature*. 2019 Sep;573(7775):526-531. doi: 10.1038/s41586-019-1576-6. Epub 2019 Sep 18. PMID: 31534217; PMCID: PMC6837873.

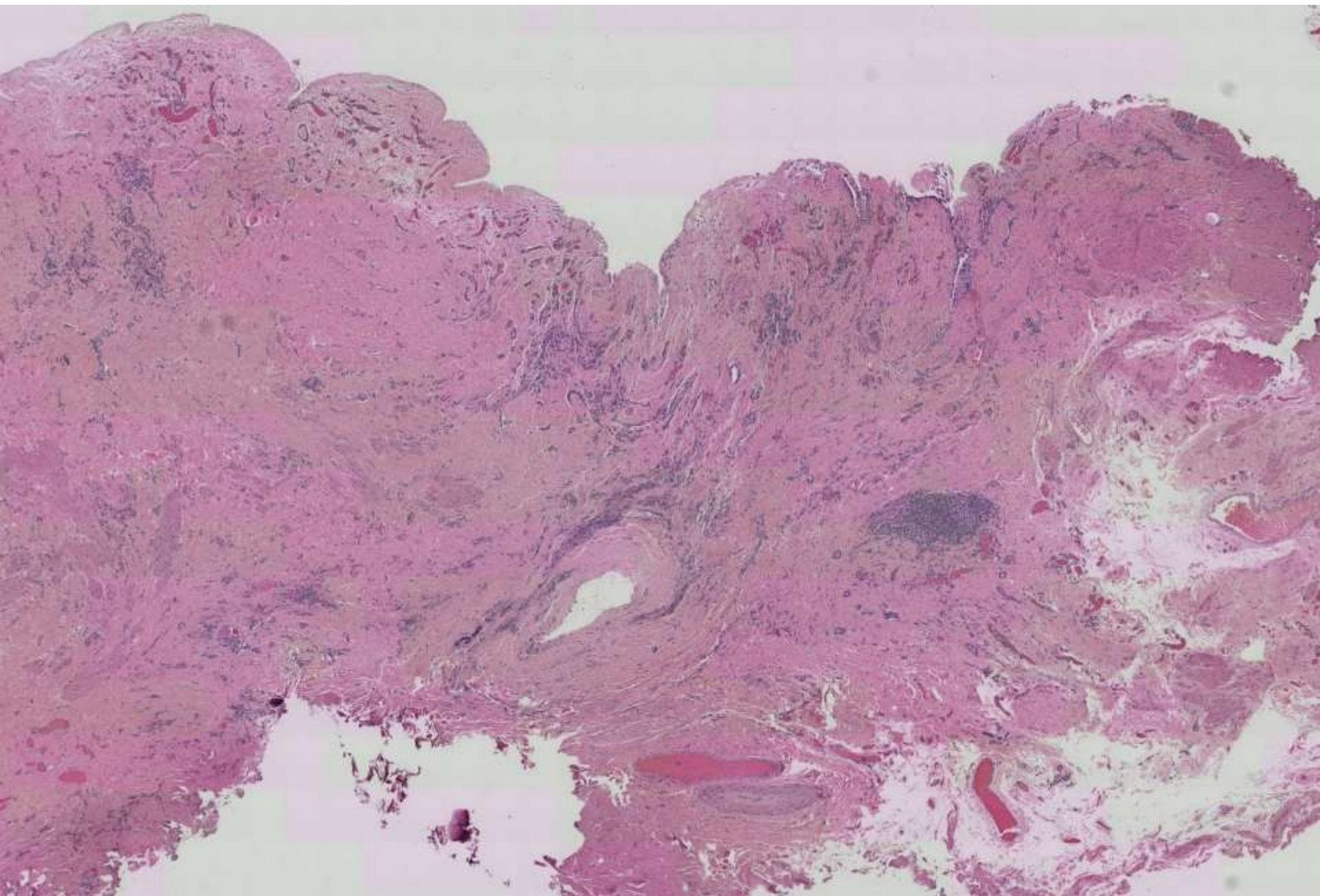
20-1007

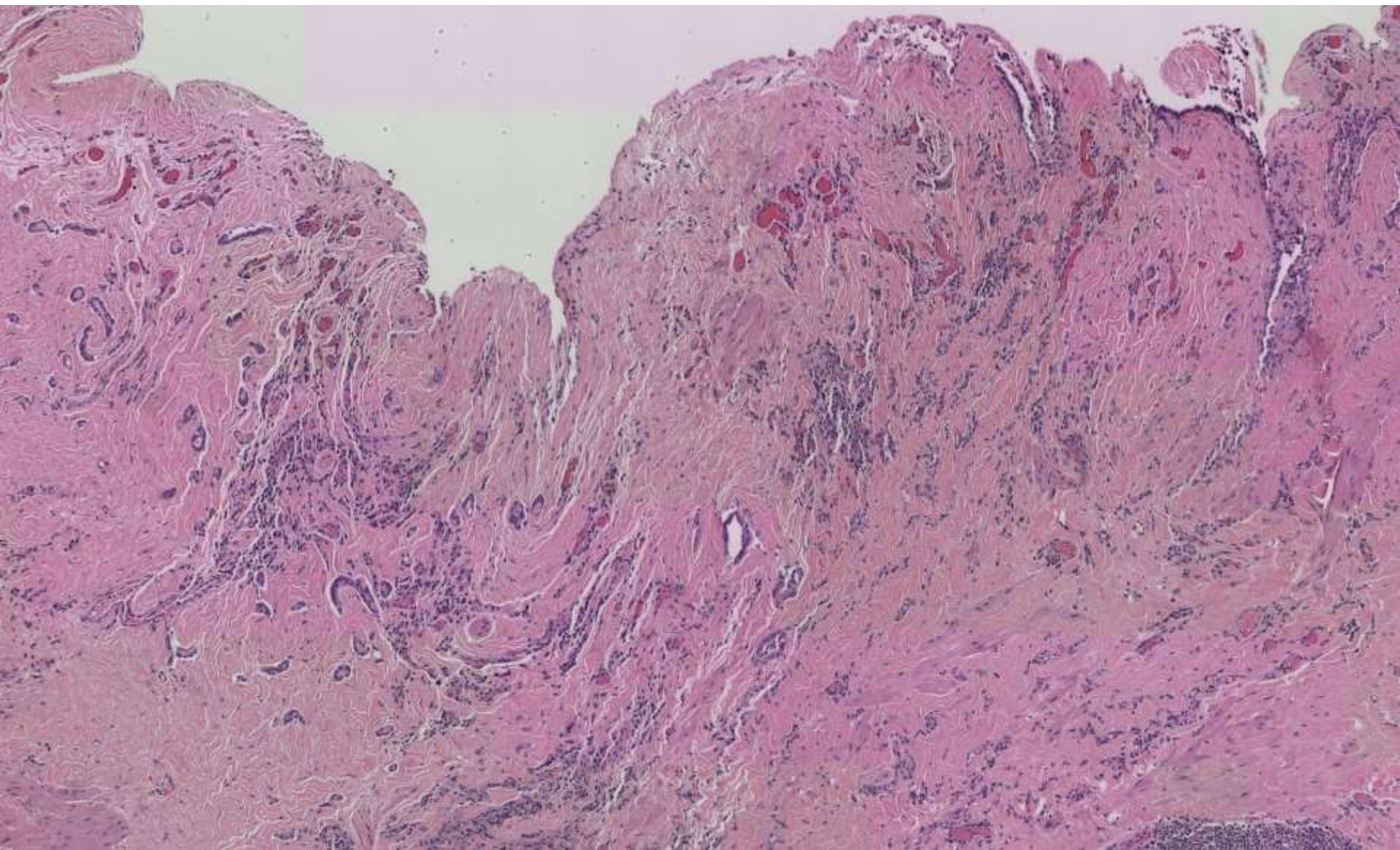
scanned slide available!

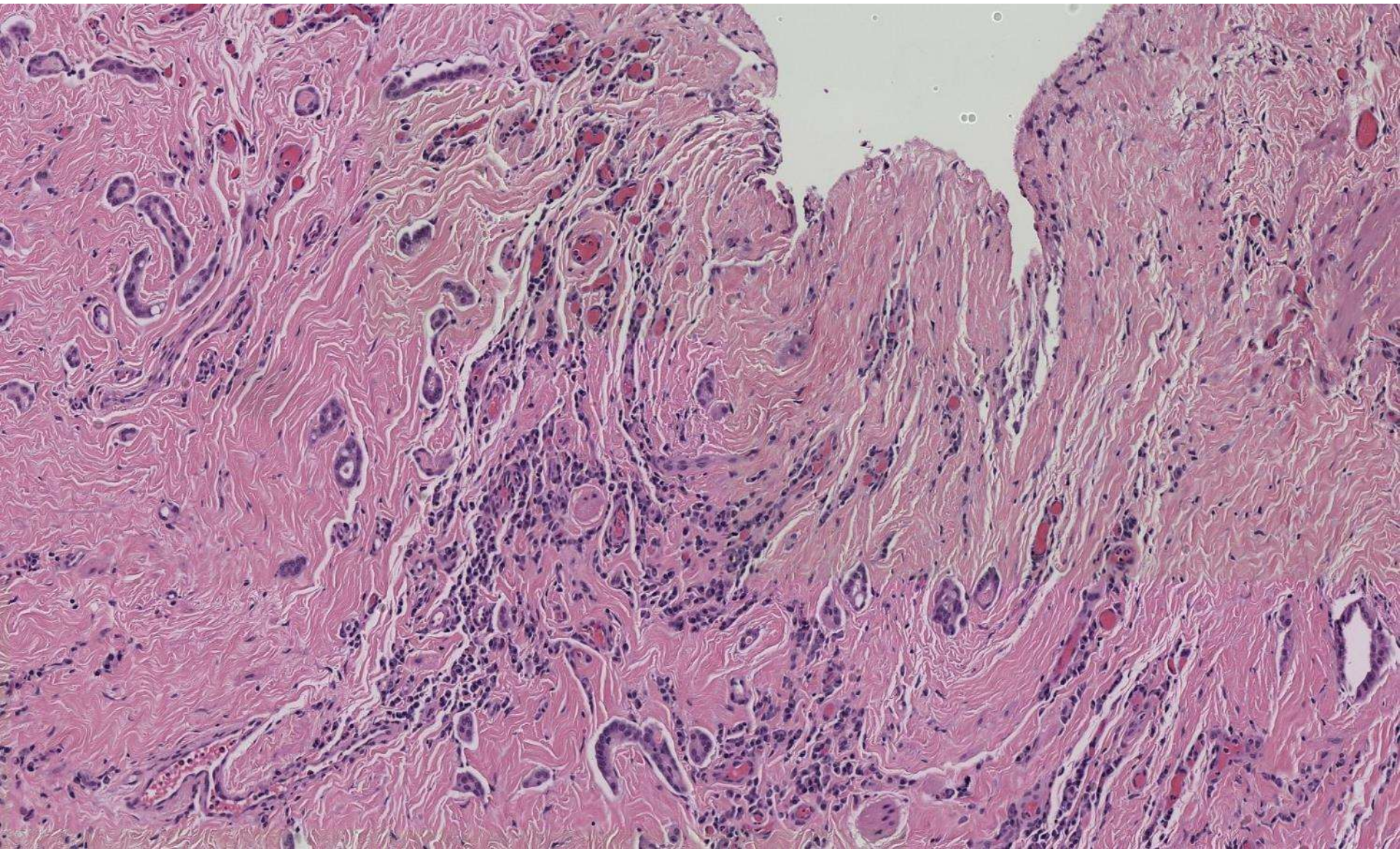
Ankur Sangoi; El Camino Hospital

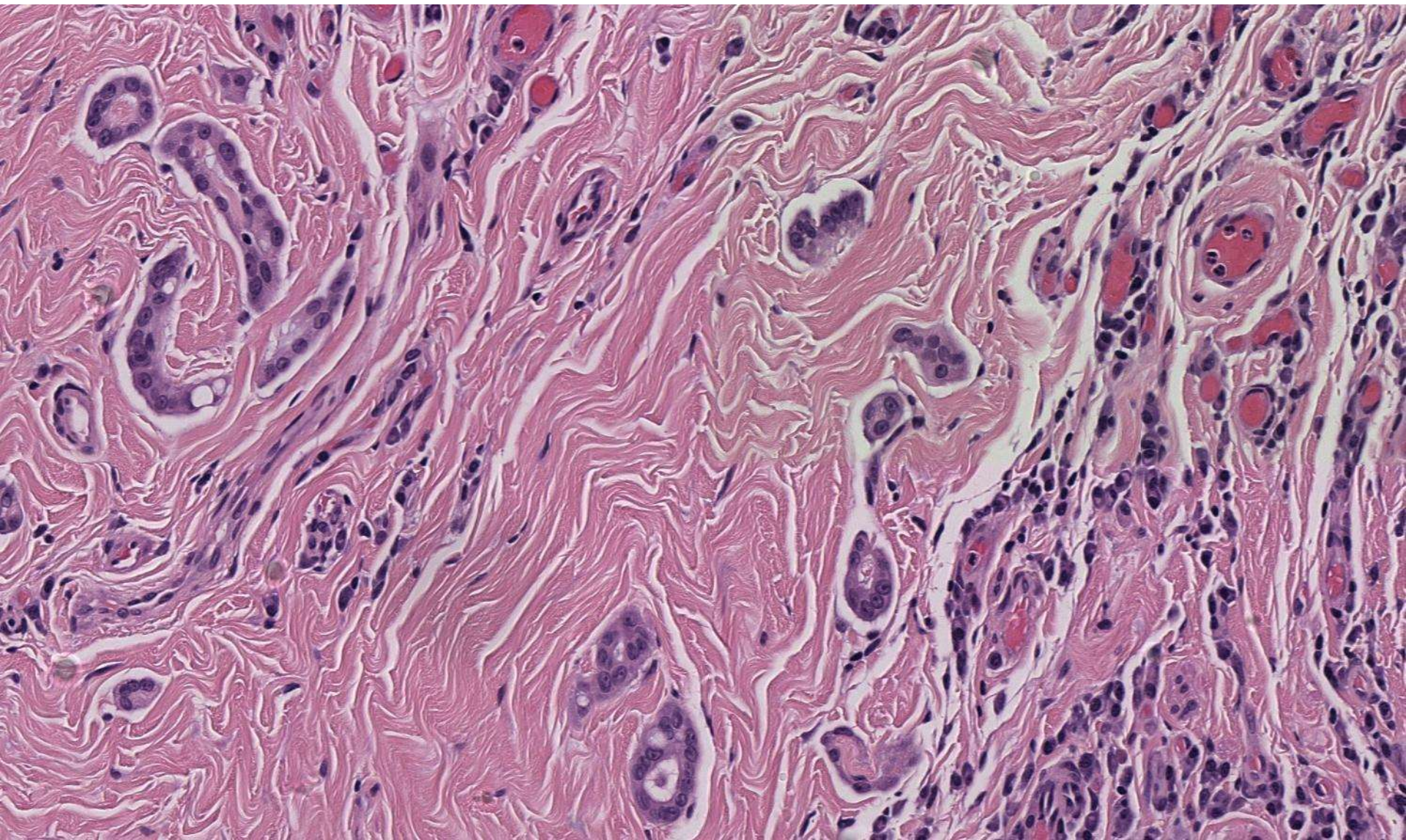
55-year-old M with paratesticular pain/swelling. Hydrocelectomy performed.

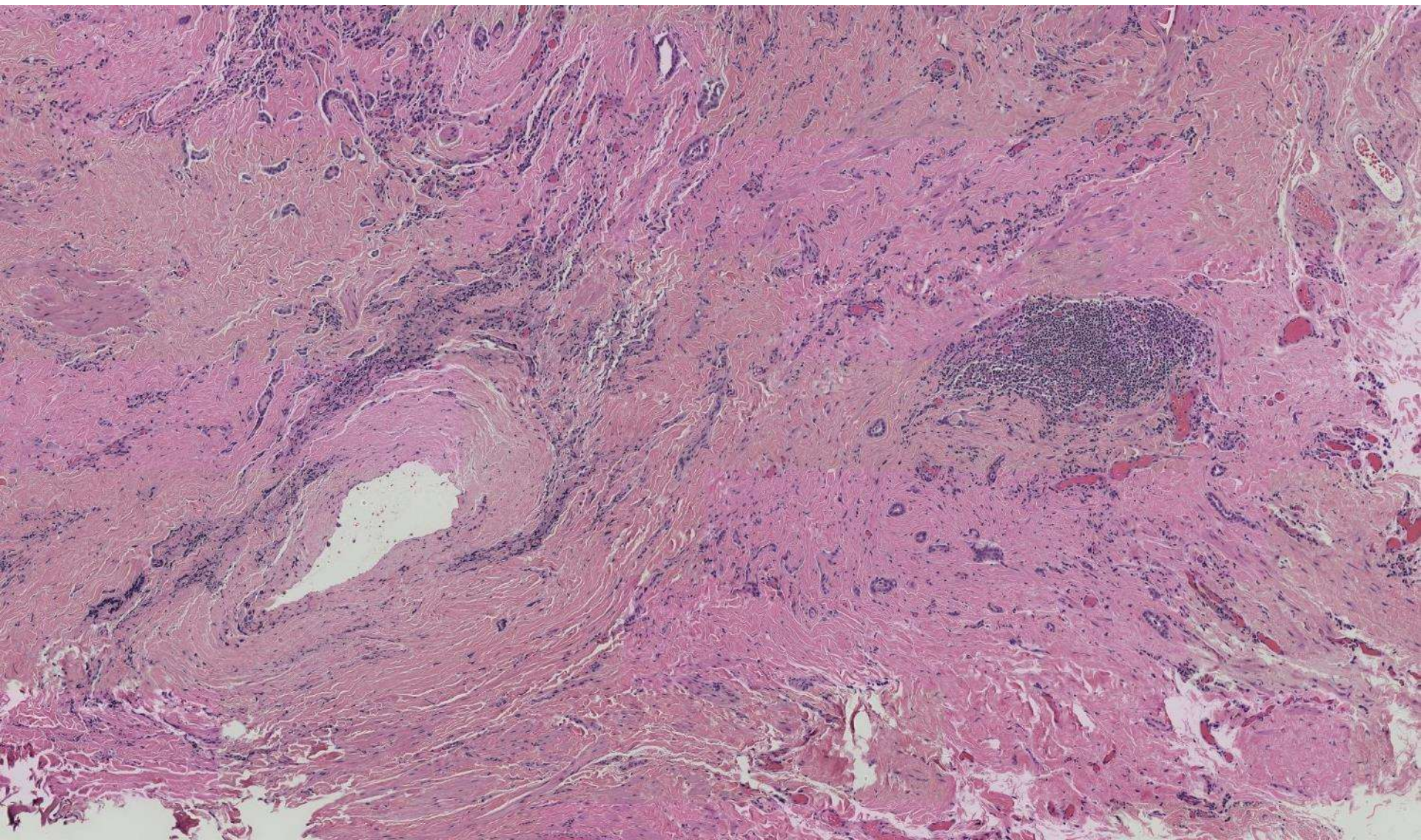


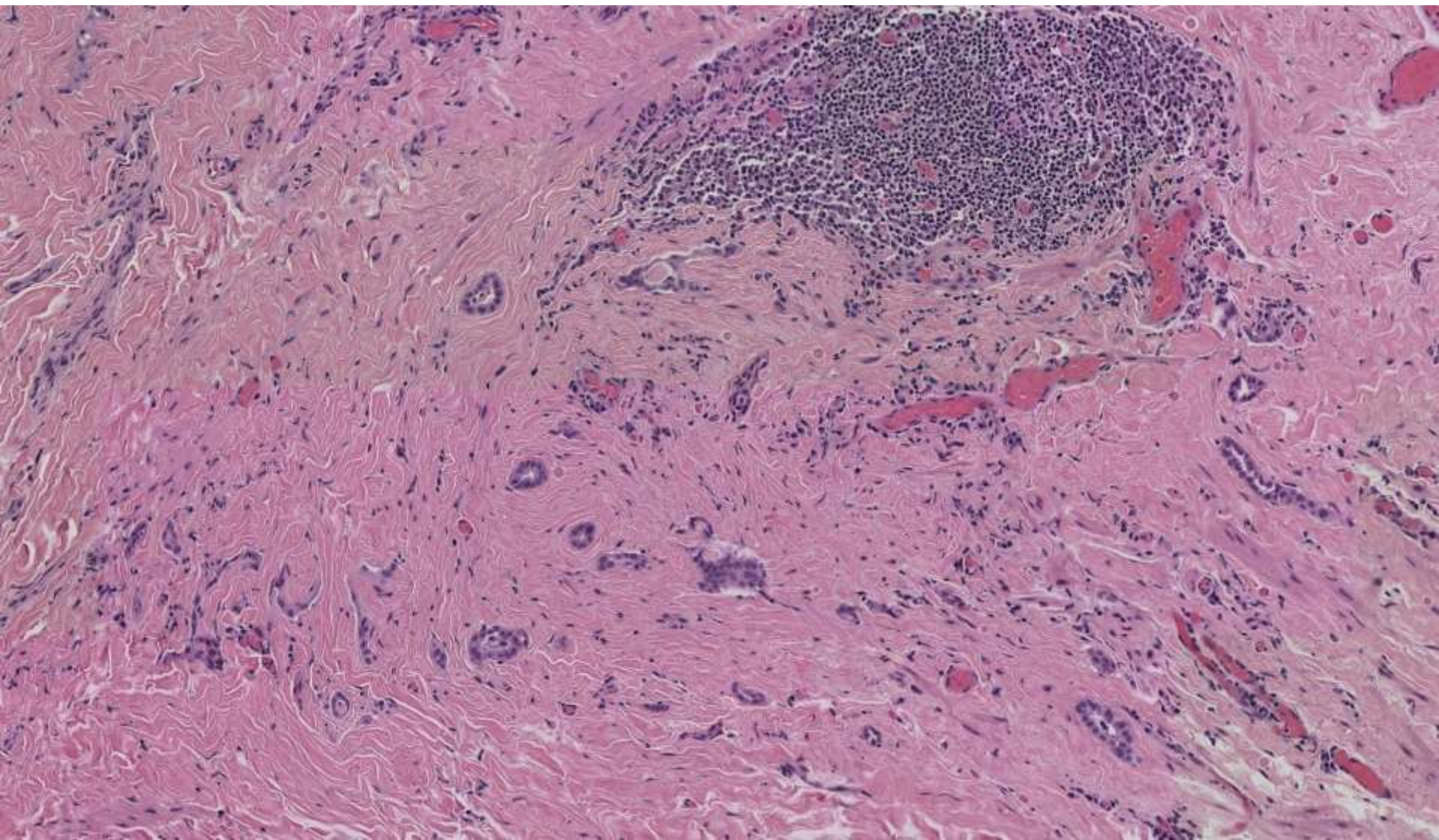












DDx

- **Adenomatoid tumor**
- **Mesothelioma**
- **Rete testis adenocarcinoma**
- **Florid mesothelial hyperplasia of tunica vaginalis**

IHC summary

- Calretinin+
- Low Ki67 (<2%)
- Wild type p53
- Intact BAP1

Follow-up

- 2-years without recurrences

Florid Mesothelial Hyperplasia of the Tunica Vaginalis Mimicking Malignant Mesothelioma

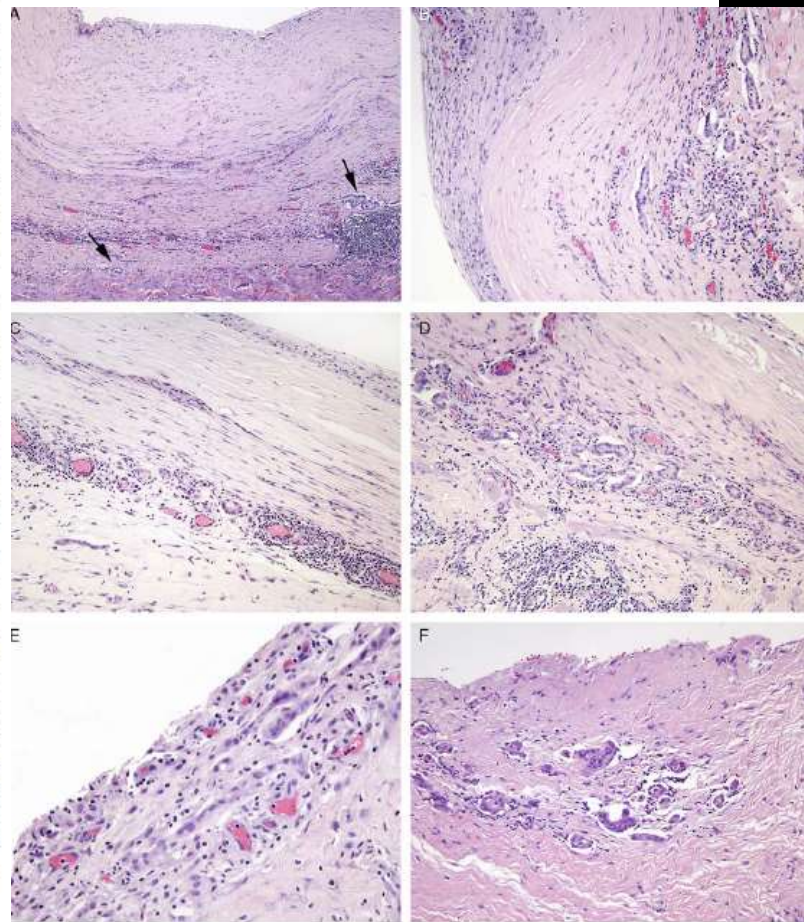
A Clinicopathologic Study of 12 Cases

Stephen Lee, MD,* Peter B. Illei, MD,* Jeong S. Han, MD, PhD,*
and Jonathan I. Epstein, MD*†‡

Abstract: The tunica vaginalis is an embryologically derived mesothelium-lined outpouching of the peritoneal cavity, which may develop neoplastic mesothelial proliferations similar to, although much less commonly than, pleural or peritoneal surfaces. We herein report our experience with 12 cases of florid paratesticular mesothelial hyperplasia, highlighting the spectrum of morphologic changes seen and the utility of fluorescence in situ hybridization analysis of homozygous deletion of 9p21 as an adjunct diagnostic tool. All cases were referred because of concern regarding the nature of the mesothelial proliferation. The median age of patients at presentation was 44.5 years (range, 16 to 71 y). Ten of 12 patients clinically presented with hydroceles (2 of which were complicated by infection or hemorrhage), 1 with “paraepididymal cyst” and 1 patient with an epididymal cyst. In contrast to the normal tunica consisting of a thin fibrous wall lined by a monolayer of flattened bland mesothelium and no significant inflammation, all of our cases were characterized by background changes of fibroblastic organization and stromal chronic inflammation. In all cases, the mesothelial proliferation within the fibrous and inflamed stroma was sparse and consisted of linear arrays of widely spaced horizontally orientated simple nonbranching elongated tubules and small solid nests and cords that were well spaced apart. There was an abrupt linear demarcation of tubules at the deep aspect of the fibrous tissue, with no evidence of definite invasion into the submesothelial tissue. Fluorescence in situ hybridization for 9p21 was negative in all 5 cases in which tissue was available for analysis. Nine patients with extended follow-up were alive (median 8 y; range, 1 to 13 y). In summary, the proliferative changes seen in reactive mesothelial hyperplasia associated with hydroceles may be florid and mimic malignant mesothelioma. In particular, the entrapment of isolated mesothelial clusters within deep fibrous tissue may be the cause of significant diagnostic difficulty. There are, however, morphologic clues such as linear arraying of widely spaced architecturally simple cell clusters that may aid in the correct identification of the benignity of these proliferations.

Key Words: paratesticular, mesothelioma, mesothelial hyperplasia

(*Am J Surg Pathol* 2014;38:54–59)



Florid mesothelial hyperplasia of tunica vaginalis

- **Reactive process secondary to persistent serosal injury in hydrocele and hernia sac**
- **Although can appear “infiltrative” especially when deep, shows linear array of widely spaced simple cell clusters lacking severe atypia**
 - Variable chronic inflammation
- **KEY DDx: mesothelioma**
 - Positive p53, positive GLUT1, loss BAP1, high Ki67, 9p21 FISH deletion